Paulo Francisco Lopes da Silva

Do senescent cells *in vivo* induce a bystander effect in muscle?

Dissertação de mestrado em Biologia Celular e Molecular,
apresentada ao Departamento de Ciências da Vida da Faculdade de Ciências e Tecnologia da Universidade de Coimbra.

Julho 2016

· U C ·

UNIVERSIDADE DE COIMBRA

Paulo Francisco Lopes da Silva

Do senescent cells *in vivo* induce a bystander effect in muscle?

Dissertação apresentada ao Departamento de Ciências da Vida da Faculdade de Ciências e Tecnologia da Universidade de Coimbra para cumprimento dos requisitos necessários à obtenção do grau de Mestre em Biologia Celular e Molecular, realizada sob a orientação científica da Doutora Olena Kucheryavenko (Newcastle University Institute for Ageing) e supervisão da Professora Doutora Emília Duarte (Departamento de Ciências da Vida, Universidade de Coimbra).

Julho de 2016

· U   C ·

UNIVERSIDADE DE COIMBRA

Experimental activities described in this thesis were performed at the Institute for Ageing and Health (IAH), Newcastle University (Newcastle-upon-Tyne, United Kingdom). The present work was developed under supervision of Dr. Thomas von Zglinicki and Dr. Olena Kucheryavenko with support from the FP7 Marie Curie Initial Training network "MARRIAGE".

O trabalho experimental descrito nesta tese foi realizado no Institute for Ageing and Health (IAH), Universidade de Newcastle (Newcastle-upon-Tyne, Reino Unido). O presente trabalho foi desenvolvido sob supervisão do Dr. Thomas von Zglinicki e da Dra. Olena Kucheryavenko com o apoio de FP7 Marie Curie Initial Training network "MARRIAGE".

Cover Image:

Injected senescent MRC5-GFP$^+$Luc$^+$ cells in gastrocnemius skeletal muscle. Tilescan of 20 merged images.

Blue: nuclei. Yellow: muscle autofluorescence. Green: GFP fluorescence signal.

Images acquired and merged using a Leica SP8 confocal and digital light sheet microscope (63x objectives; N.A. 1.4) and LASX software package.

AGRADECIMENTOS

Em primeiro lugar, devo um enorme agradecimento ao Professor Dr. Thomas von Zglinicki; por me ter aceite no seu grupo, por todas as oportunidades durante o ano que me possibilitou e encorajou a seguir, pela exigência e inspiração, que me levaram a trabalhar arduamente de modo a produzir o melhor trabalho que fosse capaz. Obrigado por conseguir sempre arranjar um tempo na agenda para esclarecer dúvidas e dar conselhos. Foi uma honra ter sido supervisionado por um cientista com tão longa carreira de excelência.

De igual modo, devo outro enorme agradecimento à Dra. Olena Kucheryavenko. Muito obrigado por toda a ajuda na integração, ao laboratório e à cidade. Muito obrigado por toda a ajuda com o projeto; sem a tua preciosa ajuda e tempo dedicado não o teria conseguido. Muito obrigado também por, mais que uma supervisora, teres sido uma amiga durante os últimos 10 meses.

Aos restantes membros do "TvZ Lab" – Satomi, Ed e Diana – obrigado por todo o apoio, sugestões e críticas. Foram sem dúvida fundamentais para o desenvolvimento do projeto. Agradeço em especial ao Glyn, por toda a ajuda e orientação com a microscopia, estatística e praticamente tudo o que fosse necessário.

À Professora Dra. Emília Duarte e ao Professor Dr. Carlos Duarte, um obrigado pelo excelente primeiro ano de mestrado, pela ajuda e encorajamento à minha ida para Newcastle.

Aos meus amigos; aos que deixei em Portugal para vir em busca das minhas "Grandes Esperanças" em Newcastle; aos que irei deixar em Newcastle e aqueles, cada vez em maior número, espalhados pelo globo, um sincero obrigado. Obrigado por estarem sempre presentes, fisicamente ou não, mesmo quando eu parecia estar ausente. Por vezes é necessário aprender a estar sozinho para perceber que nunca o estamos realmente; estes últimos 10 meses foram um exemplo disso mesmo.

Em último lugar, mas mais importante, à minha família: "Obrigado e desculpem-me." Obrigado por sempre me encorajarem a alcançar os meus objetivos através do meu próprio esforço e trabalho árduo, por sempre apoiarem as minhas decisões, mesmo as difíceis, e por estarem sempre presentes a garantir que tudo terminará bem. Desculpem-me por os meus objetivos me terem levado para longe e por nem sempre ter tido tempo ou vontade para longas conversas. O trabalho que aqui apresento não está perfeito, mas é o melhor de que fui capaz e penso que isso seja a melhor maneira de demonstrar a minha gratidão por me terem possibilitado esta experiência.

Mais uma vez, obrigado!

TABLE OF CONTENTS

LIST OF ABBREVIATIONS

53BP1	p53-Binding Protein 1
AMP	Adenosine Monophosphate
AMPK	AMP-Activated Protein Kinase
APES	(3-Aminopropyl)triethoxysilane
ATM	Ataxia Telangiectasia Mutated Protein
ATP	Adenosine Triphosphate
ATR	Ataxia Telangiectasia and Rad3-Related Protein
CDK	Cyclin-Dependent Kinase
CDKI	Cyclin-Dependent Kinase Inhibitor
C/EBPβ	CCAAT/Enhancer-Binding Protein β
CHK	Checkpoint Kinase
CNF	Centrally-Nucleated Fiber
CSA	Cross-Sectional Area
DAPI	4',6-diamidino-2-phenylindole
DDR	DNA-Damage Response
DNA	Deoxyribonucleic Acid
DSB	DNA Double-Strand Break
ECM	Extracellular Matrix
ETC	Electron Transport Chain
FISH	Fluorescence in situ Hybridization
GFP	Green Fluorescence Protein
γH2A.X	Phosphorilated Histone H2A.X
LAS	Leica Application Software
LB1	Lamin B1
MMP	Matrix Metalloproteinase
NA	Numerical Aperture
NF-kB	Nuclear Factor kappa-Light-Chain-Enhancer of Activated B Cells
OIS	Oncogene-Induced Senescence
p16 (/CDKN2A)	Cyclin-Dependent Kinase Inhibitor 2A
p21 (/CDKN1)	Cyclin-Dependent Kinase Inhibitor 1
p38MAPK	p38 Mitogen-Activated Protein Kinases
p53	Tumor protein p53
PFA	Paraformaldehyde
pRB	Retinoblastoma Protein
PCNA	Proliferating Cell Nuclear Antigen
PTEN	Phosphatase and Tensin Homolog
ROS	Reactive Oxygen Species
RS	Replicative Senescence
SA-βGal	Senescence-Associated β-Galactosidase
SAHF	Senescence-Associated Heterochromatin Foci
SASP	Senescence-Associated Secretory Phenotype
SBB	Sudan Black B
(DNA-)SCARS	DNA Segments with Chromatin Alterations Reinforcing Senescence
SIPS	Stress-Induced Premature Senescence
SMS	Senescence-Messaging Secretome

SOD	Superoxide Dismutase
TAF	Telomere-Associated Foci
TERC	Telomerase RNA Component
TERT	Telomerase Reverse Transcriptase
TIF / TAF	Telomere Dysfunction-Induced Foci / Telomere-Associated Foci
TGFβ	Transforming Growth Factor β
VEGF	Vascular Endothelial Growth Factor

LIST OF FIGURES

ABSTRACT

Cellular senescence is traditionally regarded as a state of irreversible cell cycle arrest elicited as a response to diverse stressors. Depending on cellular context, senescence can have beneficial or detrimental roles and it is currently known to be involved in tumor suppression and progression, tissue repair, organismal development and aging processes. *In vivo*, the frequency of senescent cells in certain organs can help predict lifespan and selective ablation of senescent cells was shown to postpone ageing phenotypes, showing their importance for the ageing process. The senescent phenotype can be induced by multiple stimuli and cellular contexts. These stimuli usually trigger a persistent DNA-damage response (DDR) that drives not only the irreversible loss of replicative capacity but the production and secretion of reactive oxygen species via p21-mediated signaling pathways. In addition, senescent cells develop a senescence-associated secretory phenotype (SASP). Several bioactive molecules comprising the SASP can diffuse and affect surrounding cells, suggesting that senescent cells can damage their microenvironment. Supporting this assumption, it was observed that senescent cells harboring a DDR can communicate this response to surrounding cells, leading to physiological alterations in these cells, a phenomenon termed "bystander effect". This makes senescent cells a potential cause of age-dependent tissue functional decline. While the existence and effects of the bystander effect have been previously validated *in vitro*, comprehensive proof of its role in non-pathological conditions *in vivo* is still lacking.

We present here a panel of candidate biomarkers to evaluate cellular senescence in skeletal muscle cryosections. We report age-dependent increases in frequencies of lipofuscin-containing fibers, HMGB1-negative and TAF-positive nuclei, as well as decrease in mean nuclear LB1 fluorescence. These results may prove useful to generate robust tests for identification of senescent cells within postmitotic tissues. Moreover, we show here that injection of senescent cells into skeletal muscle of young mice promotes accumulation of certain senescence biomarkers, specifically p21 and lipofuscin in adjacent, bystander muscle fibers, an effect dependent on the abundance of nearby senescent cells. Our data suggest senescent cells are capable of inducing persistent DNA damage and DDR in skeletal muscle bystander cells *in vivo* and engendering downstream senescence-like features in those same cells. These results may be the first line of evidence of a senescent bystander effect in postmitotic cells, *in vivo.* This data might contribute to understanding the reported age-related increase of senescent cells in tissues and their role in ageing/age-related pathologies, while strongly supporting a novel understanding of senescence as a dynamic phenotypic state generated and maintained by stable, self-sustainable feedback loops, driven by DDR and independent of the onset of growth arrest.

Keywords: bystander effect, cellular senescence, DDR, aging, skeletal muscle, biomarkers

Resumo

Senescência celular é tradicionalmente considerada como um estado de suspensão permanente do ciclo celular evocado como resposta a diversos agentes causadores de stress. Dependendo do contexto celular, o processo de senescência pode ter funções benéficas ou prejudiciais e actualmente, sabe-se estar envolvido em processos de supressão e progressão tumorais, reparação de tecidos, desenvolvimento do organismo e envelhecimento. *In vivo*, a frequência de células senescentes em certos órgãos pode ajudar a prever o tempo de duração de vida e a ablação seletiva de células senescentes provou ser eficaz em adiar o desenvolvimento de fenótipos de envelhecimento, demonstrando a sua importância para o processo de envelhecimento. O fenótipo senescente pode ser induzido por múltiplos estímulos e contextos celulares. Estes estímulos normalmente induzem uma "*DNA-damage response*" (DDR) persistente que controla não só a perda irreversível de capacidade replicativa mas também a produção e secreção de espécies reativas de oxigénio por vias de sinalização mediadas por p21. Além disso, células senescentes desenvolvem um "*Senescence-Associated Secretory Phenotype*" (SASP). Várias moléculas bioativas incluídas no SASP são capazes de se difundir e afetar células nas suas imediações, levando a alterações fisiológicas nestas células, um fenómeno conhecido como "*bystander effect*". Tudo isto torna as células senescentes potenciais efetores do declínio funcional observado em tecidos com o avanço de idade. Apesar de a existência e os efeitos do "*bystander effect*" terem sido anteriormente validados *in vitro*, provas compreensivas do seu papel em condições não-patológicas *in vivo* estão ainda em falta.

Apresentamos neste trabalho um painel de biomarcadores para avaliar senescência celular em criosecções de músculo esquelético. Relatamos também, aumentos nas frequências de fibras contendo lipofuscina, núcleos positivos para HMGB1 e núcleos contendo TAFs, assim como uma diminuição na fluorescência média nuclear de LB1, tudo isto em função do aumento da idade dos tecidos. Estes resultados podem vir a ser úteis para gerar testes de identificação robustos para células senescentes em tecidos pós-mitóticos. Além disso, mostramos ainda que a injeção de células senescentes em músculos esqueléticos de ratinhos jovens promove acumulação de certos marcadores de senescência, especialmente p21 e lipofuscina, em fibras musculares adjacentes, dependendo da abundância de células senescentes nas proximidades. Estes dados sugerem que células senescentes são capazes de induzir danos persistentes no DNA e uma DDR em células "*bystander*" de músculo esquelético *in vivo* e de engendrar, nessas células, o desenvolvimento de características típicas de células senescentes. Estes resultados são possivelmente as primeiras provas de um "*bystander effect*" senescente em células pós-mitóticas *in vivo* e podem contribuir para uma maior compreensão do aumento, com a idade, de células senescentes em tecidos e o seu papel no envelhecimento e patologias relacionadas. Isto suporta também uma visão do processo de senescência como um estado fenotípico dinâmico gerado e mantido por "*feedback loops*" estáveis e auto-sustentáveis, gerados por uma DDR independente da suspensão de proliferação celular.

Palavras chave: "bystander effect", senescência celular, DDR, envelhecimento, músculo esquelético, biomarcadores

CHAPTER 1. INTRODUCTION

1.1. CELLULAR SENESCENCE – HISTORICAL OVERVIEW

Human life is regulated by precise mechanisms of cellular and organismal homeostatic control, including cellular senescence[1,2]. Human life expectancy is very long when compared with those of other higher eukaryotes, however, the extended lifespan can result in increased incidence of cancer during later life, caused by a disruption of those same mechanisms[3]. Thus, there is an urgent need for a better understanding of the molecular mechanisms that maintain cellular homeostasis and the causes and consequences of its disruption, in order to improve the well-being of the aging population.

Cellular senescence was firstly described by Leonard Hayflick as a process that limited the proliferation (growth) of normal human diploid fibroblasts (HDFs) in culture[4], following the discovery that HDFs have a finite proliferative capacity in culture[5]. Presently, cellular senescence is regarded as a state of irreversible cell cycle arrest elicited in response to diverse stressors[6,7], involved in complex biological processes. Senescent cells are irreversibly arrested, predominantly in the G1 phase, and are no longer able to divide when submitted to proliferative stimuli (including ample space, nutrients and growth factors in the medium), even though they remain viable and metabolically active for long periods of time[2,6–9], thus being clearly distinct from quiescent and post-mitotic cells. The former are induced by stresses like low serum conditions but retain the ability to proliferate once the conditions are again appropriate. The latter lose the ability to divide as a consequence of developmental programs and not as a response to stress[10].

It is believed the general purpose of senescence is to eliminate abnormal/damaged cells[11], a process particularly relevant in cancer and aging, which are characterized by the accumulation of abnormal cells and cellular damage. In this context, senescence is considered a barrier against cancer development and progression by playing an important role in preventing the uncontrolled cell divisions necessary for malignant transformation[7,9].

Nowadays, the phenomenon observed by Hayflick is known to only reflect a particular type of senescence. The senescent phenotype can be induced by multiple stimuli and cellular contexts, in various physiological and pathological processes. Recent work has made a remarkable progress in understanding the causes and the nature of this process, although many questions still remain unanswered. It has been clearly demonstrated that senescence can have beneficial and detrimental roles[3,11–13]. Depending on the circumstances, senescent cells can promote tumor progression or tumor suppression; under other circumstances, they appear to aid tissue repair but can also contribute to tissue aging. Thus, senescence is currently viewed as a heterogeneous phenotype, driven by diverse inputs leading to diverse outputs[14] and associated with several effector mechanisms. This view refers to senescence as a "collective phenotype of multiple effector programs, which form functional networks of senescence"[14,15].

1.2. TRIGGERS AND MOLECULAR PATHWAYS OF SENESCENCE

As previously referred, cellular senescence can be induced by various stimuli, which engage similar molecular pathways necessary to initiate and sustain the senescence program. Besides the multiple triggers and pathways, the mechanisms that ultimately lead to senescence can also present variations, depending on the cell type and conditions, increasing even more the overall process complexity. The main triggers are a variety of potentially oncogenic stimuli, including telomere erosion[6,16,17], oncogene activation[18], oxidative stress[11,16], DNA damage[8,19,20] and mitochondrial dysfunction[21]. Other factors include epigenetic alterations[22,23], aneuploidy[23,24], inflammation[25] and extracellular matrix dysfunction[23,26]. These stimuli contribute to different types of senescence[11] by arresting cell cycle progression. In this section, an overview of the main triggers and their effector mechanisms and molecular pathways will be presented.

1.2.1. REPLICATIVE SENESCENCE

The limited growth of human cells in culture originally observed by Hayflick[5] is currently understood to, at least in part, accrue from telomere erosion. In each S phase of the cell cycle, during DNA replication, a part of the DNA chain near the ends of the chromosomes is lost because DNA polymerases are unidirectional and cannot replicate completely the ends of the lagging DNA strands (the "end replication problem")[27,28]. Normally, telomeres are in a 'capped' state; they form terminal loops which are stabilized by "shelterin" protein complexes, composed of telomere-binding proteins, including TRF1 and -2 and POT-1[29]. "Capping" renders telomeres unrecognizable by sensor proteins that elicit a DNA damage response (DDR)[30]. The progressive telomere shortening with each cell division destabilizes telomeric loops, resulting in critically short telomeres that trigger a specific type of senescence, named "replicative senescence"[6]. When telomeres reach a critical minimal length and become uncapped, they become dysfunctional and more prone to elicit a persistent DDR while, at the same time, suppress attempts of DNA repair[19,31,32]. The DDR is then responsible for arresting cell division via activation of the p53 tumor suppressor, thereby preventing the propagation of the genomic instability[8,19]. The maximum number of divisions that a cell can complete before reaching the end of its replicative lifespan ("replicative exhaustion") has since been termed the "Hayflick Limit". This value is characteristic of the cell strain but also displays a degree of heterogeneity among individual cells, suggesting telomere shortening is not exclusively a counting mechanism, as originally thought[21].

Not all cells display telomere shortening though. Some cells express telomerase, an enzyme that can restore repetitive telomeric DNA sequences *de novo*[33,34] and thus, compensate the telomere shortening. This enzyme consists of two components: 1) a functional RNA component (TERC) that serves as a template for telomere sequence synthesis and 2) a catalytic subunit (telomerase reverse transcriptase; TERT) of the enzyme[33]; both essential for telomerase activity. The ectopic expression of TERT is currently a common practice in vitro, allowing the "immortalization" of primary cells[7].

Most human tissues show significant telomere shortening during aging[33,35] and, consistently, telomerase-expressing cells are rare. Telomerase stays active in embryonic stem cells and certain adult stem cells; it can be reactivated in most cancer cells and a few somatic cells (activated T cells, for example)[8,33]. In contrast, in adult mice, many cells express telomerase[36] and there is no strong evidence that those cells undergo replicative senescence due to telomere erosion. However, even though proliferative arrest in rodent cells happens without a detectable telomere shortening[2,37], it has been reported an increase of telomeric DDR in ageing mice, irrespectively of telomere length[25,38] and also an accumulation of cells displaying several markers of senescence in various organs[39,40].

1.2.2. STRESS-INDUCED PREMATURE SENESCENCE

In addition to replicative exhaustion, other stimuli prematurely induce cell senescence independently of telomere length. *In vitro*, inadequate culturing conditions can cause a "culture shock", resulting in stress-induced senescence[7]. Recently, evidence for the existence of premature senescence *in vivo* has been increasing, pointing to a potential role in tumor suppression. This senescence type also occurs in rodent cells expressing telomerase[36,39] and is often referred to as "stress-induced premature senescence" (SIPS)[41]. In fact, many cells undergo senescence in response to genomic damage at nontelomeric sites, eliciting a DDR, needed for the senescence-induced cell cycle arrest[20]. The DDR is associated with the presence of nuclear DNA damage foci that contain a variety of activated DDR proteins, including p53[8,20,42]. Phenotypically, replicative senescence appears similar to SIPS, but there have been shown key differences in protein expression[43].

DNA double-strand breaks (DSBs) are particularly effective senescence inducers that can be formed by multiple types of stressors, including ionizing radiation, UV light, chemotherapeutic drugs and topoisomerase inhibitors[3,7,39]. Exposure to these and other stressors is normally followed by pathological increases in, both intracellular and extracellular, reactive oxygen species (ROS) levels, causing oxidative stress in the cell. The notion that ROS can trigger cellular senescence derives from the observations that antioxidant treatments delay cellular senescence[11,16], however if this process plays a role in normal physiological aging is still questionable. For instance, human fibroblasts overexpressing extracellular superoxide dismutase (SOD) presented extended lifespan under normoxic and hyperoxia conditions[44], however, animals haploinsuficient for SOD2 did not seem to have a shortened lifespan[45].

Besides inducing DSBs, oxidative stress can also accelerate telomere shortening, since telomeres are highly sensitive to damage caused by stressors, thus suggesting a modulatory role for stress in replicative senescence[16,17]. In fact, it was demonstrated several decades ago that the replicative lifespan of cultured cells is affected by the oxygen pressure[46]. These evidences indicate replicative senescence is not stress-independent. With this into account, the 'Hayflick limit' can only be applied to mass populations of cells since the lifespan of individual cells is governed not only by a genetic program, but also by stochastic factors, related to oxidative stress[21]. Telomere-driven senescence

thus gains a new role as a tumor-suppressive mechanism, responding to genome damage[17]. In addition, oxidative stress can also hasten telomere shortening by diminishing telomerase activity[21].

1.2.3. ONCOGENE-INDUCED SENESCENCE

Consistent with its role in suppressing tumorigenesis, cellular senescence can also be induced by strong mitogenic signals, including activation of oncogenes and loss of tumor suppressors. Oncogenes are mutant versions of normal genes with the potential to transform cells into a malignant state when combined with additional mutations. In normal cells, however, oncogene activation can also induce cellular senescence[18], referred to as "oncogene-induced senescence" (OIS). Because activated oncogenes can stimulate cell proliferation, this process of senescence is, therefore, an important mechanism that counteracts excessive mitogenic stimulation, functioning as a brake during early stages of tumorigenesis *in vivo*[9].

OIS was originally observed following the expression of an oncogenic form of RAS, a cytoplasmic transducer of mitogenic signals, in normal human fibroblasts[47]. Subsequently, the list of oncogenes capable of inducing senescence has increased greatly[48] and it counts in several members of the RAS signaling pathway as well as pro-proliferative nuclear proteins[6,48]. Phenotypically, senescent cells induced by oncogene activation resemble those induced by replicative exhaustion; however there are substantial differences between the two types[49].

Although OIS is established independently of any telomere dysfunction, as showed by the inability of the expression of TERT to bypass the induction of senescence[50], numerous studies suggest that OIS is mediated, partially, by the induction of DNA damage and activation of a DDR[51,52]. Again, this response is often associated with high ROS levels[3,47]. The mechanisms underlying the generation of a DDR following oncogene activation are still not completely understood but aberrant DNA replication seems to be on its genesis, since oncogene expression does not trigger a DDR in the absence of DNA replication[51]. Furthermore, the expression of an oncogenic form of RAS increases the number of simultaneously active DNA replication origin sites. Increased DNA-replication-origin usage is associated with increased rates of replication errors caused by increased fork stalling and reduced symmetry between DNA replication forks departing from the same origin site[51,53], which can cause an increase in DSBs' frequency.

As stated above, loss of tumor suppressors can also trigger cellular senescence in a similar fashion to oncogene activation. Loss of PTEN tumor suppressor was demonstrated to accompany the induction of p53 and triggered senescence in mouse embryonic fibroblasts[7,54].

1.3. THE SENESCENT PHENOTYPE

1.3.1. THE DNA DAMAGE RESPONSE AND CELL-CYCLE ARREST

Changes in the genome can be potential threats to cell and organismal survival. Thus, damage that introduces a discontinuity in the DNA double helix from proliferative cells can trigger an immediate cellular reaction. If damage is promptly and properly fixed, cells quickly resume normal proliferation; in contrast, when DNA damage is severe, cells may undergo apoptosis or initiate senescence[53]. A host of factors sense DNA damage and engage a signaling cascade known as the DNA-damage response (DDR)[6,53,55] [FIG 1]. This response has two main coordinated functions: 1) arrest DNA replication to prevent propagation of corrupted genetic information and 2) coordinate several mechanisms to repair DNA damage and maintain genome integrity[53]. A response to mild DNA damage normally generates a transient growth arrest and transient DDR signaling, allowing cells to repair their damage. Yet, the genomic lesions that induce senescence, or even apoptosis, trigger a persistent DDR signaling. The three different outcomes are probably determined by the cell type, intensity and duration of the signal, as well as the nature of the damage[53,54]; however, the mechanisms involved in the decision of cells' fate are yet poorly understood.
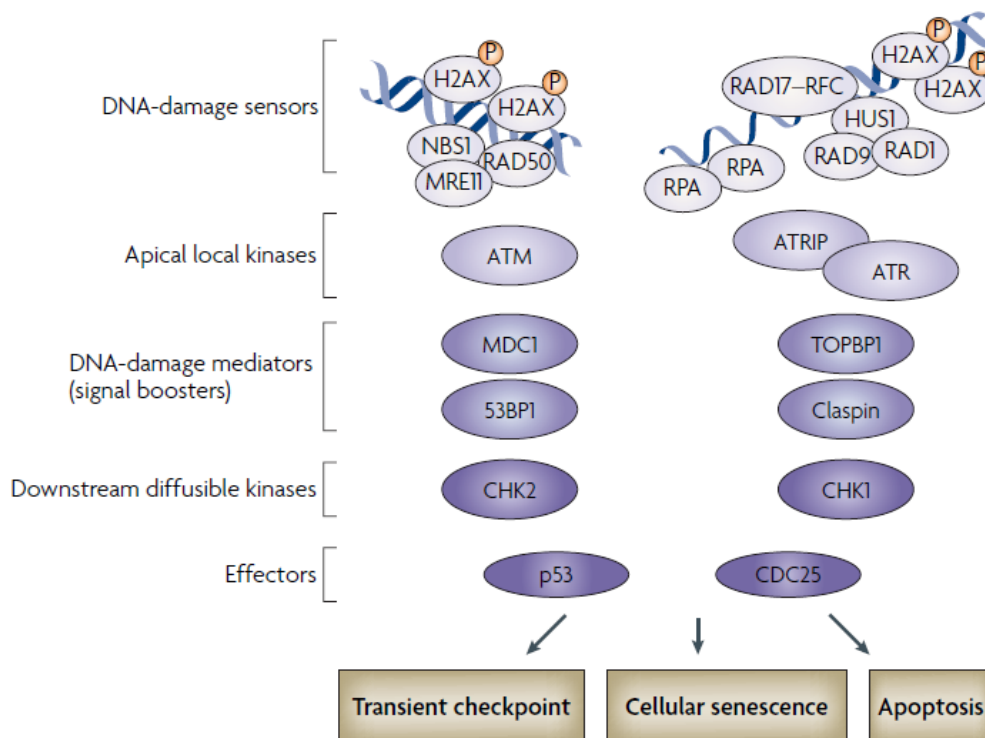
FIGURE 1. THE DNA-DAMAGE RESPONSE. DNA damage in the form of DSBs or RPA-coated single-stranded DNA is sensed by a host of factors that activate signaling cascades, amplifying the DNA-damage signal and eliciting a cellular response. Besides DNA-damage sensors, signaling cascades also involve local and downstream diffusible kinases, signal boosters and effector proteins. Effector proteins act as an interface between this pathway and the cell-cycle machinery. 53BP1, p53-binding protein 1; ATM, ataxia-telangiectasia mutated; ATR, ataxia telangiectasia and Rad3-related; ATRIP, ATR-interacting protein; MDC1, mediator of DNA-damage checkpoint 1; MRE11, meiotic recombination 11; NBS1, Nijmegen breakage syndrome 1; RPA, replication protein A; RFC, replication factor C; TOPBP1, DNA topoisomerase-II-binding protein 1. Adapted from [53].

Telomere uncapping, DSBs, exposure of RPA-coated single-stranded DNA and overexpression of certain oncogenes, among other stressors, are powerful activators of the DDR. Many different proteins are involved in the DDR, including sensor proteins, kinases, adaptor proteins and chromatin modifiers[6,53]; many of them translocate to the DNA-damage foci detected by the cell.

DNA damage in the form of DSBs is sensed by the MRN complex (MRE11-RAD50-NBS1)[56]; in the form of single-strands, however, is sensed by the 911 (RAD9-HUS1-RAD1) and RAD17-RFC complexes[53]. Detection of DNA damage by the sensors then leads to the activation of apical local kinases. NBS1 is responsible for recruiting ATM[55], which activates through autophosphorilation and then phosphorylates the histone variant H2A.X at the site of DNA damage[53]. On the other hand, RPA-coated single-stranded DNA recruits a heterodimeric complex composed of ATR (a paralog of ATM) and ATRIP (a DNA-binding subunit), whose activity is boosted by the 911 and RAD17-RFC complexes[53,57]. Therefore, DSBs primarily activate ATM whereas RPA-coated single-stranded DNA activates ATR.

γH2A.X modifies chromatin and leads to the recruitment of several other mediator proteins[58] which will boost the signaling from apical local kinases, participate in the transduction of the DNA-damage signal and optimize repair activities of other proteins (the identity of these repair-proteins depends on the nature of the damage, cell type and position in the cell cycle, among other factors). In particular, γH2A.X recruits 53BP1 and MDC1, DNA-damage mediator proteins that promote additional accumulation of MRN complexes, which will amplify the local ATM activity and spread γH2A.X along the chromatin, creating an overall positive feedback loop and forming cytologically detectable foci[6,53]. 53BP1 and MDC1 are also required to promote the activation of protein kinase CHK2 by ATM[59]. In similar fashion, in DNA-damage foci originated by exposure of single-stranded DNA, γH2A.X recruits TOPBP1 and claspin, which are necessary for CHK1 phosphorylation[6,53]. Downstream kinases like CHK2 and CHK1 then propagate the damage signal to effector molecules, such as p53 and CDC25, respectively, which are the ones that halt cell-cycle progression, either transiently or permanently[6].

p53 induces cell-cycle arrest partially via activation of p21 transcription, a CDKI that blocks cell-cycle progression. In contrast, CDC25 is an important phosphatase that promotes cell-cycle progression due to its ability to activate CDKs. After DNA-damage, CHK1 causes CDC25 inactivation, causing a rapid cell-cycle arrest[53].

The DDR appears to be the mechanism underlying senescence; however, DDR-independent senescence has also been reported in some experimental conditions, where ATR and p38MAPK were constitutively activated[14,60,61]. In addition, recent studies have identified a new "programd" type of cellular senescence, relevant during mammalian embryonic development[62,63].

Two main pathways establish the connection between the DDR and cell-cycle arrest – the p53 and p16-pRB (Retinoblastoma Protein) tumor suppressor pathways. Each pathway can independently halt the cell-cycle but interaction between pathways has also been verified[6]. The likelihood of engagement of one of the pathways and its ability to induce senescence in the cell is

dependent on cellular context and on the nature of the detected stimuli. Cases in which senescence is independent of these pathways have also been reported[64], suggesting other unknown senescence pathway(s) may exist.

The p53 pathway is elicited primarily in response to a DDR; both signaling pathways serving as a first line of defense against tumor development by ceasing the proliferation of cells at risk of developing and propagating oncogenic mutations[65]. Several proteins regulate the pathway, including HDM2 (an E3 ubiquitin-protein ligase), which promotes p53 degradation, and ARF ("Alternate-Reading-Frame protein"), which inhibits HDM2 activity[6,66].

The p16-pRB pathway can also be elicited after a DDR, but frequently it occurs secondarily to the engagement of the p53 pathway. However, this is not always the case; for instance, epithelial cells are more prone to arrest proliferation after inducing p16 than fibroblasts[6]. Senescence signals inducing this pathway do so by promoting the expression of p16, another CDKI which, similarly to p21, prevents pRB phosphorylation and inactivation. pRB is then able to suppress the activity of E2F, a transcription factor that stimulates the expression of genes required for cell cycle progression[66]. E2F also promotes the expression of ARF, indicating a reciprocal regulation between the p53 and p16-pRB pathways, where loss of p16-pRB activity upregulates the p53 pathway[67]. The p16-pRB pathway is crucial for generating SAHFs or equivalent chromatin states in cells do not displaying these structures; however, once established, SAHFs are self-maintaining, no longer requiring p16 or pRB[68]. Similarly, growth arrest elicited by this pathway is also self-maintaining. After engaging this pathway, cells no longer can resume growth, even after inactivation of p16, pRB or p53[69]. In contrast, cells engaging solely the p53 pathway can resume growth after inactivation of p53 and p21, until a mitotic catastrophe occurs, eventually[6,51]. The p16-pRB pathway has also been shown to cooperate with mitogenic signals to increase intracellular levels of ROS, causing activation of PKCδ, a downstream mediator of ROS signaling pathways, leading to a cytokinetic block that might provide an additional safeguard against proliferation of senescent cells, even after inactivation of pRB or p53[2,70]. Of note, the p16-pRB pathway is highly deregulated in several human cancers, suggesting an important role for this pathway in mediating tumor suppression[2].

1.3.2. MITOCHONDRIAL EFFECTORS OF SENESCENCE

The hypothesis that ageing could be driven by free-radical-associated macromolecular damage has been around for decades. Originally proposed in 1956 by Denham Harman, the so-called "Free Radical Theory of Aging"[71] was posteriorly revised to include mitochondria as the main drivers of this process[72]. Mitochondria are important generators of reactive oxygen species (ROS). During ATP generation via oxidative phosphorylation, reduction of oxygen can generate potentially harmful intermediates[73]. These types of ROS are believed to serve as important signaling molecules as they appear to be tightly regulated within the cell. They can, however, react with themselves and other ROS, creating highly reactive, not tightly controlled, secondary ROS, which are able to induce DNA lesions[74,75].

As previously noted, senescent cells have also been associated with increased levels of ROS[21,76,77]. This increase appears to be linked to the increased mitochondrial mass, decreased mitochondrial membrane potential and deficient antioxidant defense mechanisms observed in senescent cells[78,79]. By inducing DNA damage, particularly on telomeric DNA, ROS can be responsible for activating a DDR, consequently halting cell cycle progression[17,80]. Consistent with this, treatments using free radical scavengers[80] and overexpression of antioxidant enzymes[44] have proven efficient in decelerating telomere shortening and development of cellular senescence in vitro. Yet, while ROS can activate a DDR, DDR effector proteins can too promote an increase in ROS levels, thus generating a positive feedback loop. In particular, activation of p21 promotes ROS generation while also being an important mediator between the DDR, MAPK and TGFβ signaling pathways, which have also been shown to promote ROS generation themselves[76,81]. These observations support the assumption that ROS may be senescence-stabilizing agents, continuously generating DNA damage, thus maintaining a persistent DDR activation[76]. Another study also reported a role of ROS in inducing senescence in neighbor cells in a paracrine form[82], proposing a possible explanation to how senescent cells can contribute to decrease of tissue function with ageing.

While the importance of ROS in the context of cellular senescence has been demonstrated in a great number of cases, some studies have shown that ROS production may not affect lifespan[83] and that it may not be the main inductor of cellular senescence[84], thus suggesting the free radical theory of aging may not be enough to explain aging-associated phenotypes and the transition to a senescent state. Mitochondria are indeed required for the establishment of senescence and the development of the pro-ageing features of the senescent phenotype[85]. Their contribute to the development of senescence however, may be connoted to different mechanisms. In addition to ROS production, other mitochondrial effectors, including a defective electron transport chain (ETC), unbalanced bioenergetics processes and altered redox state, impaired mitochondrial dynamics and altered metabolism play an important role in establishing a permanent growth arrest and inducting senescence (Reviewed by[86,87]) [FIG 2].

Damage to the mitochondrial ETC is considered a form of mitochondrial stress shown to induce cellular senescence even when perturbations affect different respiratory complexes[88–90]. While studies suggest that there is an age-dependent decrease in the ETC[91], the exact mechanism leading to this still remains unclear. One hypothesis predicts that a defective ETC generates high levels of ROS that, in turn, further decrease ETC efficiency, thus generating a positive feedback loop contributing to additional mitochondrial damage and possibly resulting in senescence[86,87,92]. Decrease in ETC efficiency can also result in defects in ATP production, another important contributor to cellular senescence, mainly because it leads to an increase in the AMP/ATP ratio, creating a bioenergetics imbalance in the cell[93]. The increased AMP/ATP ratio is known to stimulate AMP-activated kinase (AMPK)[94]. AMPK activation has been shown to induce and maintain cellular senescence in different cell types, by different mechanisms[86,87]; in particular, by promoting a p53-dependent senescence[95]. Another consequence of decrease of ETC efficiency is the reduction of NAD+ levels in the cell. It has been suggested the depletion of cytosolic NAD+ levels may trigger the

implementation of cellular senescence as NAD+ serves as an essential co-factor to important enzymes involved in DNA repair signaling processes, including Poly-ADP ribose polymerases (PARPs) and Sirtuins[96].

Finally, altering mitochondrial dynamics can also lead to the development of senescence[97–99], with senescent cells typically presenting abnormally elongated mitochondria due to an overall shift towards fusion events. Mitochondrial elongation is as well associated with a decrease in membrane potential and increased ROS production[97] and increased resistance to apoptosis[100].

1.3.3. CHARACTERISTICS OF SENESCENT CELLS

Several features and molecular markers, identified mainly by cell culture experiments, are used to identify senescent cells. After cells face potentially oncogenic stimuli, they activate molecular pathways leading to a permanent proliferation arrest, often become resistant to apoptotic signals and alter their gene expression patterns. These three prevalent features comprise the so-called senescent phenotype[3,6].
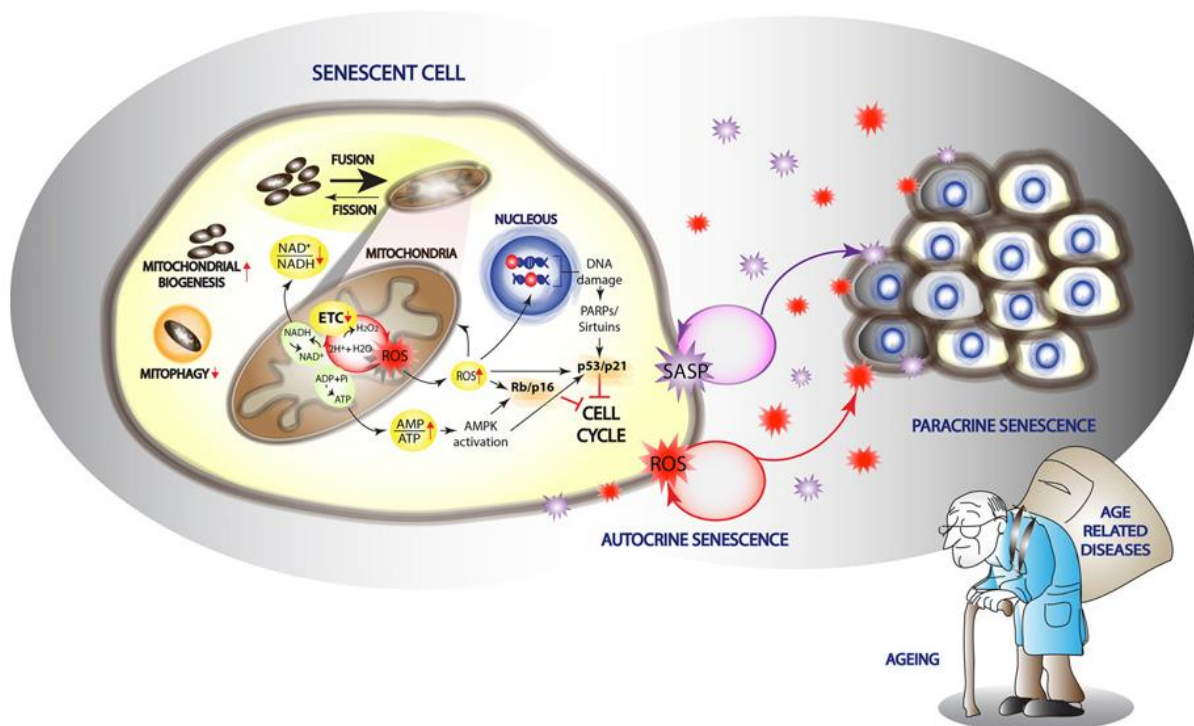
FIGURE 2. MITOCHONDRIAL EFFECTORS OF SENESCENCE. Mitochondrial homeostasis impairment induces cellular senescence and may contribute to the ageing process. Increased mitochondrial biogenesis, decreased mitophagy and decreased fission/fusion ratios have been suggested to induce cellular senescence. Perturbations on the electron transport chain (ETC) resulting in decreased ATP production and increased ROS generation can activate tumour suppressor pathways and induce a senescence cell cycle arrest. Increased ROS levels can originate telomeric and non-telomeric DNA damage, activating the p53/p21 pathway via PARPs/sirtuins activation. Decreased NAD+/NADH ratio has also been linked to senescence. Senescent cells have been shown to generate increased levels of ROS and secrete a variety of growth factors, ECM degrading proteins and pro-inflammatory cytokines, collectively known as SASP. Both ROS and the SASP have been shown to stabilise senescence in an autocrine fashion, but also to induce paracrine senescence, which may contribute to the detrimental effects of senescence during ageing. Adapted from[86].

Promiscuous gene expression. Senescent cells show striking changes in gene expression, not normally associated to the non-senescent counterpart of the same cell type. This was observed in microarray data and other analysis of gene expression by comparing gene expression of both senescent and non-senescent cells[101,102]. The data showed the invoked gene expression patterns differ greatly in a cell-specific manner, suggesting that many of the observed alterations may be dependent of collateral activation of pathways set by the cell lineage[102]. The major changes in expression can be related to known cell-cycle inhibitors or activators. Senescent cells often overexpress two important cell-cycle inhibitors, both cyclin-dependent kinase inhibitors (CDKIs) termed p21 (also termed CDKN1a or p21Cip1) and p16 (also termed CDKN2a or p16INK4a), components of DDR pathways[6]. Senescent cells also repress the expression of proteins that promote cell-cycle progression such as replication-dependent histones, c-FOS, cyclin A, cyclin B and PCNA (proliferating cell nuclear antigen)[6,68].

Apoptosis resistance. Like senescence, apoptosis is a possible response to cellular stress, responsible for the fast elimination of damaged cells. The cell type and the nature and intensity of the stressor are believed to be key factors that help determine whether a cell undergo senescence or apoptosis[103] but the effector mechanisms behind it are still poorly understood. Senescent cells frequently become resistant to certain apoptotic signals; however this is not always the case[104]. This feature can partly explain why senescent cells can be very stable in culture and even why the number of senescent cells accumulates with age *in vivo*[105].

Growth arrest. The essentially permanent growth arrest is the classic hallmark of cellular senescence in mitotic cells. This proliferation arrest is dependent on the expression of dominant cell-cycle inhibitors that halt DNA replication[6] and its general features depend greatly on cell type. Of note, while senescence cannot result in loss of proliferation of postmitotic cells such as neurons and skeletal muscle fibers, those cells display many other molecular characteristics of senescence, including a promiscuous gene expression and a senescence-associated secretory phenotype (SASP)[40].

Besides these three primary features, several other markers can help identify senescent cells both *in vitro* and *in vivo*. As previously stated, senescent cells are distinct from quiescent and terminally differentiated (postmitotic) cells, even though the distinction appears difficult at first. As yet, no marker identified is entirely exclusive to the senescent state and, likewise, not all senescent cells display all the senescence markers identified so far. Thus, senescent cells are generally identified by an aggregate of phenotypes [Reviewed by [6,8,12,13]] which, taken together, define the senescent state. Next, the more prominent senescence-associated features are presented.

Absence of DNA replication and proliferation markers. Since the cell cycle of senescent cells is permanently arrested, there is no DNA replication during the S phase of the Interphase. The lack of DNA replication is an obvious marker for senescent cells, since it can be easily detected by incorporation of 5-bromodeoxyuridine (BrdU). Alternatively, the general absence of proliferation markers, such as Ki67 or PCNA can also be an indicator of the proliferation arrest[6]. These markers

are, however, insufficient because they do not distinguish senescent cells from quiescent or post-mitotic cells.

p21 and p16 overexpression. Upregulation of p21 levels was one of the first markers of replicative senescence induction[106], even though can also be involved in the regulation of other fundamental cellular programs[107]. p16, on the other hand, is not commonly expressed by quiescent or terminally differentiated cells and is present at very low or even undetectable levels in most normal cells and tissues, thus also being used to identify senescent cells[108]. Its expression is induced by culture stress and as a response to DNA damage, becoming easily detected in senescent cells[47]. Besides, p16-positive cells have been observed to accumulate in tissues with ageing[109], making them a robust biomarker for cellular aging *in vivo*.

Senescence-Associated Heterochromatin Foci (SAHFs). Many senescent cells expressing p16 also contain SAHFs[68], detectable heterochromatin domains that contain and silence critical pro-proliferative genes, required for cell cycle progression. The formation of SAHFs is dependent upon the activation of the pRB tumor suppressor by p16[68]. Once activated, pRB promotes the reorganization of chromatin into discrete foci[68], silencing certain genes and contributing to the alteration of gene expression profiles, a typical feature of senescent cells.

Persistent DNA damage foci. As previously referred, many inducers of senescence cause genomic damage, resulting in a DDR and persistent DNA damage foci. These foci were classified as DNA segments with chromatin alterations reinforcing senescence (DNA-SCARS)[8,42] and were shown to co-localize with Promyelocytic Leukemia Protein (PML) nuclear bodies, subnuclear domains involved in cellular responses to stress and associated with p53 activation[110,111]. When located on telomeres, DNA damage foci can also be termed telomere-associated foci (TAF)[8,112]. Both foci contain several markers, including phosphorylated histone H2A.X (γH2A.X), 53BP1 and several activated DDR proteins such as phospho-CHK2, phospho-ATM and ATR[19,113]. These features help distinguishing this type of foci from transient DNA-damage foci[42].

Senescence-Associated Secretory Phenotype (SASP). Not all the changes in gene expression contribute to growth arrest. Senescent cells harboring a persistent DDR signaling secrete several growth factors, cytokines, chemokines, proteases and other soluble factors and, possibly, microvesicles[114] with potent autocrine, paracrine and synaptic signaling activities that can alter tissue microenvironment, possibly contributing to the age-related decrease in tissue structure and function[101,102]. This senescence-associated secretory phenotype (SASP)[8,115] has numerous biological activities and is viewed as the most striking feature of senescent cells and also as the key to understand many of the diverse biological roles of cellular senescence, in both organismal aging and age-related pathologies[12,13,115].

Morphological changes. Senescent cells generally increase in size, sometimes doubling in volume[5]. Depending on the senescence trigger and conditions of the medium, cells can also adopt a flattened morphology, become multinucleated or refractile[7].

Alterations in nuclear lamina. Accompanying the increase in cell size, nuclei from senescent cells also increase their size and display an irregular nuclear envelope[116] known to be associated with gene regulation[117]. Recently, the downregulation of expression of the nuclear lamina protein Lamin B1 (LB1) was established as an easily-detected but robust marker of senescence in both *in vitro* and *in vivo*[116,118].

Senescence-Associated β-galactosidase (SA-Bgal) expression. Senescent cells express a form of β-galactosidase, whose activity is detectable at a near-neutral pH. SA-Bgal was first observed in 1995, by Dimri and colleagues[105] and became the first marker to allow the detection of senescent cells *in situ* in tissues. This marker also provided evidence that senescent cells exist and accumulate with age in tissues *in vivo*[105]. The overexpression of SA-Bgal is a reflection of the altered cell function inherent to the senescent state, particularly the increase in lysosomal mass[119]. Histochemical staining for SA-Bgal has since become a commonly used marker for senescent cells.

All the characteristics above described clearly indicate that senescent cells develop a phenotype much more complex than just proliferation arrest. In fact, the conventional idea of proliferation arrest being the defining feature of senescent cells can no longer be sustained. Recently, mature postmitotic neurons were shown to develop a phenotype, which worsens with age, identical to the typical state of senescence, as a result of p21-mediated DDR signaling[40]. Again, p21 appears to be involved in major signaling pathways connecting ROS levels, the DDR and downstream phenotypic alterations during the transition to senescence. As explained in the previous section, p21 signaling results in the increase of ROS levels, which in turn escalate DNA damage and DDR, generating a stable and self-sustainable feedback loop, necessary and sufficient for the establishment of senescence[76]. In light of the recent findings in postmitotic neurons, it appears the p21-mediated positive feedback loops may be independent of the onset of growth arrest, emphasizing the need to redefine senescence beyond those terms. Instead, growth arrest must be seen as just one of many phenotypic changes downstream of the DDR mediated by p21 signaling pathways.

1.3.4. THE SENESCENCE-ASSOCIATED SECRETORY PHENOTYPE

As stated in the previous section, one of the main features of senescent cells is an altered gene expression. Cells undergoing senescence exhibit profound changes in their transcriptome and, subsequently, an increased expression of certain genes encoding a series of secreted proteins. This new secretory phenotype implemented by senescent cells is termed the senescence-associated secretory phenotype (SASP)[113,120] or the senescence-messaging secretome (SMS)[2,121].

Consistent with the overall senescent phenotype, the SASP can be beneficial or deleterious, depending on biological context[7,12]. SASP factors can be classified into three major categories: 1) soluble signaling factors; 2) secreted proteases and 3) ECM components[115]. Among the diverse host of secreted factors are inflammatory cytokines, chemokines, growth factors, interleukins and matrix-remodeling proteins, which are able to modify the local tissue microenvironment and promote a vast number of biological activities[8,115]. Among other effects, the SASP can promote cell

proliferation or can drive cells into senescence, depending on the context[8,82]; it can stimulate blood vessel formation (due to secretion of VEGF)[122], sometimes contribute to tumorigenesis or, inversely, to tumor suppression (through stimulation of the innate immune system)[115,123]. Many SASP factors, including IL-6, IL-8, several MCPs (monocyte chemoattractant proteins) and MIPs (macrophage inflammatory proteins) also promote inflammation, either directly or indirectly[115,124]. Secretion of these factors causes local chronic inflammation, an important contributor to major age-related diseases[8,115,125]. When secreted by senescent cells, proinflammatory cytokines can trigger distinct cellular responses. In certain cases, they seem to promote the conversion of premalignant cells into full malignant cells. Other cytokines seem to be key factors in establishing and maintaining the senescence arrest[7]. For instance, signaling through the IL-6 and IL-8 receptors is essential for cells to enter senescence after being exposed to a trigger[126]. Finally, the proinflammatory component of the SASP can also be responsible for senescent cell clearance by phagocytosis[127].

Thus, it appears senescent cells have contradictory roles, promoting tumorigenesis in certain settings but acting a tumor suppressing mechanism in others. In this context, the SASP is one of the most prominent features of senescent cells because it can potentially explain the role of senescence in both organismal aging and age-related pathologies[8,115]. The SASP is a very heterogeneous phenotype: the factors being secreted vary among cell types and with the senescence trigger. Senescent cells with a SASP appear to be physiological different from OIS cells. It is reported that secreted molecules of OIS cells clearly inhibit cancer cells proliferation[128] whereas the secretome of a SASP cell can have the diverse effects referred above. These apparently contradictory results suggest that the secretory characteristics of the SASP are dependent on cell type and cellular context, which could suggest cell type-specific feedback loops (possibly driven by secreted inflammatory mediators) are involved in promoting autocrine senescence[129]. Nonetheless, expression of proinflammatory cytokines appears to be its most conserved feature[7,8,113,115].

The SASP has been observed in senescent cells triggered by RS, OIS and SIPS and it arises normally due to, or accompanied by, DNA damage or epigenomic perturbations[113,120]. Loss of certain DDR proteins has been correlated to decreased expression of some SASP factors[113]. Altogether, these results suggest at least one of the functions of the SASP may be to communicate the compromised state of the cells to their neighboring cells, preparing the tissue to repair[14,115]. In support of this assumption, cells that senesce exclusively due to ectopic overexpression of p53 or p16 and do not develop a DDR also do not express a SASP despite displaying other characteristics of senescent cells[130]. Contrarily to its effects on the DDR, p53 negatively regulates the SASP[113] and genetic alterations leading to loss of p53 result in a more rapid acquisition of the SASP[115]. These findings disclose that the SASP can be uncoupled from the senescence-associated growth-arrest[115].

An early cellular response to senescence triggers is an increased IL-1α expression, which binds to its receptor (IL1R), initiating a signaling cascade that ultimately activates NF-kB and C/EBPβ (CCAAT/enhancer-binding protein)[131] [FIGURE 3]. The onset of the SASP is thought to be dependent on activation of both these transcription factors and on the DDR[61,121,132], however, it remains

unclear how exactly these two distinct events cooperate to modify the secretion patterns of the cell. NF-kB and C/EBPβ can promote the transcription of certain inflammatory factors[126]. Similarly, some DDR proteins, including ATM, NBS1 and CHK2 positively regulate certain SASP components, but only after the initial rapid and robust DDR subsides and a persistent DDR signaling has been established. DNA-SCARS and TIF appear to mediate the effects of the DDR on the SASP[42], for they contain proteins required for the establishment of a persistent DDR. For all this, another hallmark of the SASP is its dynamic development over time [FIGURE 3]. After being exposed to potentially oncogenic stimuli, cells arrest their growth within a period of 24h; however the SASP only fully develops approximately 5 days after senescence induction [FIGURE 3][12,115,120].

As noted, the NF-kB signaling system, a very important regulator of innate immunity responses, is also one of the major signaling pathways responsible for stimulating the appearance of the SASP[129]. The p65 subunit of the NF-kB complex was observed to accumulate into SAHF-positive nuclei when phosphorylated on Ser536, a modification that correlated with increased expression and secretion of inflammatory markers[133]. It was also demonstrated that the inhibition of NK-kB signaling could overcome cell growth arrest caused by p53 signaling[134], implying a causative role of NF-kB in the induction of SASP.

Several studies have shown that DNA damage, particularly with activation of ATM, can trigger the activation of the NF-kB system via several signaling complexes, including the NEMO shuttle and p38MAPK signaling pathway, also an important inducer of cellular senescence[135,136]. In addition, genomic instability caused by cellular stress can also potentiate NF-kB signaling due to epigenetic alterations involving HMGB1 proteins. HMGB1 is a high mobility group protein, chromatin associated, with an important role in controlling transcription, replication and DNA repair. HMGB1 is also a secreted cytokine, functioning as an alerting danger signal and recruiting new immune cells to tissues[129,137,138]. When secreted, HMGB1 induces inflammatory signaling by binding and activating several receptors associated to the NF-kB pathway[138]. A recent study has demonstrated that in conditions of cellular stress, HMGB1 is released from the nuclei to facilitate cellular defense and to alert the immune system[139].
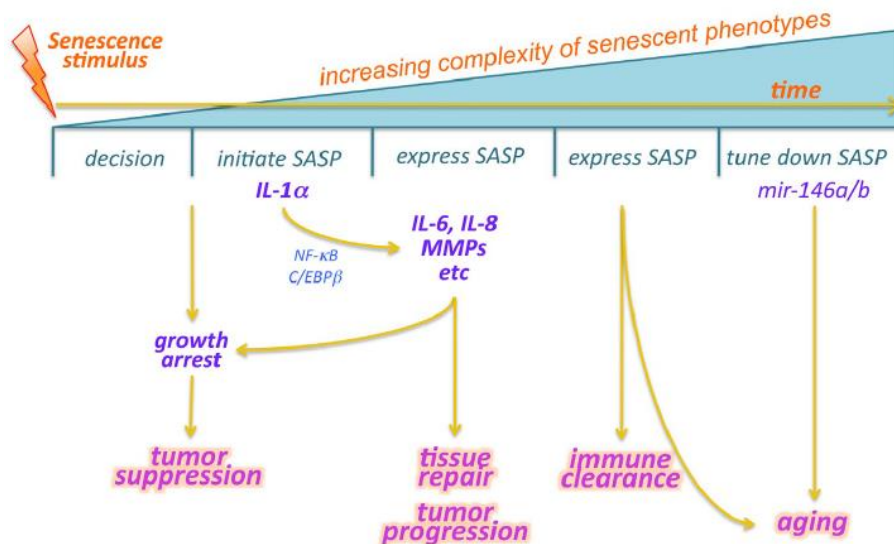
FIGURE 3. TEMPORAL ORGANIZATION OF THE SENESCENT PHENOTYPE. After being exposed to a senescence stimulus, cells enter a decision period during which they coordinate repair mechanisms and "decide" if there is need to undergo senescence. If a cell initiates senescence, after the decision period, the growth arrest and the DDR become essentially permanent, serving as tumor suppressing mechanisms. Next, the SASP starts to develop. One factor expressed early is IL-1α which leads to activation of the transcription factors NF-kB and C/EBPβ. These transcription factors subsequently promote the expression of many SASP proteins, contributing to SASP full establishment. SASP proteins, recently expressed, can promote tissue repair but also tumor progression and immune clearance of senescent cells. The accumulation of senescent cells over time seems to drive aging phenotypes. Finally, to prevent the SASP from generating a persistent acute inflammatory response, cells express mir-146a and mir-146b, which reduce the expression of certain inflammatory cytokines and other SASP factors. Adapted from[12].

1.4. THE BYSTANDER EFFECT

The SASP originates a complex signaling network in which the secreted factors affect not only the cells producing them, but also neighboring cells and the local microenvironment. In sum, SASP signals by both autocrine and paracrine mechanisms and the ultimate effect of the signaling depends on three main factors: 1) genetic composition of the cell that is signaling; 2) genetic composition of the affected cell and 3) the local microenvironment in which cells are located. In certain conditions, through paracrine and autocrine signaling, the SASP forms an inflammatory microenvironment leading to the clearance of senescent cells. In other conditions, paracrine signaling can instead trigger senescence in neighboring cells ("bystander effect"), sometimes through mechanisms that generate DNA damage and ROS[82,140,141].

Thanks to co-culture and co-transplantation experiments, it has been known for some time that senescent cells stimulate proliferation and invasiveness of premalignant and malignant epithelial cells[142,143]. However, the impact of senescent cells upon normal proliferative cells only recently started to be examined. In 2012, Nelson *et al*[82] co-cultured replicatively senescent fibroblasts (founder cells) with young (recipient/bystander cells) fibroblasts *in vitro* and observed that the founder cells induced a DDR as bystander effect in surrounding proliferating cells. In this study, induction of the senescent phenotype in recipient cells was evaluated through foci kinetic data and it was observed that blocking gap-junctions and scavenging extracellular ROS blocked the increase of foci formation rate. These results indicate, at least in this scenario, the bystander effect was transmitted via gap junction-mediated cell-cell contact and processes involving ROS were required for transmission of the effect. In contrast, soluble factors secreted into the extracellular medium had little effect on foci formation, suggesting they do not play an active role in propagating the bystander effect. The induction of senescence was confirmed by measurement of several markers, which helped to prove continuous exposure to senescent cells induced permanent cell senescence in bystander cells[82].

Work on this topic was rapidly followed by others. Hubackova *et al* [141] reported that founder cells undergoing replicative, oncogene- and drug-induced senescence are all capable of inducing the transition of recipient cells into cellular senescence through a bystander effect mediated by the IL-1/NF-kB and TGFβ/SMAD signaling pathways. These pathways were necessary for the increase in ROS production and induction of DNA damage (and a DDR) in recipient cells. In particular, NF-kB-dependent IL-1- and TGFβ-mediated signaling promoted the expression of Nox4, a NADPH oxidase capable of regulating ROS production to induce DNA damage[141]. Nox4, together with Nox1, was recently recognized as a key gene involved in mediating the senescence response, since the overexpression of both genes is sufficient to induce senescence via a DDR[144]. Thus, the activation of NF-kB seems to represent an important upstream trigger of a cascade of events that will ultimately result in establishment of senescence[141,145]. This conclusion is in accordance to the observation that fibroblasts expressing a constitutively active form of NF-kB exhibit aggravated cell senescence, result of enhanced autocrine and paracrine feedback between NF-kB, COX-2 and ROS[25]. Another

study, from Acosta *et al* [140] also delved into the regulation of paracrine senescence by the inflammasome and IL-1 signaling.

These and other works demonstrate a causal relation between certain SASP components, particularly TGFβ-1 and TGFβ family ligands[140,145,146], and the establishment of genotoxic stress and a DDR, which was excluded from the paper by Nelson *et al*. In these cases, the bystander effect was clearly mediated by secreted soluble factors released to the microenvironment but the discrepancies may reflect differences between the scenarios evaluated. With this into account, the bystander effect appears to be a cell-specific mechanism[146], varying according to the factors affecting the signaling by the SASP (presented above), while being sensitive to qualitative and quantitative differences in the SASP itself.

One particular element of the bystander effect linking several studies seems to be the role of ROS and their contribution to DNA damage. Several studies reported an increase in ROS levels in bystander cells[146,147] even with significantly different types of founder cells, suggesting a common mechanism, independent of the trigger mechanism and genetic composition of the signaling cell, inducing DNA injury in bystander cells and causing cells to undergo senescence.

The results above described suggest the bystander effect may contribute to the age-dependent increase in senescent cell frequency and to the impact these cells have on their local microenvironment. However, comprehensive proof of the induction of senescence through a bystander effect in tissues *in vivo* is still lacking. There are reports on the impact of the SASP in causing paracrine senescence and impacting tumor suppression and senescence *in vivo* [140] but are somewhat limited to effects on cells surrounding preoplastic lesions undergoing OIS. There is also evidence that reinforcement of cellular senescence caused by chronic inflammation can accelerate ageing via ROS-mediated telomere dysfunction[25]. This effect importantly implies that frequencies of senescent cells can help predict lifespan in certain tissues[25]. So far, however, it is still not clear whether the bystander effect is relevant for the accumulation of senescent cells in normal tissues *in vivo*.

Of note, proper tissue homeostasis is dependent on bidirectional communication between cells. Bidirectional communication allows cells to react to external damage in a more flexible way and so, it is not implausible that reciprocal bystander responses, possibly mediated by p53, may be establishing intercellular feedback loops responsible for augmenting or attenuating responses in both founder and bystander cells[148]. It remains unclear however how cell-intrinsic and cell-extrinsic pathways interact to determine cell fate.

1.5. SENESCENT CELLS *IN VIVO*

The discovery of cellular senescence was followed by speculation about possible physiological and pathological roles of the process *in vivo*. Owing to its ability to halt cell cycle progression and proliferation, senescence was proposed to be a tumor-suppressive mechanism and considered beneficial. Still, cellular senescence was associated with decrements in tissue renewal and function and, in this context, was considered deleterious. In fact, it is currently known the short-term induction of senescence has beneficial roles in tumor suppression and tissue repair while the long-term presence of those same cells can promote tumor development and age-related diseases[3,8]. Recent studies have also pointed out possible contributions of the senescence program to organismal development[62,63] and its impact in various diseases (Reviewed by[11]). Next, the main roles played by cellular senescence in context of tumor suppression and promotion, tissue repair, aging and organismal development will be discussed and the process will be analyzed in light of the evolutionary theory of antagonist pleiotropy.

1.5.1. TUMOR SUPPRESSION

Currently, it is clear cellular senescence prevents the proliferation of cells at risk for neoplastic transformation, thus suppressing development of cancer[8,18]. To form lethal tumors, cancer cells must expand their growth potential and be able to proliferate while expressing activated oncogenes[149], traits suppressed by the senescence program, making it an ideal mechanism to counter tumor formation. Moreover, senescence-inducing stimuli are potentially oncogenic and cancer cells usually acquire mutations (commonly affecting the p53 and p16-pRB pathways) allowing them to bypass senescence[6,54]. However, failure to undergo senescence is usually not enough for malignant transformation[6]. For instance, human fibroblasts expressing hTERT and unable to undergo replicative senescence do not display malignant properties[150].

In mouse models of PTEN deletion, biomarkers of cell senescence were abundant in preneoplastic lesions, suggesting a senescence response may be halting the progression of lesions into malignancy. In contrast, the same biomarkers were scarce in cancers that eventually developed from the same lesions[54]. Similar results were observed in human premalignant melanocytic lesions[151]. Still, it is unclear how tumors eventually emerge from premalignant lesions. In the mouse models of PTEN deletion, the inactivation of p53, with consequent disassembly of the senescence program lead to a striking acceleration in the development of malignant tumors[54], confirming that defects in the p53 (or p16-pRB) pathway(s) greatly increase organismal susceptibility to cancer. In addition, some tumor cells retain the ability to senesce after reactivation of p53, which is associated with tumor regression[123]. Combined, these studies clearly demonstrate cell senescence act as a potent tumor suppressor mechanism by imposing a cell-autonomous block to the proliferation of premalignant cells.

Cellular senescence suppresses malignant tumorigenesis mainly by promoting growth arrest but accumulating evidence show that certain SASP components, including IL-6, IL-8, IGFBP-7 (insulin-

like growth factor binding protein 7) and PAI-1 (plasminogen activator inhibitor 1) can help reinforce growth arrest in an autocrine manner[8,13,126].

1.5.2. TUMOR PROMOTION

Paradoxically, long-term presence of senescent cells within tissues can potentiate cancer formation[3,7,8] due to three main features of senescent cells: 1) inability to proliferate alone; 2) impaired cellular function and 3) negative impact on the local microenvironment[3]. These three features yield a detrimental impact on the tissues where senescent cells reside and can be responsible for impairment of tissue regeneration, decline of stem and progenitor cells potential to regenerate tissues and tissue dysfunction, which eventually compromises tissues' structure and function[3]. Accumulation of senescent cells in tissues with age creates a tissue microenvironment permissive for development and progression of cancer[8].

Studies with mouse xenograft experiments in which senescent cells are co-injected with premalignant epithelial cells have demonstrated the SASP can facilitate cellular proliferation and tumorigenesis in neighboring cells; in particular, through direct cell contact between the two types of cells[142]. At least in some cases, the effects of senescent cells can be attributed to secretion of MMPs[143]. Another prominent feature of the SASP is its ability to cause inflammation through secretion of inflammatory cytokines, contributing to cancer development since cancer is a pathology fueled by inflammation[13]. SASP factors can also promote epithelial-to-mesenchymal transition, a transition that enables transformed cells to migrate and invade tissues and is critical in the development of metastasis. This transition also seems to be dependent of inflammatory cytokines, in particular IL-6 and IL-8[152]. Further, senescent fibroblasts can also secrete VEGF, which also stimulates endothelial cell migration and invasion[12,122].

The effects of senescent cells within the tumor microenvironment are highly dependent on physiological context. In some cases, cells that senesce in response to chemotherapeutic agents can secrete factors that protect neighboring cells from the same chemotherapeutic agents[153] while, in other cases, SASP factors can be chemosensitizing, promoting the ablation of neighboring cells[132].

1.5.3. TISSUE REPAIR

Human and mouse tissues accumulate senescent cells chronically during aging. Cellular senescence is usually viewed as a promoter of tissue dysfunction during the aging process and its beneficial effects are often overlooked. When transiently present, particularly in the skin, senescent cells promote tissue repair and optimal wound healing through cell non-autonomous mechanisms[10]. Tissue repair is a complex process comprised by four distinct overlapping stages, each one promoted by soluble factors, some of which SASP factors[154]. A recent study showed the elimination of senescent cells in young mice bearing cutaneous wounds delayed wound closure but

this phenotype could be rescued after topical application of the SASP factor PDGF-AA (platelet-derived growth factor AA)[154].

Chronic wounds commonly present tissue fibrosis, characterized by excessive collagen deposition during tissue repair. Impairment of the senescent response during wound healing leads to fibrosis[13,155], suggesting limiting fibrosis is another important function of senescent cells[10,156]. In fact, several MMPs that comprise the SASP promote collagen degradation[120], thus maintaining tissue homeostasis during wound healing and contributing to optimal tissue repair. In this context, the senescence response, particularly the SASP, seems important in limiting the extent of fibrosis after tissue damage and in propagating a cellular-damage signal to neighboring cells to stimulate repair[3,13]. The attenuation of fibrosis can occur in various tissues in different pathological contexts[11], emphasizing the beneficial effects of senescence in certain diseases. In light of this, senescence is not just a failsafe mechanism, redundant to apoptosis, but a complex process, selected during evolution to promote tumor suppression and optimize tissue repair[12].

1.5.4. AGING

The idea that senescence may be on the genesis of organismal aging has been around for decades and, in recent years, has garnered increasing experimental support. Senescent cells have been shown to drive degenerative changes and have been implicated in several age-dependent pathologies. Senescent cells can disrupt normal tissue structures essential for normal tissue function, impairing tissue homeostasis[12]. Senescent cells increase *in vivo* with age, accumulating primarily but not exclusively in tissues composed by mitotic cells[39,40,105,157]. Accumulation of senescent cells in the organism not only contributes to the depletion of the pool of mitotically competent and functional cells within tissues but also alters the microenvironment, compromising tissue repair[158].

Cellular senescence may drive aging/age-related pathology mainly by three mechanisms. First, senescence of certain stem cells in adult organisms may be responsible for the age-related decline in tissue repair and regeneration. Corroborating this hypothesis, it has been observed that p16 accumulate in tissue stem and progenitor cell compartments in an age-dependent manner, limiting their regenerative capacity[159,13]. Second, the SASP might contribute to disruption of normal tissue structure and function thanks to secretion of extracellular-matrix-degrading enzymes, inflammatory cytokines and growth factors[115,13]. In particular, the potent pro-inflammatory component of the SASP may explain the low-level chronic inflammation observed in aging tissues. Third, the reprogramming of mitochondrial function and nutrient-sensing pathways can lead to metabolic failure[160]. These three mechanisms might, at least partly, explain the functional decline of several organs/tissues with increasing age and the development of several age-related diseases[161].

Evidence that senescent cells drive aging still remains mainly circumstantial. Nevertheless, accumulating evidence from transgenic mice models suggests senescent cells are causally implicated in age-related dysfunction[162,163]. In 2004, Maier *et al* developed a transgenic mouse

model that constutively expressed a truncated form of p53, which resulted in chronically elevated p53 activity[163]. Surprisingly, these mice displayed a shortened lifespan and premature aging, however without exactly phenocopying normal aging. *In vitro*, cells from these mice also underwent rapid senescence and, *in vivo*, tissues rapidly accumulated senescent cells[163]. More recently, Baker *et al* (2011)[162] designed a transgenic strategy for clearing senescent cells in mice. The model developed allowed specific elimination of p16-expressing cells after administration of a drug. The mouse model created, termed INK-ATTAC, was crossed with a progeroid mouse model (BubR1[H/H]) that exhibit a shortened lifespan and several age-related phenotypes. Surprisingly, the group observed that BubR1[H/H];INK-ATTAC mice did not live longer. Nonetheless, both life-long and late-life clearance of p16-expressing cells selectively delayed several age-related pathologies in tissues that accumulated those cells. This study provided the first direct evidence that senescence can drive degenerative age-related pathology. Clearance of p16-expressing senescent cells did not show apparent side-effects[162], suggesting clearance of senescent cells could represent a promising approach to anti-aging therapies. Of note, this study used a premature aging mouse model; further studies using "normal" aging models are still lacking.

Finally, although the studies here discussed, along with several others, provide evidences for a strong association between cellular senescence and aging phenotypes, other processes, including cell death and simply loss of functionality, certainly contribute to those same phenotypes[12].

1.5.5. ORGANISMAL DEVELOPMENT

The roles of cellular senescence have been mostly studied in contexts of cellular damage. Recently, however, the identification of senescent cells in a large number of embryonic structures and in some specialized normal adult cells has expanded the role of senescence to development and physiology[3,11]. Analysis of embryos from different vertebrate models revealed senescence occurs during development and it may be a conserved feature of embryonic development across vertebrates[11,62,63]. The exact reasons why the senescence program may be useful in embryonic development are still unknown. The SASP seems to have important roles in maintaining normal placental function since secretion of certain proteases and cytokines – both associated with senescent cells – can help maintain feto-placental homeostasis and regulate placental growth during pregnancy, respectively[164].

Senescent cells were identified at multiple embryonic structures, however without displaying DNA-damage markers, suggesting developmental senescence has distinctive features compared to damage-induced senescence. These cells also establish independently of p53 and p16 expression and are dependent, instead, on p21, which is regulated by the TGF-β/SMAD and PI3K/FOXO pathways[3,11]. Of note, although SA-βGal-positive cells have been identified in mice embryo structures, they did not display other markers of senescence[165]. Whether these cells display a somewhat distinct type of senescence or cannot be classified as senescent cells remains uncertain.

During embryonic development, failure to undergo senescence activates a compensatory apoptotic program[62,63], albeit not enough to prevent the development of some morphological defects that will affect adult animals[62]. This compensatory mechanism suggests a connection between senescence and apoptosis during development.

Finally, senescence also occurs in a physiologically programd manner in adult organisms. In particular, certain mammalian cells that undergo endoreduplication (which leads to polyploidy) also undergo senescence as part of their natural maturation programs[166]. Similarly, fusion of different cell types, including cancer cells, can also induce senescence (cell-cell fusion induced senescence; FIS). FIS might also play a physiological function in the placenta[167].

1.5.6. CELLULAR SENESCENCE AS A CASE OF ANTAGONISTIC PLEIOTROPY

It seems paradoxically that cellular senescence can act as a tumor suppressor mechanism and contribute to tissue repair and, at the same time, promote tumor development and aging. Still, the senescent phenotype has a temporal organization[12] [FIGURE 3], and so, albeit the induction of cell senescence can initially have beneficial effects, the long-term presence and accumulation of senescent cells within tissues, can have a detrimental impact.

Since senescent cells accumulate with age in different tissues[39,105,157], they can contribute to age-related declines in tissue function and promote age-related diseases. Thus, paradoxical effects of senescent cells can be explained by the theory of antagonistic pleiotropy, which states that aging phenotypes, including age-related diseases, are a consequence of the declining force of natural selection with age[168]. Most organisms have evolved in environments rich in fatal extrinsic hazards (predation, starvation, etc.); in these environments, aged individuals are rare and so, natural selection against processes with detrimental impact in late life is weak. Consequently, traits selected to maintain fitness during early life can have unselected deleterious effects during late life, after the organisms' reproductive period, thus escaping the force of natural selection. From this perspective, the senescence response may have evolved primarily as a tumor suppressor mechanism and a promoter of tissue repair. By contrast, some of the changes induced may be unselected consequences of the growth arrest[13,142], having a small impact on young organisms but becoming more prominent late in life, as senescent cells accumulate. With this in mind, the apparent redundancy between apoptosis and the secretory phenotype of senescent cells can be denied. Both processes act as tumor suppressive mechanisms but only the senescence response seems to have evolved to allow damaged cells to send a signal to the surrounding tissue, preparing it to repair[6,13].

1.6. AGING OF SKELETAL MUSCLE FIBERS AND SARCOPENIA

The world's population over 60 years is expected to double by 2050, with approximately 2 billion people aged 60 or older in the world[169]. This increase itself does not constitute a problem; however, aging is associated with an increased incidence of chronic health conditions and an increase prevalence of impairment and disability. In particular, musculoskeletal disorders, frailty and sarcopenia cause mobility limitations that reduce physical activity and promote the loss of functional independence[170,171]. Sarcopenia, a hallmark of aging in humans, is the age-related loss of skeletal muscle mass and function, resulting in muscle weakness, atrophy and impaired performance[172]. Due to this, sarcopenia is considered as an emerging threat by investigators and recent research has focused on possible interventions to slow down the development of sarcopenia in the elderly. However, a clear understanding of the cellular and molecular alterations associated with sarcopenia is still lacking, thus research in this field that could lead to the development of specific interventions and effective treatments is currently of high importance.

Currently, several cellular and molecular changes at the level of muscle fibers have been identified to contribute to muscle aging (Reviewed by[170]). In particular, there is an age-related decrease in muscle fibers' size and number that are reflected in a gradual loss of overall muscle mass, strength and power. Other factors, such as adipocyte infiltration[173], loss of mitochondrial content[174] and function and loss of satellite cells[175,176] also contribute to the age-related muscle function decline, the latter by impairing the regeneration machinery of skeletal muscle. Skeletal muscle homeostasis and regeneration are dependent on a population of Pax7-expressing, normally quiescent stem cells[177,178] that turn into a senescent-like state at geriatric age, resulting in the inhibition of the regenerative capacity of the muscle[179].

In contrast to muscle satellite cells, skeletal muscle fibers consist of fully differentiated post-mitotic cells, where classification of a senescent state is very difficult. While there are reports of accumulation of senescent cells in mitotic tissues with age *in vivo*[39,105,112,157], reports of accumulation of senescent cells in post-mitotic tissues such as the skeletal muscle are majorly inconclusive. Hampering this task, is the inexistence of specific biomarkers for cellular senescence and the shared common features between post-mitotic and senescent cells (e.g. general absence of proliferation markers; particular cell morphology), which makes the identification and quantification of senescent post-mitotic cells, in particular myofibres, a very difficult task. Due to these and other difficulties, exhaustive reports on the presence of senescent cells and their importance *per se* in different tissues of aging mammals still need to be done. An age-related increase in γ.H2A.X-positive foci was reported for different mitotic tissues, including both low- and high-turnover tissues such as the liver and small intestine, respectively, in mice[39] and the same was observed for 53BP1-positive foci in the skin of baboons[157]. In both studies and both animal models, double-strand DNA break foci did not appear to accumulate in skeletal muscle of aged individuals, maintaining consistent low numbers throughout the animal lifespan[39,157]. Moreover, only a low abundance of telomere damage was detected in skeletal muscle fibers, suggesting telomere-dysfunction induced senescence does not occur universally in tissues and, therefore, may not

contribute significantly for sarcopenia, unless when, possibly, affecting satellite cells[157,179]. These studies clearly show that different tissues undergo distinct pathways during aging, resulting in different types of tissue aging, some of them apparently more closely related to cellular senescence than others. Nonetheless, an exhaustive evaluation of important features associated with cellular senescence in skeletal muscle fibers of elderly animal models, that will give a better insight on the intrinsic aging process of myofibers, is still lacking.

1.7. AIMS OF THE PROJECT

As previously referred, it was recently observed that replicatively senescent fibroblasts were capable of inducing a persistent DDR as bystander effect in surrounding young fibroblasts when co-cultured *in vitro*, via gap junction-mediated cell-cell contact[82]. Other studies also demonstrated the role of ROS-mediated processes[82,146,147] and secreted soluble factors released to the microenvironment[126,145,146] in mediating a bystander effect. Together, these results highlight the high variability of scenarios promoting a bystander effect, suggesting a cell-specific mechanism. Even though evidences that senescent cells lead to aging of tissues are still somewhat circumstantial, the bystander effect may contribute to the age-dependent increase in senescent cell frequency observed in tissues *in vivo*. Still, there is not concrete proof of the induction of senescence through a bystander effect or of its overall relevance in normal, non-tumorigenic tissues *in vivo*.

As discussed earlier, cellular senescence is currently viewed as a dynamic phenotypic state generated and maintained by stable, self-sustainable feedback loops, driven by DDR[76], which can be independent from the onset of proliferation arrest[40,76]. In light of this, the use of postmitotic tissues such as skeletal muscle can prove useful in studies assessing the effect of the senescent bystander effect in tissue microenvironment and its contribute to the increase in senescent cell frequency. Thus, we hypothesize that senescent cells are capable of inducing persistent DNA damage and DDR in skeletal muscle bystander cells and *in vivo* contributing to skeletal muscle fibre ageing by inducing senescence-like features similar to those observed in other postmitotic cells. To confirm this hypothesis, senescent fibroblasts will be xenotransplanted into skeletal muscle of immunodeficient mice and the expression of senescence markers in muscle fibers adjacent to and further away from transplanted cells will be compared. To use the most sensitive markers, a panel of proposed senescence markers will first be validated by comparing their expression in skeletal muscles from young and old mice.

CHAPTER 2. MATERIALS AND METHODS

2.1. Biological and Chemical Material

PRODUCT NAME	COMPANY	CATALOG NUMBER
(3-AMINOPROPYL)TRIETHOXYSILANE (APES)	Sigma-Aldrich	A3648
ACETONE	VWR	20065.327
AMMONIUM HYDROXIDE	VWR	83870.260
AVIDIN	Vector Laboratories	SP-2001
BIOTIN	Vector Laboratories	SP-2001
BLOCKING REAGENT	Sigma-Aldrich	11096176001
BOVINE SERUM ALBUMIN (BSA)	Sigma-Aldrich	A1470
DEOXYNUCLEOTIDES (DNTPS) MIX 10MM	Thermo-Scientific	R0192
DPX	Thermo-Scientific	UN1866
DULBECCO'S PHOSPHATE BUFFER SALINE (PBS)	Sigma-Aldrich	D5652
EOSIN Y	Sigma-Aldrich	HT110316
ETHANOL	Fisher Scientific	64-17-5
ETHYLENE GLYCOL	Sigma-Aldrich	E9129
FLUORESCEIN AVIDIN DCS	Vector Laboratories	A-2011
FORMAMIDE (DEIONIZED)	Amresco	0606 75-12-7
GELATIN FROM COLD WATER FISH SKIN	Sigma-Aldrich	G7765
HEMATOXYLIN	Sigma-Aldrich	H3136
HISTO-CLEAR (D-LIMONENE)	Fisher Scientific	12358637
ISOPENTANE	Fisher Scientific	2011428
NORMAL GOAT SERUM BLOCKING SOLUTION	Vector Laboratories	s-1000
NORMAL HORSE SERUM BLOCKING SOLUTION	Vector Laboratories	s-2000
NUCLEAR FAST RED (NFR)	Sigma-Aldrich	60700
PARAFORMALDEHYDE (PFA)	Sigma-Aldrich	158127
PNA PROBE	PNA Bio	F1002
PROLONG DIAMOND MOUNTING MEDIA WITH DAPI	Thermo-Scientific	P36962
PROLONG GOLD MOUNTING MEDIA	Thermo-Scientific	P36934
PROLONG GOLD MOUNTING MEDIA WITH DAPI	Thermo-Scientific	P36935
SODIUM CHLORIDE	Sigma-Aldrich	S9625
SODIUM CITRATE TRIBASIC DIHYDRATE	Sigma-Aldrich	S4641
SUDAN BLACK B (SBB)	Sigma-Aldrich	199664
TRITON X-100	GE Healthcare	17-1315-01
TWEEN®-20	Sigma-Aldrich	P1379

2.2. Cell Culture

Primary human fibroblasts MRC5 were cultured at 5% CO_2, in ambient oxygen in DMEM supplemented with 10% foetal calf serum, 100 U/ml penicillin, 100 mg/ml streptomycin and 2mM L-Glutamine media. To generate MRC5-GFP$^+$Luc$^+$, early passage of cells was transfected with a pSLIEW lentiviral vector (kind gift from Dr. Helen Blair), overexpressing enhanced green fluorescent protein (EGFP) and Luciferase (Luc). To assess efficiency of transfection, the intensity of GFP fluorescence and the number of GFP-positive cells were analyzed. To evaluate efficiency of cells to luminesce, *in vitro* luciferase assay was performed on cells in a range of dillutions of cell suspension

from 150 cell/well to $2X10^4$ cell/well in 96-well plate using plate reader. To generate replicatively senescent cells, MRC5-GFP$^+$Luc$^+$ cells were cultured under normal conditions until cells reached population doubling rate below 0.1 per week.

2.3. ANIMALS

All animal experiments were carried out in compliance with the Home Office regulations and FELASA guidelines. Immuno-deficient mice were purchased from Charles River (UK breeding facility) or from locally maintained colony (8 and 32 months old mice) at CBC, Newcastle University. Upon arrival, mice were housed under 12 hours day/night cycle, in individually ventilated cages. We injected adult, 4- to 6-month-old, NSG male mice (n=6) with 50 µl of $1,5X10^6$ cell/ml suspension of senescent MRC5-GFP$^+$Luc$^+$ cells sub-cutaneously in right flank and intra-muscular in right hind limb. Control mice (n=5) were injected with the same amount of proliferation-competent MRC5-GFP$^+$Luc$^+$ cells. Procedures were performed under general inhalational anaesthesia followed by administration of analgesic to provide pain relief after the intra-muscular injection.

To verify localization of injected cells, mice were subjected to *in vivo* imaging 24 hours after injection of the cells using IVIS Spectrum system. To extend the length of exposure of tissues to replicatively senescent cells, injections were repeated two more times in weekly intervals and cells were followed by *in vivo* imaging bi-weekly during this period. Five weeks after the first injection, the site of injected cells was marked based on the results of the last *in vivo* imaging. Mice were euthanized, and skin and muscle tissues from injected and non-injected sites were collected and cryo-preserved.

2.4. TISSUE PROCESSING

Following dissection, gastrocnemius and biceps femoris muscles of both injected and non-injected limbs were placed into isopentane, cooled with liquid nitrogen, for approximately 30 seconds until frozen. Specimens were stored at -70ºC until sectioning. Tissues were sectioned into 10µm sections in a Leica CM1950 clinical cryostat (Leica Biosystems) between -18ºC and -20ºC and collected to 4% (3-Aminopropyl)Triethoxysilane (APES)-coated microscopy slides. Injected tissues were fully sectioned, following a repeating pattern of collection and discard of sections [FIG 4]. In short, each collected section was interspersed between two discarded sections. Each unit of the collection pattern corresponded to 160µm of tissue and consisted of 8 collected sections distributed through 4 microscopy slides, the first two (Slides A and B) containing one section each and the last two (Slides C and D) containing three sections each. Following sectioning, slides containing muscle cryosections were again stored at -70ºC until analysis.
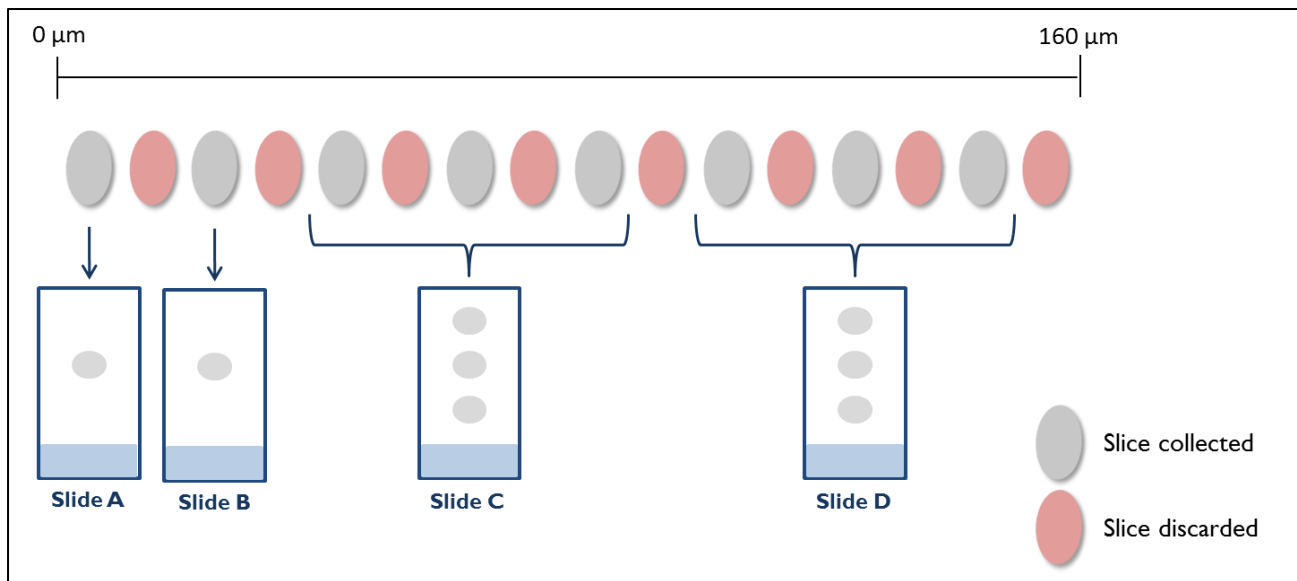
FIGURE 4. Schematic representation of the collection pattern of sections from injected tissues.

2.5. *In situ* Luciferase Assay

Slides were placed in a FujiLAS4000 chemoluminescent chamber (GE Healthcare Life Sciences; 28-9558-10). One slide, containing one cryosection, was analyzed for each 160μm distance (slide A of each unit of the section collection pattern). After the slides were placed in the chamber, 10-20μL (depending on section size) of a 0.1% dNTPs and 0.1% D-Luciferin solution in 1X-PBS were applied to each section and the luminescent signal was collected for 3 min. Immediately after, tissue sections were fixed for 10 min in 4% paraformaldehyde (PFA) in PBS, washed 2 times for 5 min with 1X-PBS and mounted with Prolong Gold/Diamond mounting media incorporated with DAPI. Slides were left mounting for at least 24 hours before being screened for Native GFP-positive cells.

2.6. Immunofluorescence

Gastrocnemius and biceps femoris muscle cryosections were taken from -70ºC storage and left at room temperature for 5 min. Next, sections were fixed in 4% PFA in PBS for 10 min, washed 2 times for 5 min with 1X-TBS and permeabilized with 0.1% Triton X-100 in 1X-PBS for 10 min. To block non-specific staining, tissues were incubated with 1% BSA and 1% Gelatin in TBS at room temperature for at least 1 hour. Sections were then incubated with primary antibody diluted in blocking solution and left overnight at 4ºC in a humidified chamber. The following primary antibodies and dilutions were used: Anti-Lamin B1 polyclonal antibody (rabbit; ab16048; 1:1000 dilution), anti-HMGB1 polyclonal antibody (rabbit; ab18256; 1:500 dilution) and anti-p21 polyclonal antibody (rabbit; ab7960; 1:250 dilution). After that time, sections were washed 3 times for 5 min with 1X-TBS and incubated with an Anti-rabbit IgG, Alexa Fluor® 594 conjugated secondary polyclonal antibody (goat; A-11037; 1:1000 dilution) diluted in blocking solution for 1 hour at room temperature. After washing sections again 3 times for 5 min, sections were mounted with Prolong Gold/Diamond mounting media with DAPI and allowed to mount for 12-24 hours in the dark.

33

2.7. Hematoxylin & Eosin Staining

Gastrocnemius and biceps femoris muscle cryosections were taken from -70ºC storage and left at room temperature for 5 min. Next, sections were fixed in 4% PFA in PBS for 5 min and washed 2 times for 5 min with 1X-TBS. Tissues were stained in Hematoxylin for 2 min and washed in water 2 times for 1 min, in 1% acid alcohol for 5 seconds, again in water for 1 min, in ammonia water for 20 seconds and finally, in water for 1 min. Tissues were then counterstained with Eosin Y for 30 seconds and washed several times in water until no more staining was running from the tissue. To dehydrate tissues, slides were incubated in 95% and 100% ethanol, 2 times for 1 min in each solution. Finally, slides were incubated in Histo-Clear clearing agent 2 times for 5 min, drained in tissue paper and mounted with DPX mounting media.

2.8. Sudan Black B Staining

Preparation of Sudan Black B solution and staining procedure were based on[180,181], with some modifications. In short, SBB powder was dissolved in 100% in Ethylene Glycol (7 mg/mL), covered with parafilm, in order to avoid evaporation, and stirred overnight. After, the solution was filtered through filter paper and through a Polyethersulfone syringe filter (30 mm membrane diameter, 0.22μm pore size) and stored in an airtight container.

For the staining procedure, OCT-frozen muscle cryosections mounted onto 4% APES-coated microscopy slides were left at room temperature for 5 min, fixed in 1% PFA in PBS for 5 min and then washed three times for 1 min with deionized water. Next, sections were incubated in 100% ethylene glycol for 5 min. After that, two/three drops of SBB solution were dropped on a clean glass slide and, in order to avoid SBB precipitation, the slide containing the muscle cryosections was placed, facing down, in the glass slide, with the cryosections in direct contact with the drops of SBB solution and left facing down for 3 hours at room temperature. After that period, the coverslip was carefully lifted and the excess SBB staining was removed with 2-3 quick rinses with deionized water. Tissues were then incubated for 3 min in 80% ethylene glycol, followed by several quick rinses with deionized water. For the evaluation of the frequency of lipofuscin-positive skeletal muscle fibers, cryosections were then counterstained with Nuclear Fast Red for 10 min, rinsed 2-3 times with TBS and mounted in Prolong Gold mounting media. Tissues were left to mount for 12 to 24 hours and observed with a Nikon E800 wide field upright microscope. For the assessment of the accumulation of lipofuscin-positive fibers around sites of injection, cryosections were not counterstained. Instead, they were directly mounted in Prolong Gold mounting media incorporated with DAPI and observed with a Leica DM5500 wide field fluorescence microscope following a mounting period of 12 to 24 hours. In both cases, SBB staining was considered positive when fibers displayed a clear darker coloration than the rest of the fibers in the section and/or presented small, dark granules dispersed throughout the entire fiber.

2.9. Immuno-FISH (γH2A.X-Telomere FISH) Staining

Staining and *in situ* hybridization procedures were performed mainly as described by Hewitt et al 2012[38]. Muscle cryosections were removed from storage and immediately fixed with 2% PFA in PBS for 20 min in a shaker, followed by 2 washes with PBS for 15 min each. Next, sections were incubated with 70% ethanol, chilled to -20ºC, for 20 min, washed with PBS 3 times for 10 min each and blocked with a 8% BSA in PBS-TT solution for 1 hour at room temperature in a humidified chamber. Afterwards, sections were washed once, for 5 min, with PBS-TT, blocked with Avidin and then Biotin, for 15 min each and washed for 5 min with PBS. After removing excess buffer around the tissue with soft tissue paper, sections were incubated overnight at 4ºC with 100µL of primary polyclonal anti-phospho-histone H2A.X antibody (rabbit; cs9718S; 1:250 dilution in 1% BSA in PBS). Posteriorly, sections were washed 3 times for 5 min each with PBS-TT and incubated with 100µL of biotinylated anti-rabbit secondary antibody (VectaShield ZA0520; 1:250 dilution in 1% BSA in PBS) for 1 hour, in the dark and at room temperature. Following, sections were again washed 3 times for 5 min each with PBS-TT, incubated for 20 min with DSC-Fluorescin (1:500 dilution in PBS), washed 2 times with PBS-TT and 2 times with PBS, for 5 min each. Tissues were then crosslinked with 4% (wt/vol) PFA in PBS for 20 min, washed 3 times with PBS for 5 min each, dehydrated gradually with 70%, 90% and 100% ethanol solutions, chilled to -20ºC, for 3 min each and allowed to air dry. Afterwards, sections were denatured for 10 min at 80ºC in 10µL hybridization mix (2.5µl 1M Tris pH 7.2, 21.4µl Magnesium chloride buffer, 175µl De-ionised Formamide, 12.5µl Blocking Buffer (1:9 Roche Blocking reagent in autoclaved malic acid and 33.6µl deionized H_2O)), containing 1µl Cy-3-labelled telomere specific (CCCTAA)[3] peptide nucleic acid (PNA) probe and hybridized in a humidified chamber for 2 hours in the dark at room temperature. Posteriorly, sections were washed once with a 70% formamide/2X-SSC solution (300 mM NaCl, 30 mM Sodium Citrate), 2 times with 2X-SSC solution and once with PBS for 10 min each. Finally, tissues were mounted with Prolong Gold mounting media incorporated with DAPI and allowed to mount overnight in the dark at 4ºC until imaging.

2.10. Image Acquisition and Analysis

2.10.1. Analysis of Biomarkers

For immunofluorescence pictures, digital images were acquired using a Zeiss Axio Observer microscope equipped with a Yokogawa CSUX1 spinning disk head and a QuantEM camera; EC plan Neofluar (40X; Numerical Aperture (N.A.) 1.3) and Plan Apochromat (63X; N.A. 101.4) objectives were used. Z stacking was performed, with 10 (when 40X objective was used) or 15 (when 63X objective was used) optical slices obtained per image. Acquisition was performed using Zeiss' Axiovision software package, with optimal exposure settings established for each biomarker evaluated. 8-12 pictures were taken per tissue. For SBB- and H&E-stained muscle sections, digital images were acquired using a Nikon E800 wide field upright microscope; 10x (N.A. 0.3) and 20x (N.A. 0.5) objectives were used. Image acquisition was performed using LASX software package. For

immuno-FISH stained sections, digital images were acquired using a DMi8 fluorescence inverted microscope; 100x (N.A. 1.44) objectives were used. In depth Z stacking was used, with approximately 40 optical slices obtained per image. A minimum of 50 nuclei were imaged per tissue. Image acquisition was performed using LASX software package. Images were composed and edited with ImageJ image analysis free public software (https://imagej.nih.gov/ij/), optimal brightness and contrast adjustments were applied to the whole image; parameters for image analysis were quantified using the same software.

To assess myofibre cross-section area, individual fibres were manually outlined and their cross-sectional area (CSA) was measured. To quantify centrally-nucleated (CNF) and SBB-positive fibres in muscle sections, it was counted the number of positive fibres per field, in 8-14 fields for each animal of both age groups.

For quantification of HMGB1- and p21-positive nuclei, first a nuclear mask was created using the DAPI channel of the acquired image. Touching nuclei were separated and the particles identified in the mask were used to measure the mean nuclear fluorescence intensity in the channel of the protein being analyzed. To classify nuclei as positive/negative, a threshold (cytoplasm's fluorescence intensity + 2X (standard deviation of cytoplasm's fluorescence intensity)) was calculated for each image taken and applied to all measured nuclei. For the Lamin B1 analysis, a mask of only the peripheral area of the nuclei was created for the DAPI channel using the Image Calculator function in ImageJ software and inverted. This mask was used to measure the mean nuclear fluorescence intensity in the LB1 channel.

To quantify γH2A.X-positive nuclei, nuclei with distinct γH2A.X foci or an overall high intensity signal throughout the entire/large part of their area were manually counted. Nuclei were considered TAF-positive when containing at least one telomere co-localizing with a distinct γH2A.X foci in unstacked tilescans.

2.10.2. *IN SITU* LUCIFERASE DETECTION AND NATIVE GFP SCREENING

During the *in situ* luciferase assays, for every slide analyzed, two images were collected in the chemoluminescent chamber (FujiLAS4000): one image of the luminescent signal emitted by the tissue and a simple photography of the slide containing the tissue. These two images were stacked together with ImageJ software, creating an image with two different channels. Next, the tissue section was delineated in the photography channel and the signal intensity in that exact region was measured in the "luminescent signal" channel. The signal was considered positive when its value was above the established threshold (background signal + standard deviation of background signal). Tissue sections with positive signal were imaged with DMi8 fluorescence inverted microscope, using 10x (N.A 0.4) objectives. Tilescans of the entire tissue sections were acquired and used to identify areas containing injected cells.

2.10.3. ANALYSIS OF BIOMARKERS AROUND SITES OF INJECTION

To assess the effects of xenotransplanted cells in adjacent skeletal muscle fibers, a cutoff value of 100μm was established to separate adjacent from further away fibers. For the analysis of biomarkers expression in immunofluorescence images, 3 groups were considered: 1) injected GFP$^+$ cells, 2) cells between 0-100μm distance and 3) cells further away from the injection site. For the analysis of p21 and HMGB1 expression, cells in the 0-100μm distance were further divided in function of the quantity of adjacent injected cells. Thus, cells in 0-100μm distance of 1/2 isolated injected cells were separated from cells in 0-100μm distance of more than 2 injected cells. For analysis of SBB stained sections only groups 2 and 3 were considered.

For immunofluorescence pictures, digital images were acquired using a Leica SP8 confocal and digital light sheet microscope; 63 x (N.A. 1.4) and 40x (N.A. 0.85) objectives were used. Images were acquired using the LASX software package. LASX software Multipoint x,y with tiling (2D) image mode was used to obtain two tilescans per analyzed section: one containing areas of injection and fibers in the immediate surroundings and another, from a different region of the tissue, with no injected cells in the surroundings. Quantification of p21- and HMGB1-positive nuclei and measurement of LB1 fluorescence intensity were performed as described in Section 2.10.1. Nuclei were classified as positive for p21 and HMGB1 when their mean fluorescence intensity was higher than the average mean fluorescence intensity of all the nuclei in the tilescan (nuclei from GFP-Positive cells were excluded from this measurement).

For SBB-stained sections, digital images were acquired using a Leica DM5500 wide field fluorescence microscope; 10x (N.A. 0.3) and 5x (N.A. 0.15) objectives were used. DAPI and GFP filters were used in combination with bright field monochrome imaging, resulting in images with a bright field channel combined with 2 fluorescence channels. Classification of fibers as SBB-positive was performed as described in Section 2.8. Measurement of fibers' CSA and quantification of CNFs were performed as described in Section 2.10.1.

2.11. STATISTICAL ANALYSIS

For the evaluation of biomarkers, no specific blinding method was used; for the assessment of a bystander effect, mice were given number codes and experiments in injected tissues were conducted blindly, without knowing whether the injected cells were proliferative or senescent. All experiments were repeated at least with three biological replicates; the statistical test applied to compare the data is described in each corresponding figure legend. Unless stated otherwise, all data is normally distributed and presented in bar graphs as mean ± standard deviation (SD). For the Pearson's product moment correlation analysis, 5 mice were considered as only tissues from those 5 mice were tested for all biomarkers evaluated.

SigmaPlot 12.5 software (©Systat Software Inc.) was used for all statistical analyses. Student's t-test, in cases when a normal distribution was assumed, and Mann-Whitney U-test, in cases where a

normal distribution could not be assumed, were used to perform a statistical analysis of the results when comparing only two groups. Two-way ANOVA followed by Holm-Sidak multiple comparisons test was also used, to compare the cross-sectional area of CNFs and non-CNFs in young and old tissues. One-way ANOVA followed by Holm-Sidak multiple comparisons test was used to compare the expression of biomarkers around sites on injection. Statistical significance was considered for P values below 0.05.

2.12. QUANTITATIVE ANALYSIS OF CLUSTER PROBABILITY

Quantitative analysis of cluster probability of Sudan Black B-positive cells was mainly performed as described by Nelson et al. 2012[82]. 10 μm muscle cryosections from young and old mice (3 animals per age group) were stained for Lipofuscin using the Sudan Black B staining technique above described (Section 2.7). 8-16 images were taken per section with a Nikon E800 wide field upright microscope; 10x (N.A. 0.3) and 20x (N.A. 0.5) objectives were used. For each image, the total number of cells (N) and the total number of SBB-positive cells (K) were counted, as well as the total number of neighbour cells (n_i) and the number of SBB-positive cells (k_i) for each of the positive cells (i = 1...K) in the image. Cells were considered positive using the same criteria stated in Section 2.8. Fibres were only considered as neighbours when immediately in contact with a positive cell.

To test the probability of a positive cell in the tissue having one or more positive neighbour cells and test whether positive cells were clustered to a larger degree than expected by chance, a hyper-geometric p-value (p_i) for over-representation was calculated for each neighbourhood of each positive cell. All probability values were then corrected for multiple comparisons by false discovery rate (FDR) control, obtaining q-values (q_i=1...K). Finally, the fraction (F) of positive cells having more positive neighbour cells than expected by chance, according to the overall proportion of positive cells was estimated by the following equation,

$$F = \frac{Q/_{(Q<0.05)}}{K}$$

where Q stands for the total number of q_i values calculated and Q<0.05 stands for the number of q_i values below 0.05. This analysis was performed in R free public software (http://cran.r-project.org/; ©2016 The R Foundation).

CHAPTER 3. RESULTS

3.1. Biomarkers of Senescence and Sarcopenia in Mice Skeletal Muscle

As discussed previously, to use the most sensitive markers to analyze the effects of xenotransplanted cells in surrounding skeletal muscle fibers, a panel of proposed senescence markers was first validated by comparing their expression in skeletal muscles from young and old mice. Due to the inexistence of specific biomarkers for cellular senescence and some shared common features between post-mitotic and senescent cells, the identification and quantification of senescent myofibres becomes a difficult task. This analysis will provide standard values, for normal young and old tissues, of important parameters of muscle morphology and proposed biomarkers, which will later on be evaluated in injected tissues.

3.1.1. Muscle Morphology Analysis

Hematoxylin/Eosin staining is a widely used technique for visualization of tissue morphology and evaluation of signs of sarcopenia in muscle tissue. This staining allowed quantification of centrally-nucleated fibers (CNFs) and measurement of fiber cross-sectional area (CSA), two important parameters assessed to evaluate age-related tissue dysfunction and sarcopenia[179,182]. As expected, older tissues presented a significant ($p<0.05$) higher frequency of centrally-nucleated fibers (19.14% ±7.60 of total fibers) when compared to younger tissues (3.49% ±2.65 of total fibers) [FIG 5.A, B], while as well presenting fibers with significant ($p<0.001$) smaller cross-section area (2384.52 μm^2), in comparison to younger tissues (4667.59 μm^2) [FIG 5.A, C]. This difference corresponds almost to a 50% decrease in fiber cross-sectional area with age. Frequency distribution of fibers according to their cross-sectional area [FIG 5.D] also shows a narrower distribution of mostly smaller fibers in older tissues while, in younger tissues, fibers are distributed through a wider range, that include fibers of bigger size. For the evaluation of fibers' CSA, values from all measured fibers were used, as the data was not normally distributed.

Aside from the increase in older tissues of both centrally-nucleated fibers and fibers with smaller cross-sectional area, the data obtained does not seem to indicate a connection between these two features, in the sense that the fibers with reduced size are the ones with also centrally-nucleated nuclei. In fact, the two parameters appear independent of each other, as there is no significant difference in the cross-section area of fibers with and without central nuclei in both age groups (in the Young group, 4322.42±944.16μm^2 and 4318.19±536.46μm^2 for centrally-nucleated fibers and non-centrally-nucleated fibers respectively; in the Old group, 2507.50±159.22μm^2 and 2159.59±161.21μm^2 for centrally-nucleated fibers and non-centrally-nucleated fibers respectively) [FIG 6]. The only significant differences detected were in function of age ($p<0.01$) [FIG 6], as previously verified [FIG 5.C].
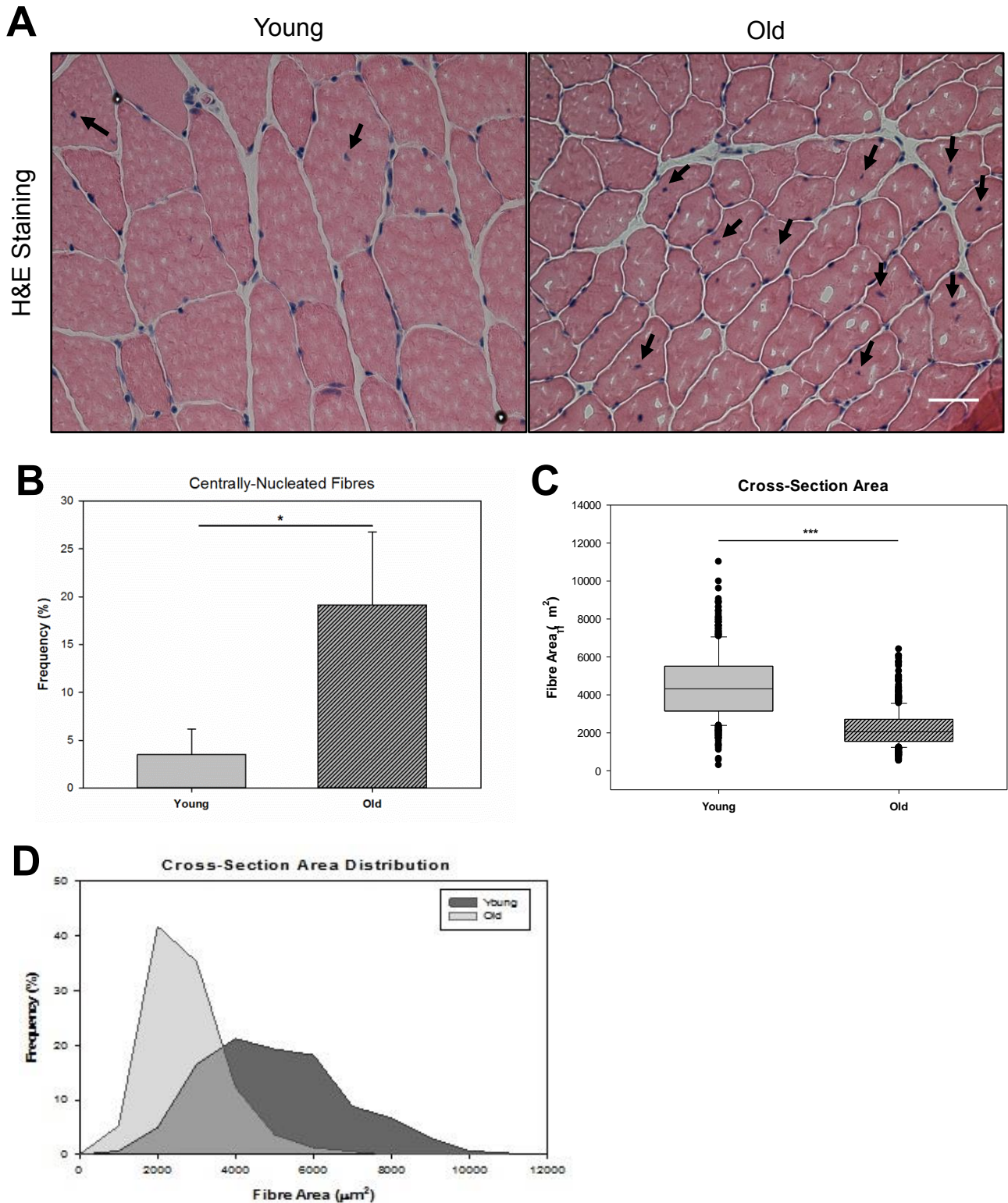
FIGURE 5. MUSCLES FROM OLD MICE DISPLAY SIGNS OF SARCOPENIA. A, Representative images of hematoxylin (blue) & Eosin (red) (H&E) stained cryosections of gastrocnemius muscle from wild-type mice with different ages: Young (8 months old) and Old (31.5, 32 and 32.5 months old. Arrows indicate centrally-nucleated myofibres. **B**, Frequency of centrally-nucleated fibres in cryosections represented by A (3 animals per group). Whiskers indicate Standard Deviation. **C**, Quantification of myofibre cross-section area. Box plots indicate median (line), upper and lower quartiles (boxes), upper and lower centiles (whiskers) and outliers (dots). **D**, Percentage frequency distribution of myofibres according to fibre cross-section area. Scale bar, 50 µm. Student's t-test (B) and Mann-Whitney U-test (C) were used to analyse the data. Significant differences between young and old tissues are represented in each graph with *, p=<0.05 and ***, p= <0.001.
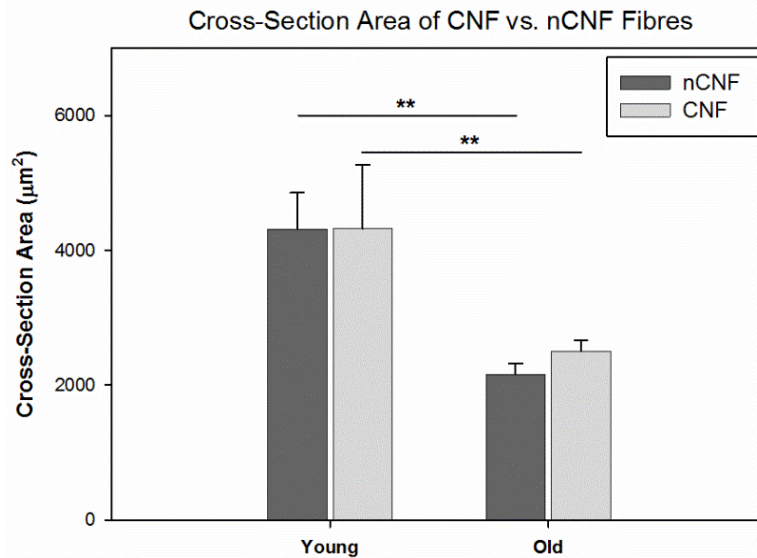
FIGURE 6. Quantification of cross-section area of both centrally-nucleated (CNF) and non-centrally-nucleated (nCNF) myofibres from two age groups: Young (8 months old) and Old (31.5, 32 and 32.5 months old). 3 animals per group. Two-way ANOVA coupled to Holm-Sidak multiple comparisons test was used to analyse the data. Significant differences between young and old tissues are represented with **, p=<0.01.

3.1.2. SENESCENCE AND DNA DAMAGE BIOMARKERS

Recently, the histochemical Sudan Black B (SBB) staining was validated as a reliable approach to detect senescent cells, independently of sample preparation and trigger of senescence[180]. SBB stains lipofuscin, an aggregate of oxidized proteins, lipids and metals known for a long time to accumulate with age, especially in post-mitotic cells[183,184] and demonstrated to co-localize with SA-βGal in senescent cells both *in vitro* and *in vivo*, justifying its use as a biomarker of cellular senescence[180]. To determine the frequency of SBB/Lipofuscin-positive skeletal muscle fibers from both young and old, muscle cryosections from both age groups were stained with SBB [FIG 7.A]. As expected, older tissues presented a significant (p<0.05) higher frequency of SBB-positive fibers (16.23±8.72% of total fibers) when compared to younger tissues (2.80±3.83% of total fibers) [FIG 7.A, B]. Moreover, in tissues from the Old group, fibers stained positive for SBB were significantly smaller than their negative counterparts (with average cross-sectional areas of 1572.06±659.57µm^2 and 2721.42±1066.53µm^2, respectively) [FIG 8.A]. In this case, the frequency distribution of fibers according to their cross-sectional area [FIG 8.B] displays a clear shift between the two groups of cells; SBB-positive fibers having mainly smaller cross-sectional areas than SBB-negative fibers. Even though the fibers that stained positive for SBB may be responsible for lowering the average cross-sectional area of fibers from older tissues, is important to note that the average cross-sectional area of the SBB-negative fibers is as well smaller than the one from younger tissues [FIG 5.C].
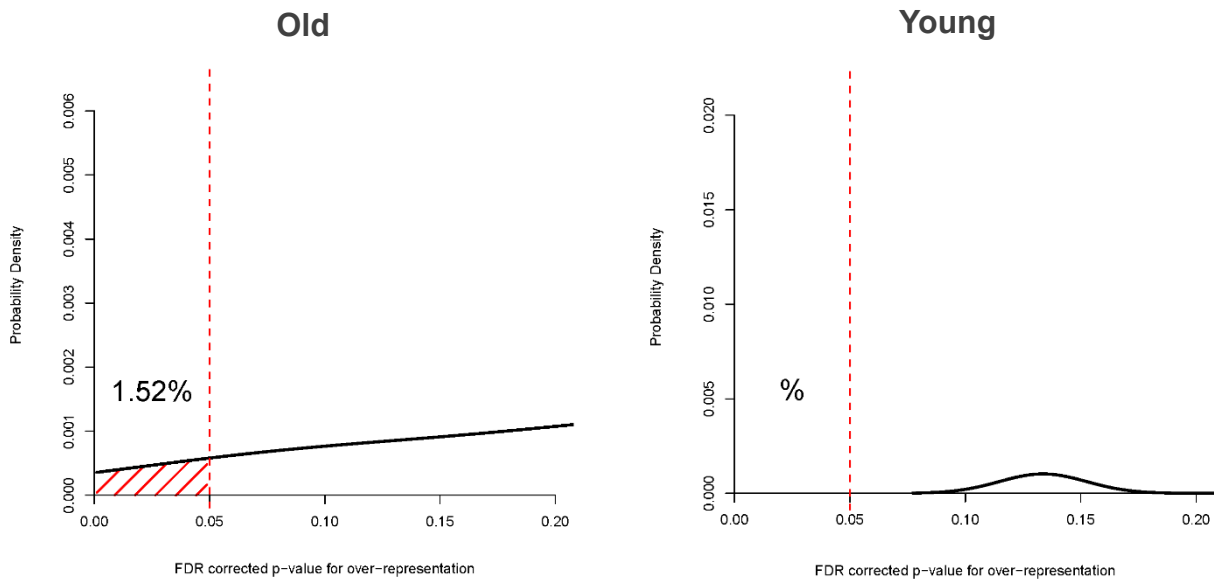
FIGURE 7. MUSCLES FROM OLD MICE HAVE HIGHER FREQUENCY OF LIPOFUSCIN-POSITIVE MYOFIBERS. **A**, representative images of Sudan Black B (SBB) and Nuclear Fast Red (NFR) double stained cryosections of gastrocnemius muscle from wild-type mice from two different age groups: Young (8 months old) and Old (31.5, 32 and 32.5 months old). 3 animals per group. Arrows indicate lipofuscin-positive myofibers. **B**, Frequency of SBB-positive fibers in cryosections represented by a. Scale bar, 50 µm. Student's t-test was used to analyse the data. Significant differences between young and old tissues are represented in the graph with *, one-tailed p-value <0.05.

FIGURE 8. SBB-POSITIVE MYOFIBERS DISPLAY SMALLER CROSS-SECTIONAL AREA IN OLD TISSUES. **A**, Quantification of cross-sectional area of both SBB-positive and SBB-negative myofibers from old mice. 3 animals per group. **B**, Percentage frequency distribution of SBB-positive and SBB-negative myofibers from old mice according to fibre cross-section area. Student's t-test was used to analyse the data. Significant differences between young and old tissues are represented in each graph with *, One-tailed p-value <0.05.

FIGURE 9. QUANTITATIVE ANALYSIS OF CLUSTER PROBABILITY OF SBB-POSITIVE CELLS. Probability density plots for the significance of over-representation of SBB-positive myofibres in contact with another positive cell in muscles from young and old mice (old group: 3 animals; young group: 1 animal). The red area indicates the percentage of all cells that have significantly (p ≤ 0.05) more positive neighbours than expected by chance, given the frequency of positive cells in the samples.

To obtain the probability value of finding a SBB-positive cell clustered with others and to determine if, overall, SBB-positive fibers tended to be clustered within the tissues analyzed, a quantitative analysis of cluster probability (Section 2.12) was performed. Given the frequency of SBB-positive cells in the tissue samples, in old tissues, 1.52% of all cells had significantly (p ≤ 0.05) more positive neighbor cells than what it was expected by chance, indicating possible clustering. In the only young tissue with a significant amount of SBB-positive cells, the value of cells with more positive neighbor cells than expected was 0%. While the percentage of clustered cells in old tissues is very low to appear impactful, the frequency of SBB-positive cells in those tissues is only 16.23±8.72% of total fibers [FIG 7.B]. With this in consideration, the clustered cells in old tissues account for approximately 10% of all SBB-positive cells in the samples.

Lamin B1 loss, another recently validated biomarker of cellular senescence[116] is believed to cause alterations in gene expression and in the chromatin landscape[185]. LB1 loss affects nuclear lamina organization and is probably strongly associated with some morphological changes associated with cellular senescence, in particular, enlarged and irregular nuclei and reorganized chromatin[68,116,117]. Trying to assess differences in the LB1 content in nuclei from myofibers of old and young tissues, tissue sections were incubated with an anti-LB1 primary antibody and imaged as described (Sections 2.6 and 2.10.1). As predicted, in myofibers from older tissues, the mean nuclear LB1 fluorescence intensity was reduced significantly (p<0.05) [FIG 10.A, B]. This reduction consisted in an approximately 20% decrease in mean nuclear LB1 intensity. The frequency distribution of the total nuclei analyzed also exhibits relevant differences between young and old tissues [FIG 10.C]. Young tissues were shown to include, somewhat consistently and with approximately the same

frequencies, nuclei with both lower and higher intensity of LB1. On the other hand, older tissues tend to accumulate nuclei with lower LB1 intensity.
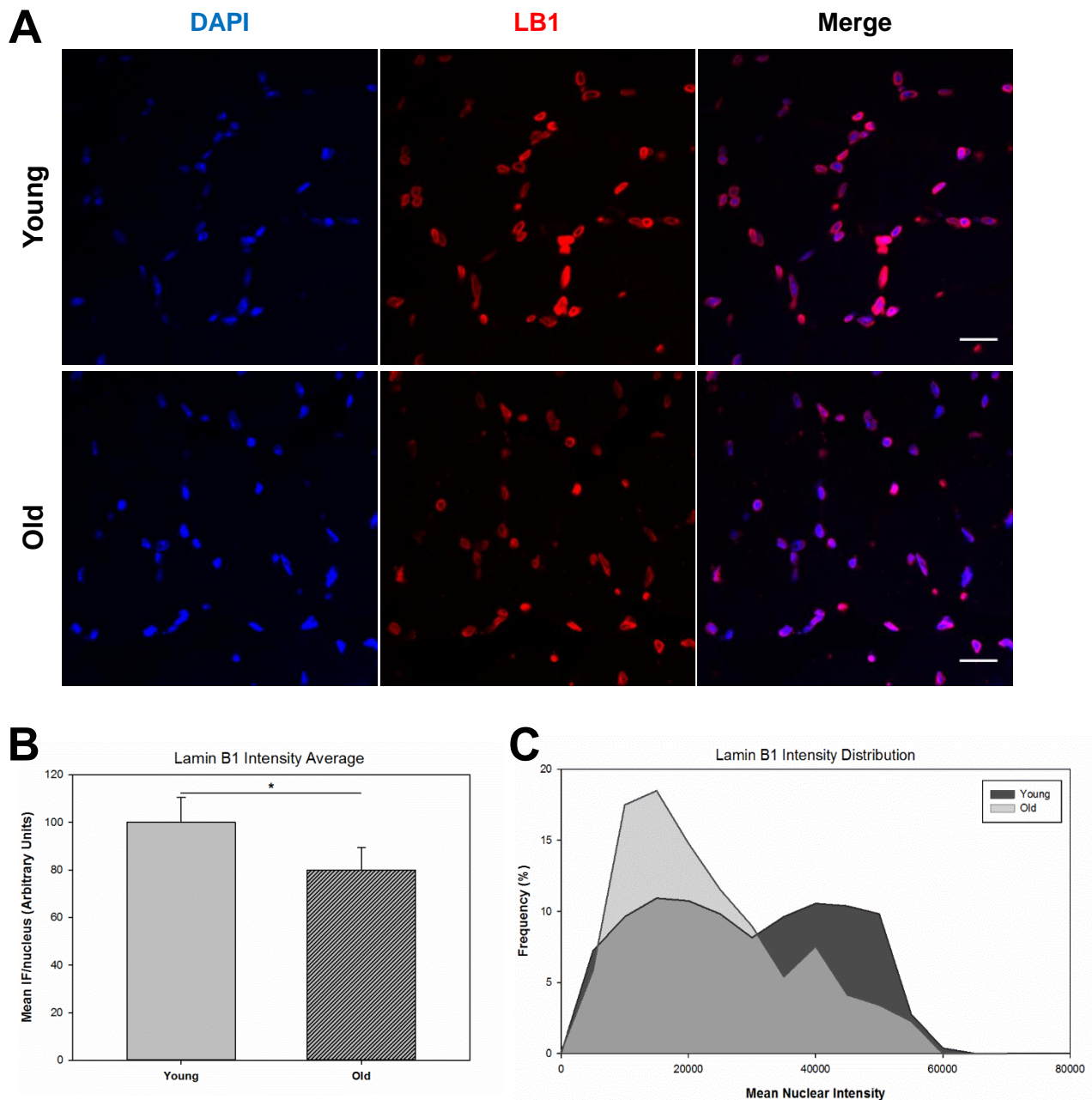

FIGURE 10. MEAN NUCLEAR LAMIN B1 FLUORESCENCE INTENSITY DIFFERS IN MUSCLES FROM OLD AND YOUNG MICE. A, Representative images of immunostained cryosections of gastrocnemius muscle from wild-type mice from two different age groups: young (8 months old) and old (31.5, 32 and 32.5 months old). 3 animals per group. Muscle sections were immunostained for LB1 (in red) and mounted with a mounting media containing DAPI (in blue) **b,** Mean nuclear intensity of LB1 fluorescence signal (arbitrary units) in tissues from the young and old age group. **C,** percentage frequency distribution of the total number of nuclei analysed from young and old mice according to Lamin B1 mean nuclear intensity. Nuclei analysed amounted to 540 and 730 for the young and old groups, respectively. Scale bars, 20 μm. Student's t-test was used to analyse the data. Significant differences between young and old tissues are represented in each graph with *, one-tailed p-value <0.05.

Despite this, no significant differences (p=0.168, one-tailed p-value) were observed in the standard deviation of the pixel-to-pixel variation of LB1 fluorescence intensity within a single nucleus [FIG 11], an indirect assessment of the existence of gaps in the nuclear lamina. In fact,
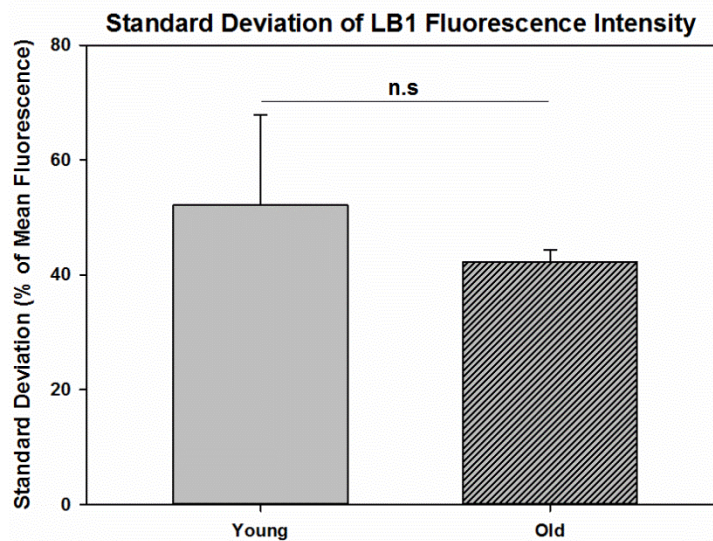
FIGURE 11. Standard deviation of pixel-to-pixel variation of nuclear LB1 fluorescence intensity, represented as percentage of mean nuclear intensity of LB1 for both Young and Old tissues (3 animals per group). Student's t-test was used to analyze the data. No significant differences were detected between groups. N.s, non significant.

contrary to expectations, younger tissues displayed higher standard deviation values (52.23±15.63%) than older ones (42.23±2.03%). Nonetheless, the overall results suit the idea of LB1 loss accompanying/ensuing as a result of the development of a senescence phenotype as it is known that senescent cells accumulate with age in certain tissues[39,105,112,157] that can also include post-mitotic cells[40].

Loss and relocalization of nuclear HMGB1, another potential, yet imperfect, biomarker of senescent cells, was demonstrated to occur in a variety of mouse and human cells[186]. To determine the localization of HMGB1 in muscle fibers, muscle cryosections were fixed, immunostained for HMGB1 and imaged as described (Sections 2.6 and 2.10.1). HMGB1 nuclear and cytoplasmic fluorescence intensity was then measured in both young and old tissues [FIG 12.B, C]. Similar to what was previously described, old tissues contained significantly ($p<0.05$) more fibers with no nuclear HMGB1 than young tissues [FIG 12.A, D]. In the young group the frequency of HMGB1-negative nuclei amounted to 57.92±7.19% while in the old group the mean frequency was 73.64±7.26% [FIG 12.B]. While tissues displayed a somewhat inconsistent HMGB1 fluorescence intensity throughout their area, in the young group, high intensity staining was observed in nuclei and perinuclear areas of fibers; older tissues displayed a more uniform and faint nuclear and cytoplasmic staining [FIG 12.A, B, C]. Nonetheless, no significant differences were observed either for cytoplasmic or nuclear HMGB1 fluorescence intensity between the two groups [FIG 12.B, C]. Overall, this data supports the idea that loss of nuclear HMGB1 can be a valid, conserved feature of senescent cells in mice post-mitotic tissues *in vivo*.
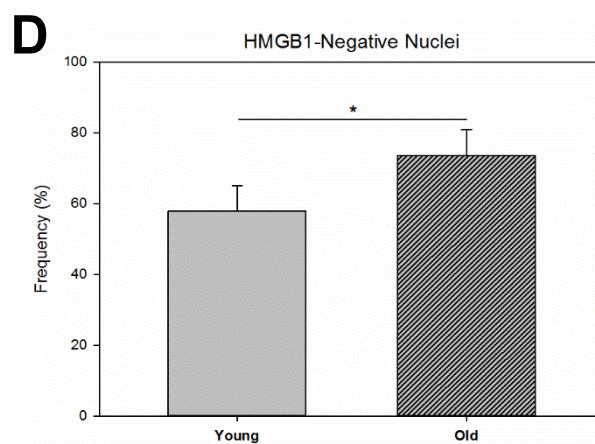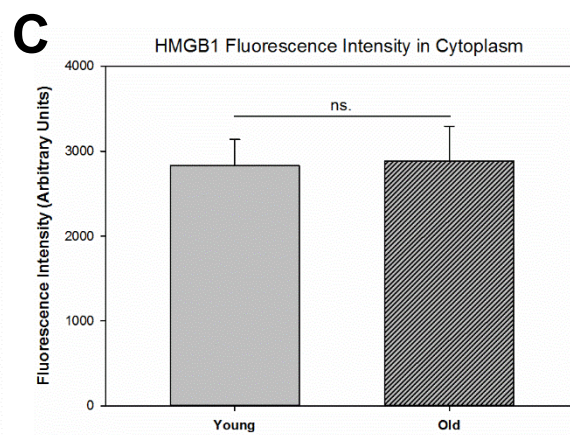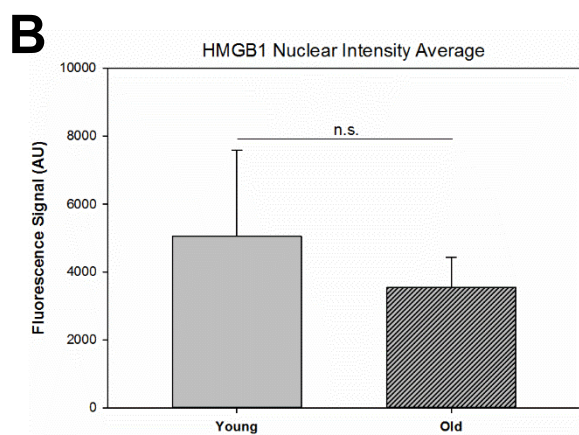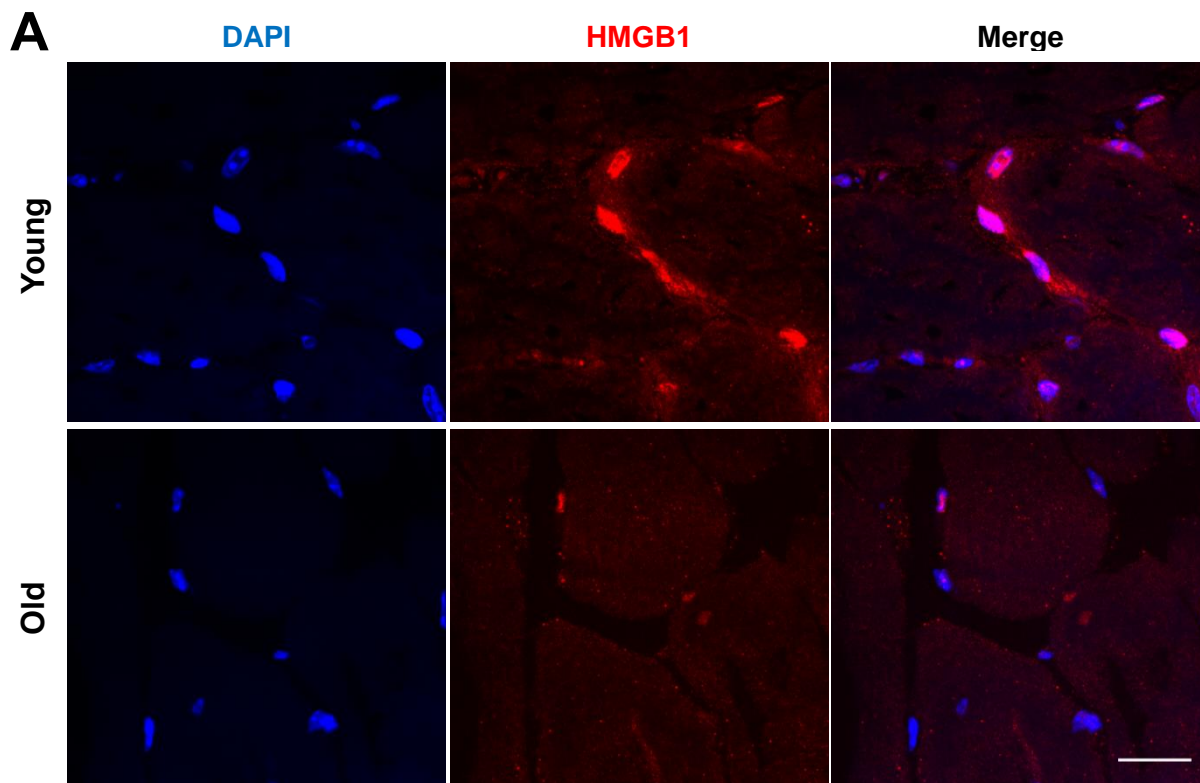
A

DAPI | HMGB1 | Merge

Young

Old

B HMGB1 Nuclear Intensity Average

C HMGB1 Fluorescence Intensity in Cytoplasm

D HMGB1-Negative Nuclei

FIGURE 12. For caption please refer to page 49.

FIGURE 12. HMGB1 DISPLAYS DIFFERENT SUBCELLULAR LOCALIZATION IN MYOFIBERS FROM OLD AND YOUNG MICE. A, Representative images of immunostained cryosections of gastrocnemius muscle from wild-type mice from two different age groups: Young (8 months old) and Old (31.5, 32 and 32.5 months old). 3 animals per group. Muscle sections were immunostained for HMGB1 (in red) and mounted with a mounting media containing DAPI (in blue). **B,** Mean nuclear intensity of HMGB1 fluorescence signal (arbitrary units; 3 tissues analysed per group). **C,** Mean cytoplasmic intensity of HMGB1 fluorescence signal (arbitrary units). **D,** Mean frequency of HMGB1-negative nuclei in tissues from the young and old age groups Samples analysed were the same as in B. Scale bar, 20 μm. Student's t-test was used to analyse the data. Significant differences between young and old tissues are represented in each graph with *, one-tailed p-value <0.05. Ns., non-significant.

As described previously (Section 1.3.1), activation of p21 transcription is a key event in p53-mediated cell-cycle arrest, with the upregulation of its levels being one of the first markers of replicative senescence induction[106]. To assess differences in p21 subcellular localization and levels between young and old tissues, muscle cryosections were immunostained for p21 and imaged as described (Sections 2.6 and 2.10.1). After measurement of nuclear and cytoplasmic p21 fluorescence intensity, p21-positive nuclei were quantified. In young tissues, the frequency of p21-positive nuclei amounted to 48.39±12.40% in contrast to the 65.83±7.05% in old tissues [FIG 13.A, B]. Even though the Student's t-test applied to the data reported no significant differences (p=0.0508, one-tailed p-value) between young and old tissues regarding the frequency of p21-positive nuclei, the data seems to suggest a tendency for an increase in p21 nuclear colocalization in older tissues. Similarly, the ratio of the p21 fluorescence intensity signal between nucleus and cytoplasm was slightly increased in older tissues (1.45±0.16) in comparison to younger ones (1.22±0.12) however, no significant differences were detected (p=0.067, one-tailed p-value) [FIG 13.C]. No statistical significance was detected for cytoplasmic p21 fluorescence intensity as well [FIG 13.D].

Telomeres are important targets of stress-related ageing, with TAFs being reported to increase with age in mitotic and postmitotic tissues[25,38,39]. To verify if the same age-dependent increase occurs in skeletal muscle fibers, yH2A.X immune-FISH was performed as described (Section 2.9) and nuclei with yH2A.X foci and nuclei with yH2A.X co-localizing with telomeres were quantified. No significant differences (p=0.191, one-tailed p value) were observed between young and old tissues regarding yH2A.X content in nuclei [FIG 14.A, B]. Both groups displayed very high frequencies of nuclei containing yH2A.X foci or bigger aggregates (41.79±9.29% in young tissues, 52.64±16.74% in older tissues) [FIG 14.B], however in very few cases there was co-localization with telomeres [FIG 14.A]. As predicted, the frequency of TAF-containing nuclei in older tissues (5.91±2.30%) was significantly (p<0.05) higher than the same frequency in younger tissues (1.49±1.31%) [FIG 14.C].
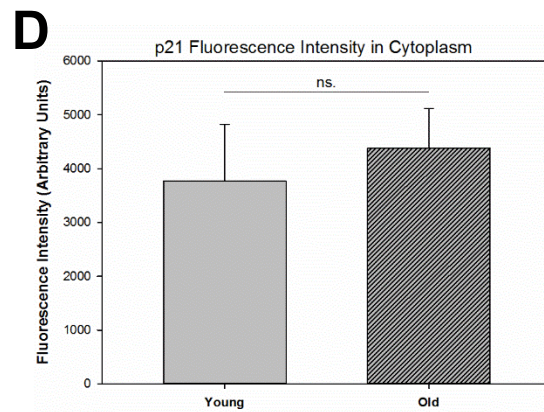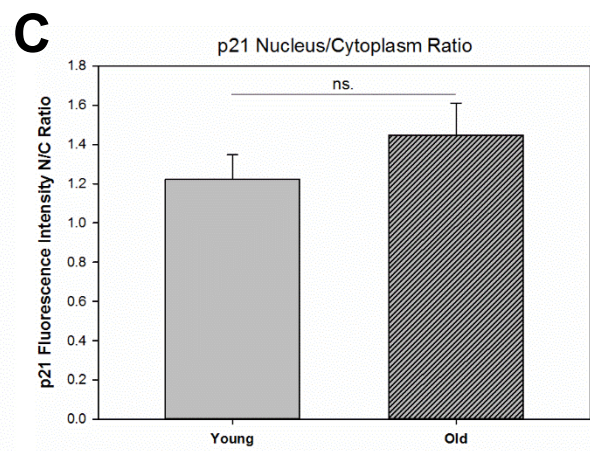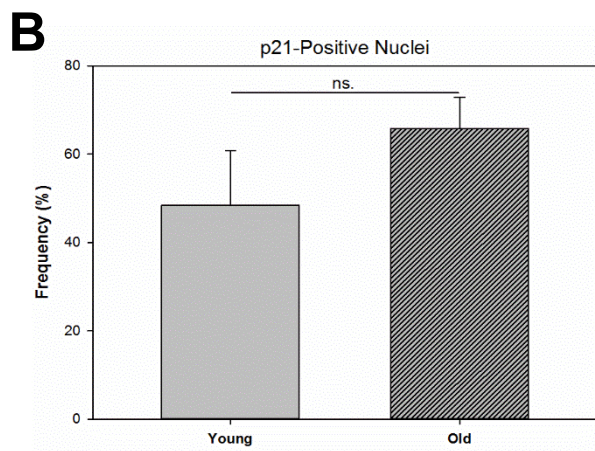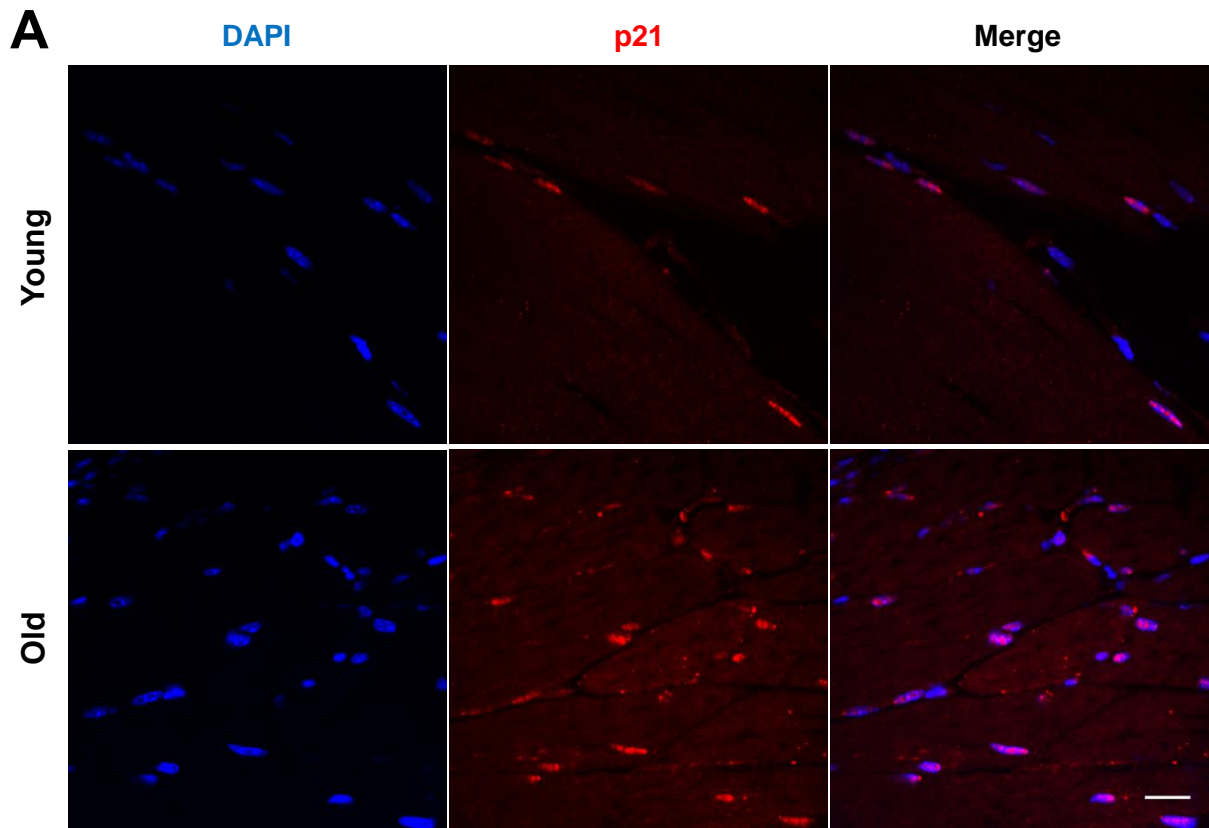
FIGURE 13. For caption please refer to page 51.

FIGURE 13. p21-NUCLEI COLOCALIZATION DISPLAYS A TENDENCY TO INCREASE IN OLDER TISSUES. A, Representative images of immunostained cryosections of gastrocnemius muscle from wild-type mice from two different age groups: Young (8 months old) and Old (31.5, 32 and 32.5 months old). 3 animals per group. Muscle sections were immunostained for p21 (in red) and mounted with a mounting media containing DAPI (in blue) **B,** Mean frequency of p21-positive nuclei in tissues from the young and old age groups (3 tissues analysed per group). **C,** Nucleus/Cytoplasm (N/C) ratio of p21 fluorescence intensity. Samples analysed were the same as in B. **D,** Mean cytoplasmic intensity of p21 fluorescence signal (arbitrary units). Samples analysed were the same as in B and C. Scale bar, 20 μm. Student's t-test was used to analyse the data. Ns., non-significant.
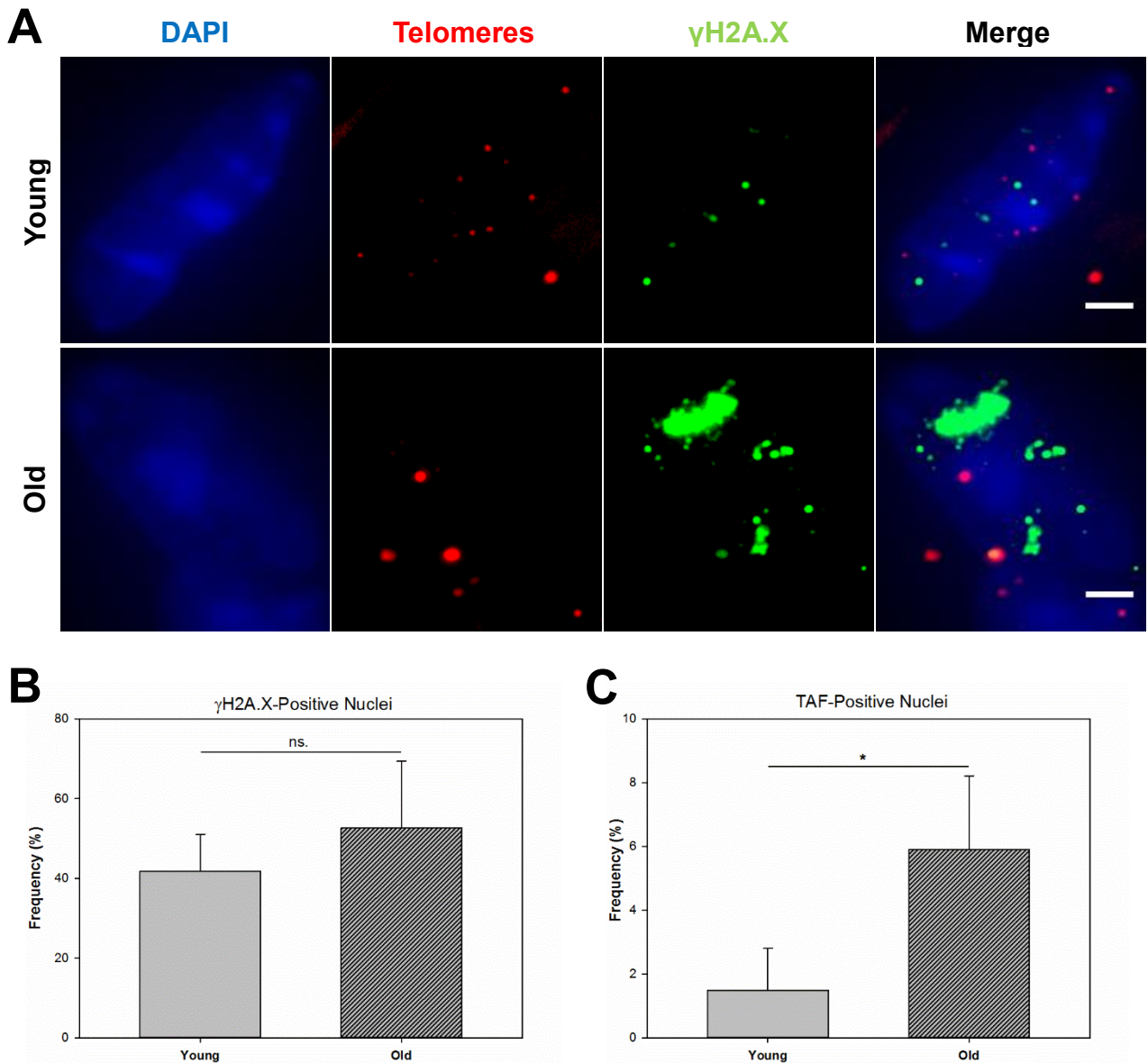

FIGURE 14. FREQUENCY OF NUCLEI CONTAINING TAF INCREASES IN OLDER TISSUES. A, Representative images of γH2A.X Telo-FISH stained cryosections of gastrocnemius muscle from wild-type mice from two different age groups: Young (8 months old) and Old (31.5, 32 and 32.5 months old). 3 animals per group. Muscle sections were immunostained for γH2A.X (in green), hybridized with a Cy-3-labelled telomere specific PNA probe to allow the visualization of telomeres (in red) and mounted with a mounting media containing DAPI (in blue) **B,** Mean frequency of γH2A.X-positive nuclei in tissues from the young and old age groups (3 tissues analysed per group). **C,** Mean frequency of γH2A.X-positive nuclei. Tissues analysed were the same as in B. Scale bar, 5 μm. Student's t-test was used to analyse the data. Significant differences between young and old tissues are represented with *, one-tailed p-value <0.05. Ns., non-significant.

Together, the results above described can prove helpful in establishing sensitive biomarkers of cellular senescence and myofibre ageing. To assess if some of the parameters analyzed were directly correlated with others, a Pearson's product moment correlation analysis was done and a scatter matrix was created [FIG 15]. 8 of the parameters above described were considered: CSA (μm^2), frequency of CNFs, frequency of SBB-positive cells (%), frequency of p21-positive nuclei (%), frequency of HMGB1-positive nuclei (%), mean nuclear LB1 intensity (arbitrary units), standard deviation of LB1 signal (% of mean intensity), frequency of TAF-containing nuclei (%). A Pearson's correlation coefficient (Pcc) and a p-value for statistical significance of linear correlation were calculated for each variable, consisting of a combination of markers. The pair(s) of variables with positive correlation coefficients tend to increase together, while the pairs with negative correlation coefficients, one variable tends to decrease while the other increases. For four pairs there was a statistical significance, thus indicating both parameters were linearly correlated: CSA-SBB^{+} cells (p=0.048), CSA-p21[+] nuclei (p=0.021), SBB^{+} cells-LB1 St Dev (p=0.022) and CNF-TAF[+] nuclei (p=0.039).

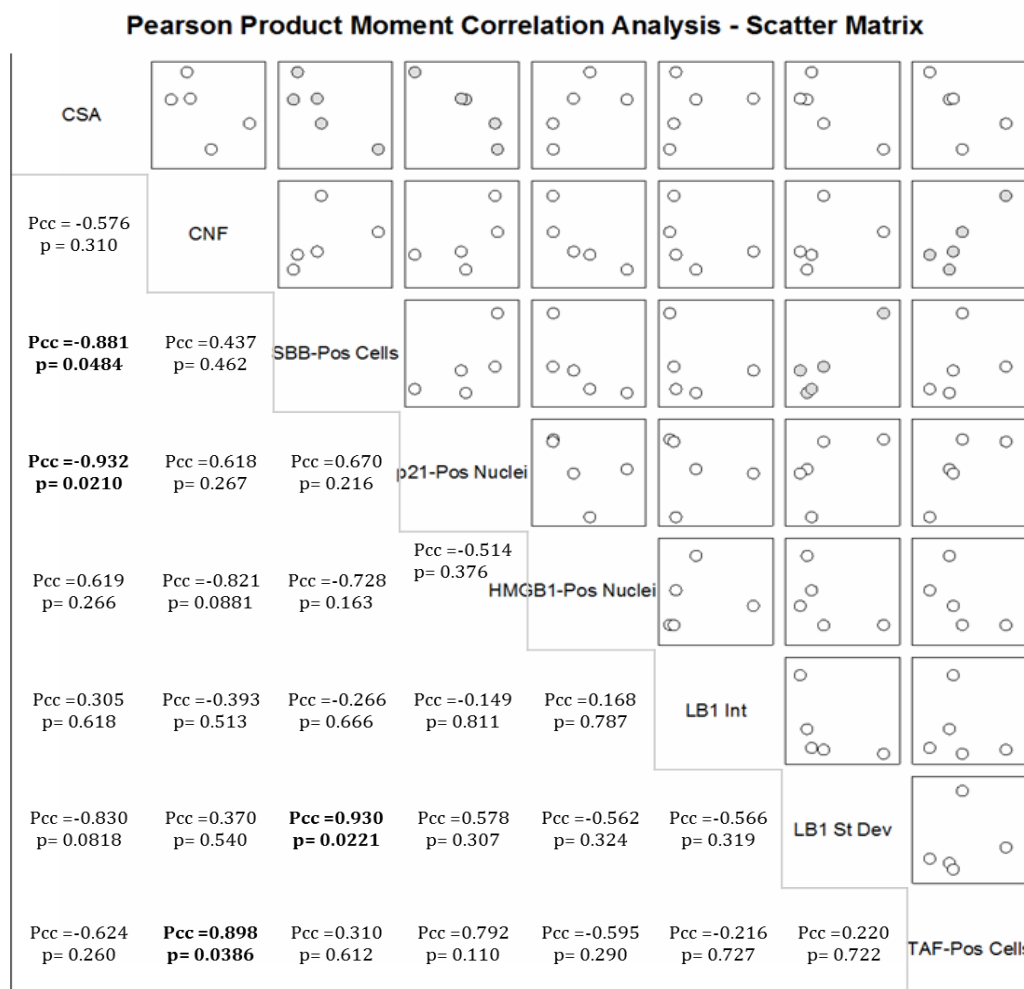**Pearson Product Moment Correlation Analysis - Scatter Matrix**

FIGURE 15. PEARSON'S PRODUCT MOMENT CORRELATION SCATTER MATRIX. Top: Scatter matrix displaying the scatter plots for each pair of variables. Bottom: Pearson's correlation coefficient and p-value for statistical significance of linear correlation between the two plotted variables. 8 parameters are represented: CSA (μm^2), frequency of CNFs, frequency of SBB-positive cells (%), frequency of p21-positive nuclei (%), frequency of HMGB1-positive nuclei (%), mean nuclear LB1 intensity (arbitrary units), standard deviation of LB1 signal (% of mean intensity), frequency of TAF-containing nuclei (%). Statistical significance was considered for p= <0.05 and is represented in the figure by bolded text (in bottom) or filled dots (in individual scatter plots). For each individual analysis. n=5.

3.2. IDENTIFICATION OF IMPLANTED CELLS

As referred previously (Sections 2.2 and 2.3), 11 mice, divided into two groups – N2 and N3, were injected in gastrocnemius muscle of the right hind limb with MRC5-GFP$^+$Luc$^+$ cells: 5 mice injected with proliferative cells, 6 mice injected with senescent cells. To identify regions containing injected cells and to restrict the area of analysis of biomarkers, *in situ* luciferase assays were conducted for all injected tissues as described (Sections 2.5 and 2.10.2), with non-injected tissues analyzed as controls [FIG 16]. This first screening allowed to restrict, at a tissue level, the regions where injected cells were most probable to be found. To confirm exactly whether the slides that came up as positive for injected cells with the *in situ* luciferase assays indeed had regions with positive cells and to restrict, on a section level, the specific area where those cells were located, the entire tissue sections were screened for native GFP [FIG 17]. This second screening allowed for a definitive identification of positive slides for injected cells. The same sections were used for both the *in situ* luciferase assays and native GFP screening. The number of analyzed and positive slides identified for each injected tissue in both screenings is summarized in Table I. In animals injected with proliferative cells, no GFP-positive cells were identified during the native GFP screening, despite the fact those same tissues had positive chemiluminescence signal reported during *in situ* luciferase assays; ultimately, all tissue sections of these animals were considered negative. In animals injected with senescent cells, however, in most of the sections with positive chemiluminescent signal reported during *in situ* luciferase assays, GFP-positive cells were identified. Tissue sections were considered positive only when both the *in situ* luciferase assay and native GFP screening exhibited positive results.

TABLE I. Number of screened and positive slides in injected muscles of each animal. 5 animals (5LN, 9NoN, 10.1, 11.2 and 12.3) were injected with proliferative cells while the remaining 6 (6RN, 72NN, 82LN, 13.4, 14.5 and 15.6) were injected with senescent cells. The same type of mice was used in both established groups (N2 and N3).

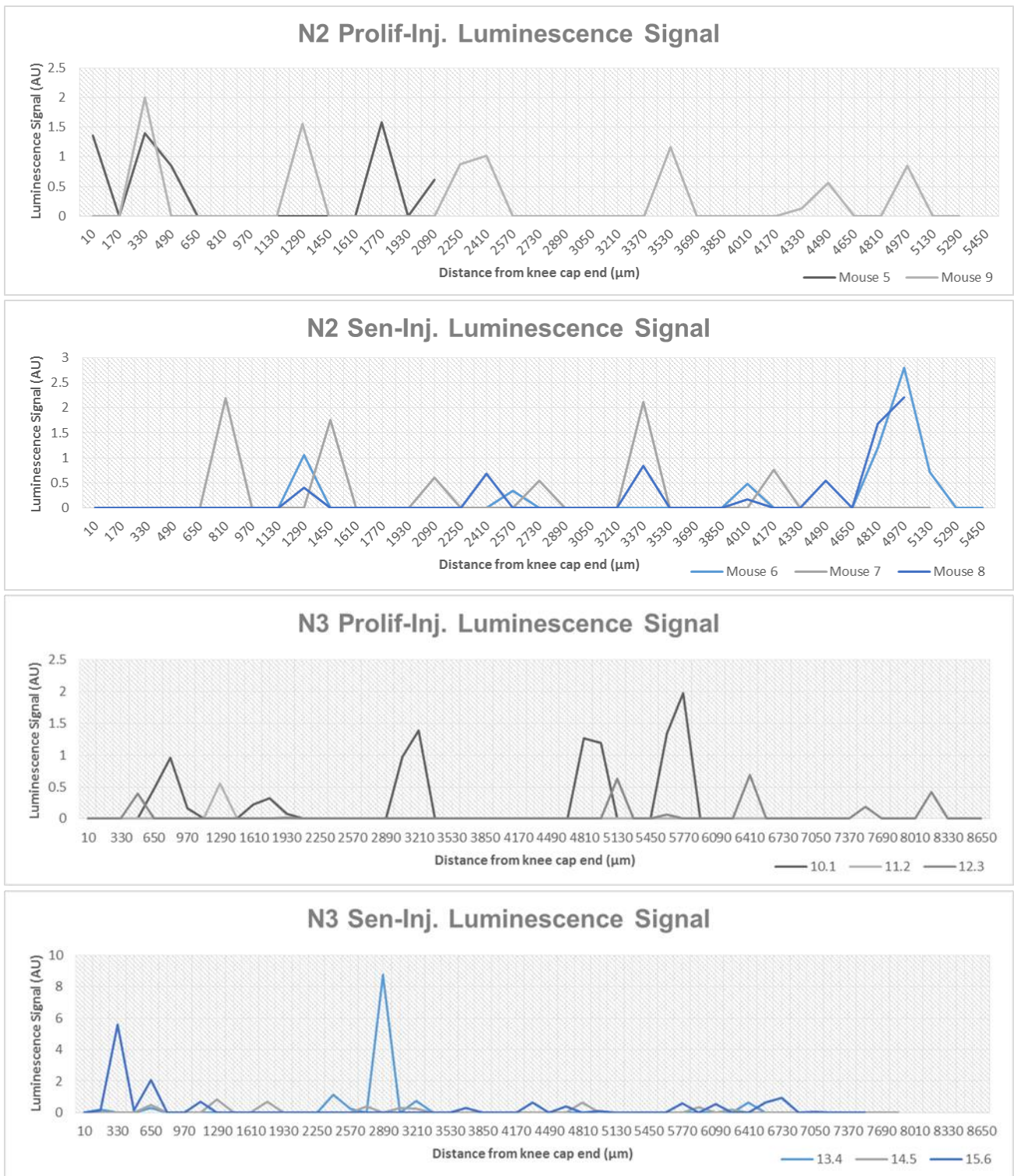| Experiment	Animal ID	Screened slides	Positive Slides	
			In situ Luciferase Assay	Native GFP Screening
N2	5LN	14	5	0
	9NoN	34	9	0
	6RN	35	6	4
	72NN	33	6	5
	82LN	32	7	4
N3	10.1	41	12	0
	11.2	42	1	0
	12.3	55	9	0
	13.4	50	7	6
	14.5	50	9	8
	15.6	48	14	7

FIGURE 16. *IN SITU* **LUCIFERASE ASSAYS' RESULTS.** Graphs display the chemoluminescence signal (arbitrary units) in function of the distance from the knee cap end of muscles sectioned. Muscles were sectioned from the knee cap end until the lower base, with the first section collected representing an increment of 10μm from the knee cap end. One section was analysed every 160μm until the end of the muscle. To facilitate representation, results were separated into four graphs in function of experiment name (N2 and N3) and the type of MRC5-GFP+Luc+ cells injected (Sen – Replicatively Senescent; Prol – Proliferative). In the first top graphs, "Mouse 5", "Mouse 9", "Mouse 6", "Mouse 7" and "Mouse 8", represent mice 5LN, 9NoN, 6RN, 72NN and 82LN, respectively.
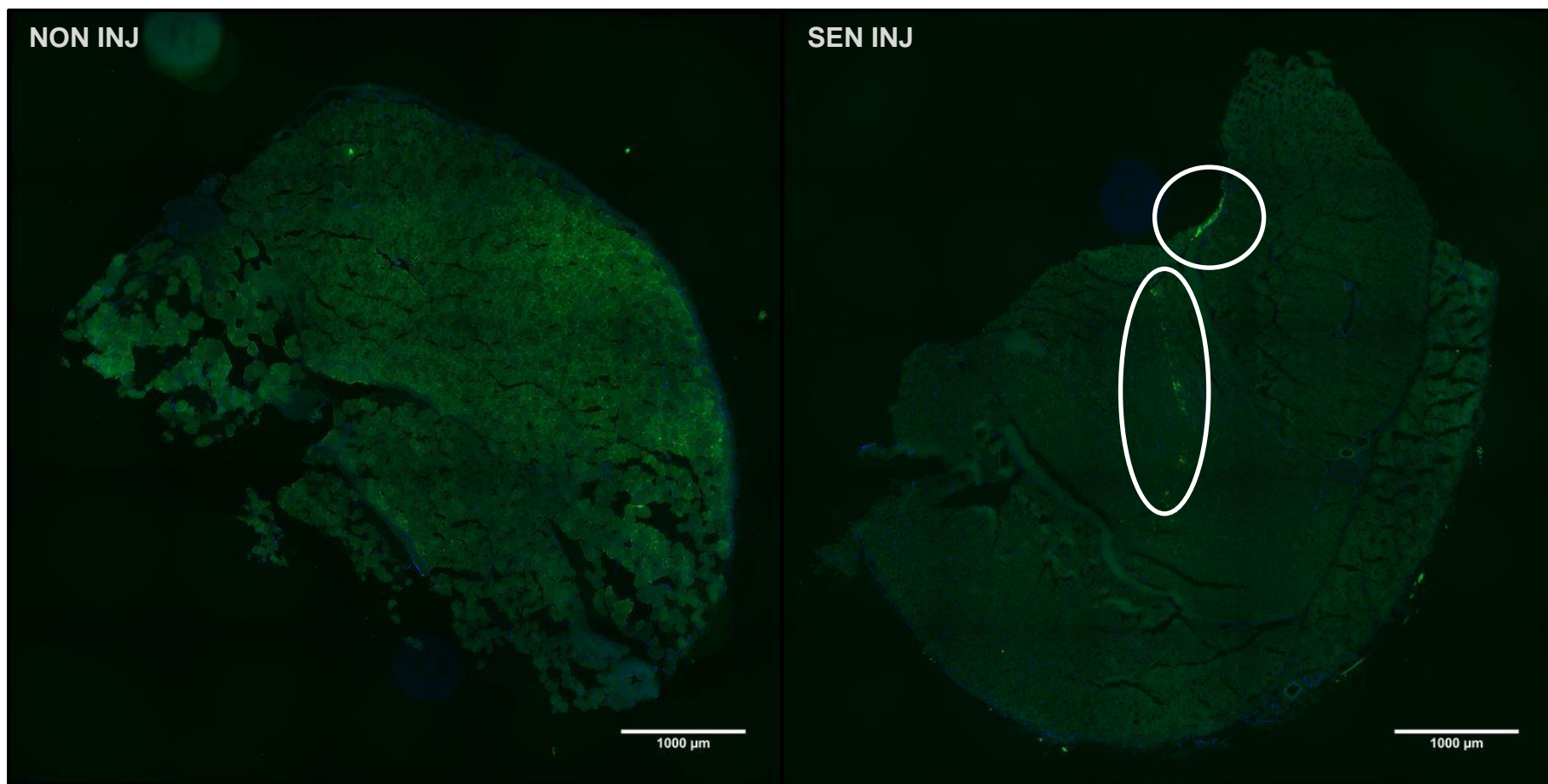
FIGURE 17. NATIVE GFP SCREENING TILESCANS. Representative images of the native GFP screening conducted for entire sections of non-injected tissues (NON INJ, left image) and tissues injected with proliferative (Not shown) and replicatively senescent (SEN INJ, right image) MRC5-GFP+Luc+ cells. To reconstruct entire tissue sections, represented tilescans were created by merging 25 images acquired with 10x magnification objectives (a variable number of images were required, in function of sections' area). White circles delineate areas containing identified injected cells. Scale bar, 1000 µm.

3.3. ASSESSMENT OF AN *IN VIVO* SENESCENT BYSTANDER EFFECT

Following identification of injected senescent cells within tissues, we wanted to investigate the effects of said cells in their microenvironment, particularly in adjacent skeletal muscle fibers. With the goal of confirming the hypothesis that senescent cells are capable of inducing persistent DNA damage and DDR in skeletal muscle bystander cells and *in vivo* contributing to skeletal muscle fiber ageing by inducing various senescence-like features, we assessed levels of several previously validated biomarkers described in Section 3.1. A cutoff value of 100μm was established to separate adjacent from further away fibers and sections were stained and imaged as described (Sections 2.6, 2.8, 2.10.3). Expression of the selected biomarkers was evaluated in fibers of both regions and also in injected GFP$^+$ cells, when possible. In tissues from animals injected with senescent cells, sections analyzed were always within a range of 160μm from a slide confirmed to contain injected cells.

Frequency of p21-positive nuclei within the tissue, p21 fluorescence intensity in cytoplasm and the ratio between p21 fluorescence intensity between nucleus and cytoplasm were shown not to be the most sensitive parameters to compare young against old skeletal muscle fibers, even though they displayed a tendency to increase in older tissues [FIG 13]. Despite this, activation of p21 transcription is, nonetheless, a key event in p53-mediated cell-cycle arrest[106] and p21 was demonstrated to be involved in signaling pathways mediating the development of senescence-like phenotypes in postmitotic cells independently of proliferation arrest[40]. Thus, nuclear p21 content was measured in injected (and non-injected, for controls) tissues, to check whether the frequency of p21-positive nuclei in fibers adjacent to injected senescent MRC5-GFP$^+$Luc$^+$ cells was different from the frequency for the remaining tissues. The One-Way ANOVA test used to analyze the data reported significant differences between the regions analyzed. Frequency (59.12±7.95%) of p21-positive nuclei in areas adjacent to sites with senescent injected cells (0-100μm, SEN-INJ) was significantly different from the frequency in other regions [FIG 18.A, B]. Importantly, it was significantly higher than the frequencies reported for regions further away (>100μm, SEN-INJ) from areas with injected cells (41.40±4.97%) within the same tissues, for tissues injected with proliferative cells (36.70±12.87) and for non-injected tissues (37.45±8.56%), although being significantly smaller than the frequency of p21-positive nuclei in injected cells (88.98±5.70%) [FIG 18.B]. No significant differences were detected between regions >100μm from injected sites in SEN-INJ tissues, tissues injected with proliferative cells (PROL-INJ) and non-injected (NON-INJ) tissues regarding frequencies of p21-positive nuclei. For this analysis, the 0-100μm SEN-INJ group was exclusively constituted of nuclei within 100μm range of clusters of injected cells containing more than 2 cells. However, around sites of injection it was common to identify isolated GFP-positive cells far from the 100μm range. Then, to check if fibers within 100μm range of 2 or less injected cells had the same frequency of p21-positive nuclei as fibers within 100μm range of larger clusters, a Student's t-test was applied to the data. Fibers within 100μm range of 2 or less injected cells had, in fact, significant (p<0.05) less p21-positive nuclei (43.23±17.15%) than their counterparts within 100μm range of clusters [FIG 18.C], suggesting the effects of injected senescent cells in tissue microenvironment is dependent on the amount of cells present.
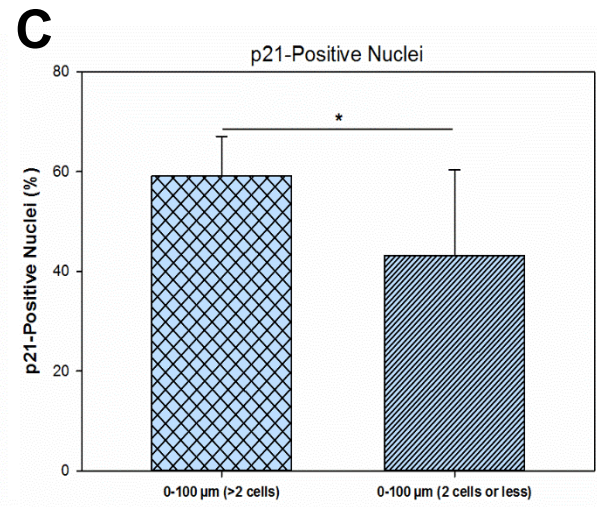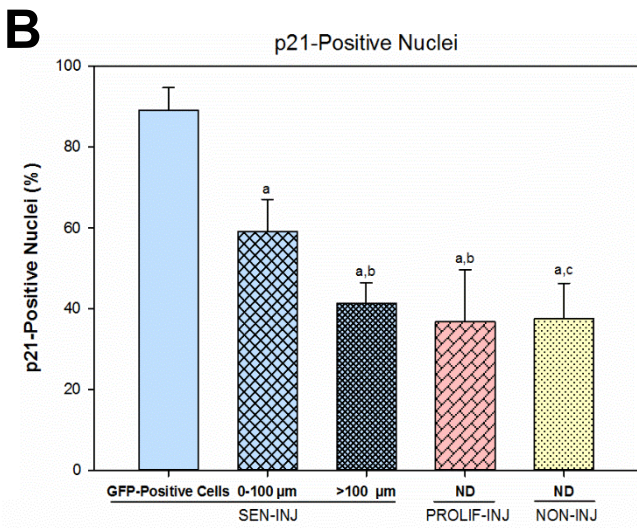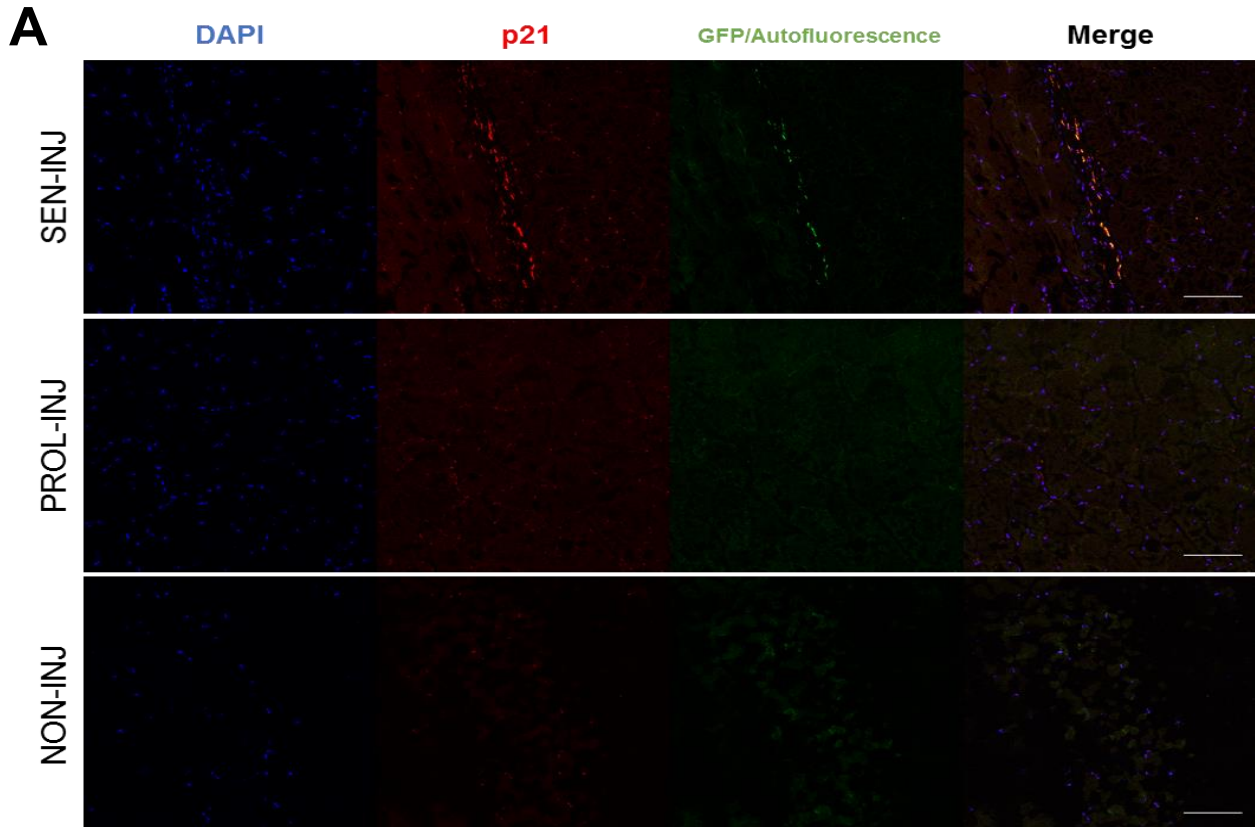
FIGURE 18. FREQUENCY OF p21-POSITIVE NUCLEI INCREASES AROUND SITES OF SENESCENT INJECTED CELLS. A, Representative images of immunostained cryosections of gastrocnemius and biceps femoris muscles from hind limbs of young mice (4-6 months old) who were injected with senescent (SEN-INJ) or proliferative (PROL-INJ) MRC5-GFP+Luc+ cells and not injected hind limbs (NON-INJ). Muscle sections were immunostained for p21 (in red) and mounted with a mounting media containing DAPI (in blue). Injected cells were tracked and muscle morphology observed through native GFP fluorescence signal and fibers' auto fluorescence, respectively (in green). **B**, Mean frequency of p21-positive nuclei from GFP-positive cells, fibers within 100µm range of clusters of injected cells (0-100µm) and fibers further distant from that same range (>100µm) from SEN-INJ tissues (n=6 for all groups) and from not defined, random regions (ND) from PROL-INJ (n=5) and NON-INJ (n=2) tissues. **C**, Mean frequency of p21-positive nuclei from fibers within 100µm range of clusters of injected cells (same data as in B) and fibers within 100µm range of 2 or less injected cells (n=6). Scale bar, 50µm. In B, One-Way ANOVA followed by Holm-Sidak's multiple comparisons test were used to analyze the data. **a**, statistical significant difference ($p<0.001$) against GFP-Positive cells group; **b**, statistical significant difference ($p<0.01$) against 0-100µm group; **c**, statistical significant difference ($p<0.05$) against 0-100µm group; remaining pairwise comparisons did not show significant differences. In C, Student's t-test was used to analyse the data. *, one-tailed p-value <0.05.

In similar fashion, the frequency of HMGB1-negative nuclei was analyzed for the same tissues and groups described above [FIG 19.A]. Because this data was not normally distributed, an ANOVA on Ranks test was applied to compare the groups. This test showed statistically significant (p<0.05) differences between the groups analyzed. The only groups significantly different, as confirmed by a Dunn's pairwise multiple comparisons test, were the GFP-positive cells and >100μm ones [FIG 19.B]. Surprisingly, these results go against our expectations, as it appears there is a tendency for the frequency of HMGB1-negative nuclei to increase as the distance from the injected senescent cells increases as well. No statistically significant differences were detected between the remaining groups [FIG 19.B] neither between fibers within 100μm range of 2 or less injected and fibers within 100μm range of clusters [FIG 19.C].

The same tissues and groups were also analyzed for the mean nuclear fluorescence intensity signal of LB1 and the standard deviation of the signal's pixel-to-pixel variation in a single nucleus [FIG 20.A]. No statistically significant differences were detected between the groups regarding mean nuclear fluorescence intensity signal of LB1 as they displayed an overall consistent fluorescence signal (in SEN-INJ tissues: 8701.83±3854.86, 11263.0.4±847.98 and 8583.22±2535.62 for GFP-positive cells, 0-100μm and >100μm fibers, respectively; in PROL-INJ tissues: 9070.89±1613.05; in NON-INJ tissues: 9075.08) [FIG 20.B]. There was, however, statistically significant differences between the groups regarding the standard deviation of the signal's pixel-to-pixel variation in a single nucleus [FIG 20.C]. Nuclei from fibers from PROL-INJ and NON-INJ have a significantly (p<0.05) lower standard deviation of the signal's pixel-to-pixel variation when compared to GFP-positive cells and >100μm fibers from SEN-INJ tissues. Despite not significantly different, the same standard deviation in PROL-INJ and NON-INJ fibers displays a tendency to decrease when compared to 0-100μm fibers of SEN-INJ tissues (p=0.060 for 0-100μm SEN-INJ vs. PROL-INJ and p=0.056 for 0-100μm SEN-INJ vs. NON-INJ).

Lastly, the same tissues were stained for SBB and mounted with a mounting media incorporated with DAPI. By combining bright field monochrome imaging (for SBB stain) with fluorescence imaging (for DAPI) it was possible to obtain images with a bright field channel combined with a fluorescence channel [FIG 21.A]. This allowed the combined analysis of the frequencies of SBB-positive cells and CNFs and fibers' CSA. GFP-positive cells were not considered for these analysis and inclusion of fibers clearly disrupted due to cryo-artifacts was avoided. For SBB analysis, the One-Way ANOVA test used to analyze the data reported significant differences between the regions analyzed. In SEN-INJ tissues, fibers from the 0-100μm group had a significantly higher frequency of SBB-positive cells (28.73±6.86%) than fibers from the >100μm group within the same tissues (17.78±4.10%; p<0.01) and fibers from NON-INJ tissues (18.54±2.18%; p<0.05) [FIG 21.C]. The difference was not significant when compared to fibers from PROL-INJ tissues (20.65±2.67%; p=0.067). These results clearly show a tendency for accumulation of lipofuscin in fibers around areas with injected cells. This accumulation, however, probably exceeds the range of 100μm as observed in some cases [FIG 21.B].
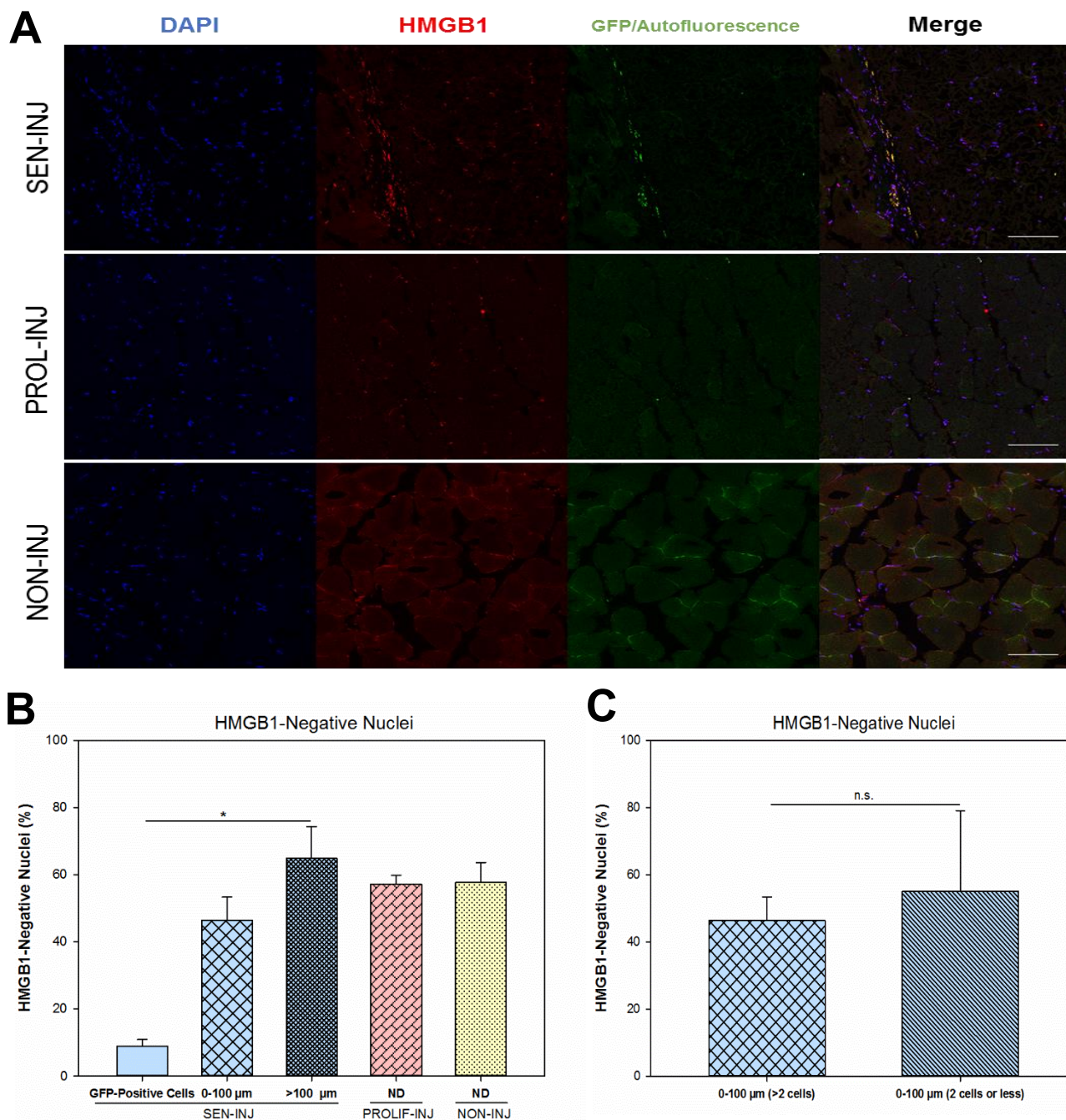
FIGURE 19. FREQUENCY OF HMGB1-NEGATIVE NUCLEI REMAINS UNALTERED AROUND SITES OF SENESCENT INJECTED CELLS. A, Representative images of immunostained cryosections of gastrocnemius and biceps femoris muscles from hind limbs of young mice (4-6 months old) who were injected with senescent (SEN-INJ) or proliferative (PROL-INJ) MRC5-GFP+Luc+ cells and not injected hind limbs (NON-INJ). Muscle sections were immunostained for HMGB1 (in red) and mounted with a mounting media containing DAPI (in blue). Injected cells were tracked and muscle morphology observed through native GFP fluorescence signal and fibers' auto fluorescence, respectively (in green). **B**, Mean frequency of HMGB1-negative nuclei from GFP-positive cells, fibers within 100µm range of clusters of injected cells (0-100µm) and fibers further distant from that same range (>100µm) from SEN-INJ tissues (n=3 for all groups) and from not defined, random regions (ND) from PROL-INJ (n=3) and NON-INJ (n=2) tissues. **C**, Mean frequency of HMGB1-positive nuclei from fibers within 100µm range of clusters of injected cells (same data as in B) and fibers within 100µm range of 2 or less injected cells (n=3). Scale bar, 50µm. In B, Kruskal-Wallis test, followed by Dunn's pairwise multiple comparisons test were used to analyze the data. In C, Student's t-test was used to analyse the data. *, one-tailed p-value <0.05; n.s., not significant.
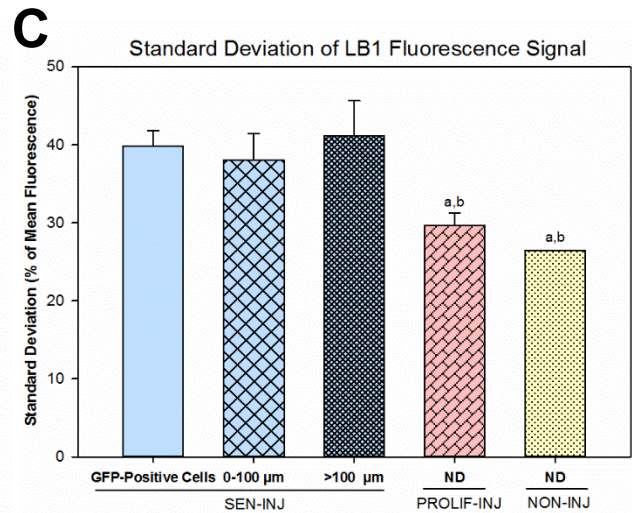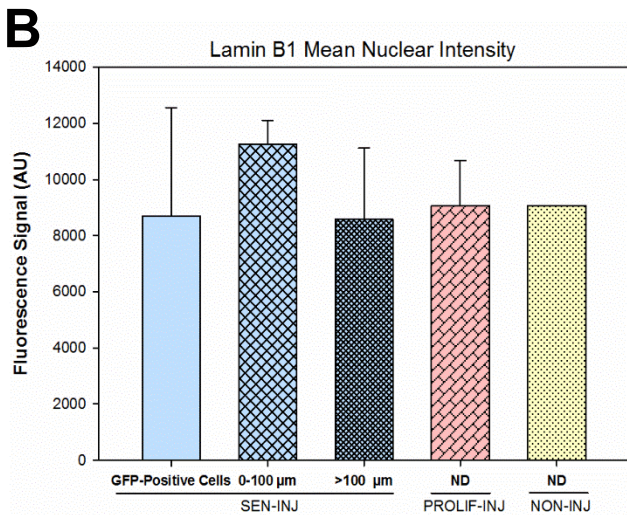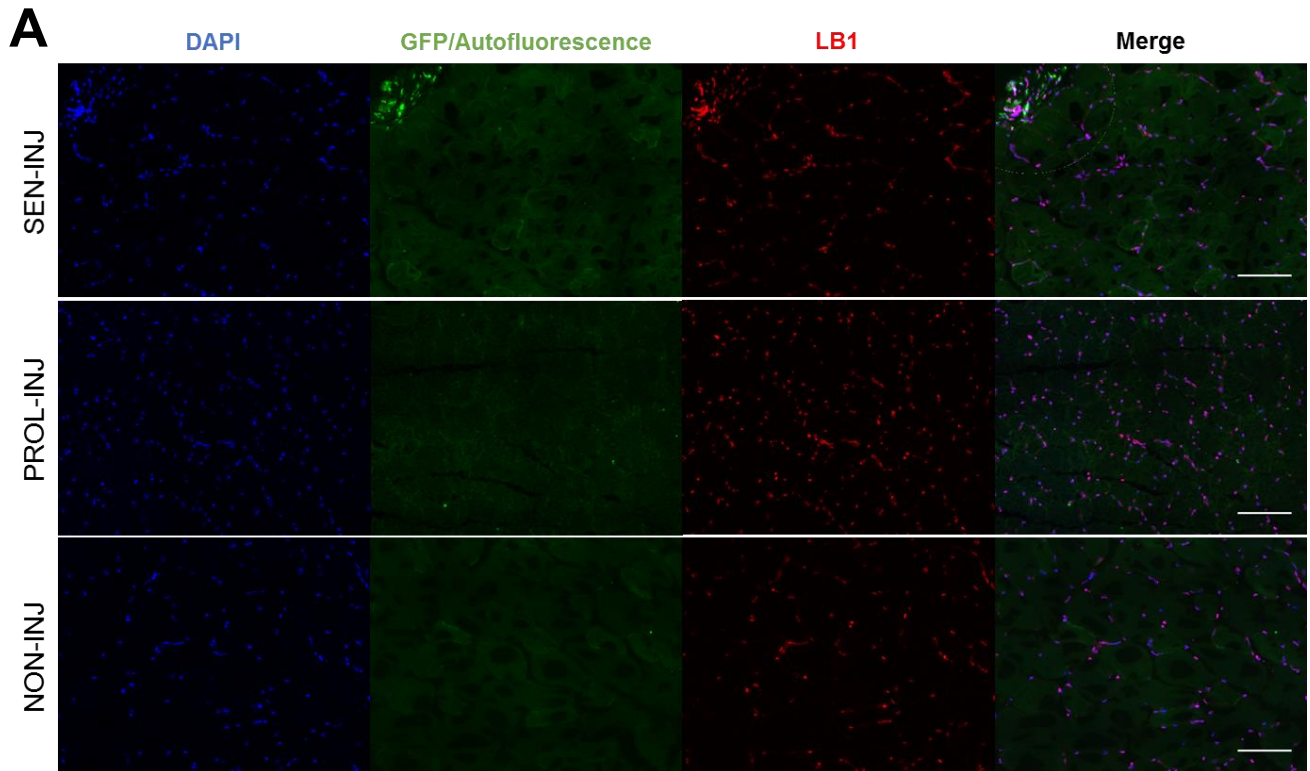
FIGURE 20. LB1 MEAN NUCLEAR INTENSITY, BUT NOT PIXEL-TO-PIXEL VARIATION, REMAINS UNALTERED IN TISSUES INJECTED WITH SENESCENT CELLS. A, Representative images of immunostained cryosections of gastrocnemius and biceps femoris muscles from hind limbs of young mice (4-6 months old) who were injected with senescent (SEN-INJ) or proliferative (PROL-INJ) MRC5-GFP+Luc+ cells and not injected hind limbs (NON-INJ). Muscle sections were immunostained for LB1 (in red) and mounted with a mounting media containing DAPI (in blue). Injected cells were tracked and muscle morphology observed through native GFP fluorescence signal and fibers' auto fluorescence, respectively (in green). **B**, Mean nuclear intensity of LB1 fluorescence signal (arbitrary units, AU) from GFP-positive cells, fibers within 100µm range of clusters of injected cells (0-100µm) and fibers further distant from that same range (>100µm) from SEN-INJ tissues (n=3 for all groups) and from not defined, random regions (ND) from PROL-INJ (n=3) and NON-INJ (n=1) tissues. **C**, Standard deviation of LB1 signal's pixel-to-pixel variation in a single nucleus. Samples analyzed and groups the same as in B. Scale bar, 50µm. One-Way ANOVA followed by Holm-Sidak's multiple comparisons test were used to analyze the data. **a**, statistical significant difference (p<0.05) against GFP-Positive cells group; **b**, statistical significant difference (p<0.05) against >100µm group; remaining pairwise comparisons did not show significant differences.

A

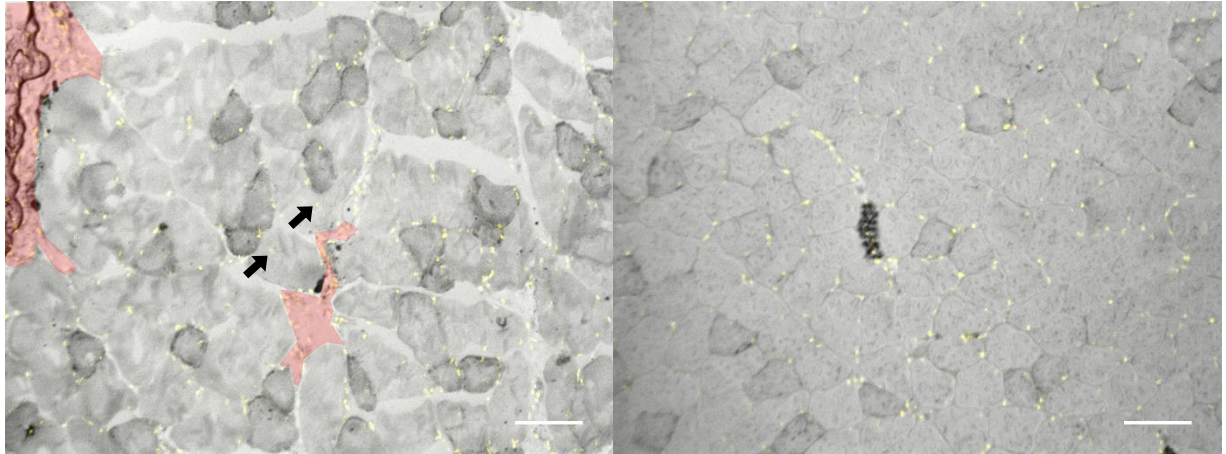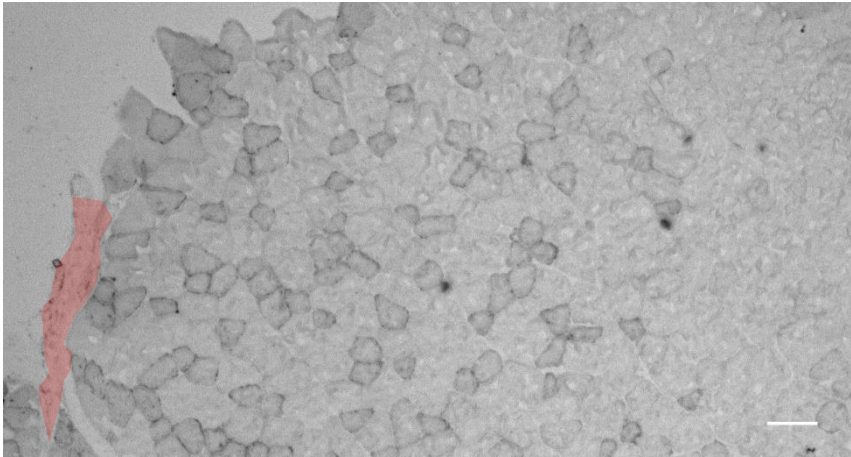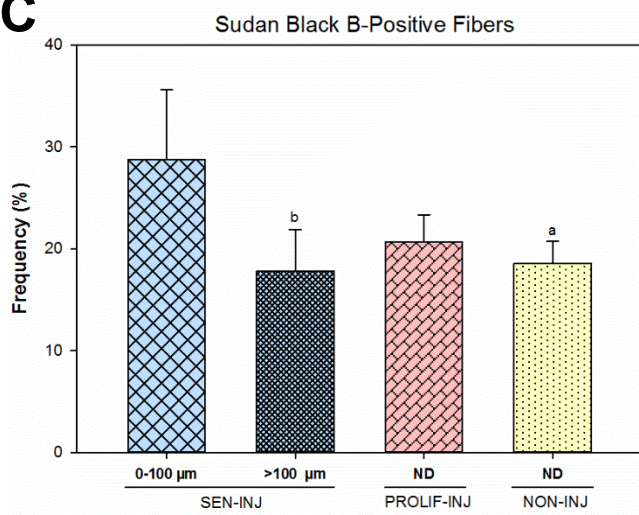**B**

C

Sudan Black B-Positive Fibers

FIGURE 21. For caption, please refer to page 62.

FIGURE 21. HIGHER FREQUENCY OF LIPOFUSCIN-POSITIVE MYOFIBERS AROUND SITES OF INJECTED SENESCENT CELLS. A, Representative images, at 10X magnification, of Sudan Black B (SBB) stained cryosections of gastrocnemius and biceps femoris muscles from hind limbs of young mice (4-6 months old) who were injected with senescent (SEN-INJ) MRC5-GFP+Luc+ cells. Bright field monochrome imaging, for SBB stain (bright field channel) was combined with fluorescence imaging, for DAPI (in yellow). Red areas indicate areas where injected cells were identified. Arrows indicate centrally-nucleated myofibers. **B,** Representative images, at 5X magnification, of Sudan Black B (SBB) stained cryosections of gastrocnemius and biceps femoris muscles from hind limbs of young mice (4-6 months old) who were injected with senescent (SEN-INJ) MRC5-GFP+Luc+ cells. Same tissues as in A. **C,** Mean frequency of SBB-positive fibers within 100μm range of clusters of injected cells (0-100μm) and further distant from that same range (>100μm) from SEN-INJ tissues (n=6 for all groups) and from not defined, random regions (ND) from PROL-INJ (n=4) and NON-INJ (n=4) tissues. Scale bar, 100μm. One-Way ANOVA followed by Holm-Sidak's multiple comparisons test were used to analyze the data. **a,** statistical significant difference (p<0.05) against 0-100μm group; **b,** statistical significant difference (p<0.01) against 0-100μm group; remaining pairwise comparisons did not show significant differences.

As to parameters of muscle morphology, injection of senescent cells appears to have limited effects. While significant (p<0.05) differences were detected between the 0-100μm group of SEN-INJ tissues and NON-INJ tissues regarding the frequency of CNFs (3.63±1.99% and 0.82±0.69%, respectively), no significant differences were detected for the remaining pairwise comparisons. No significant differences for fibers' CSA were detected between any of the established groups.
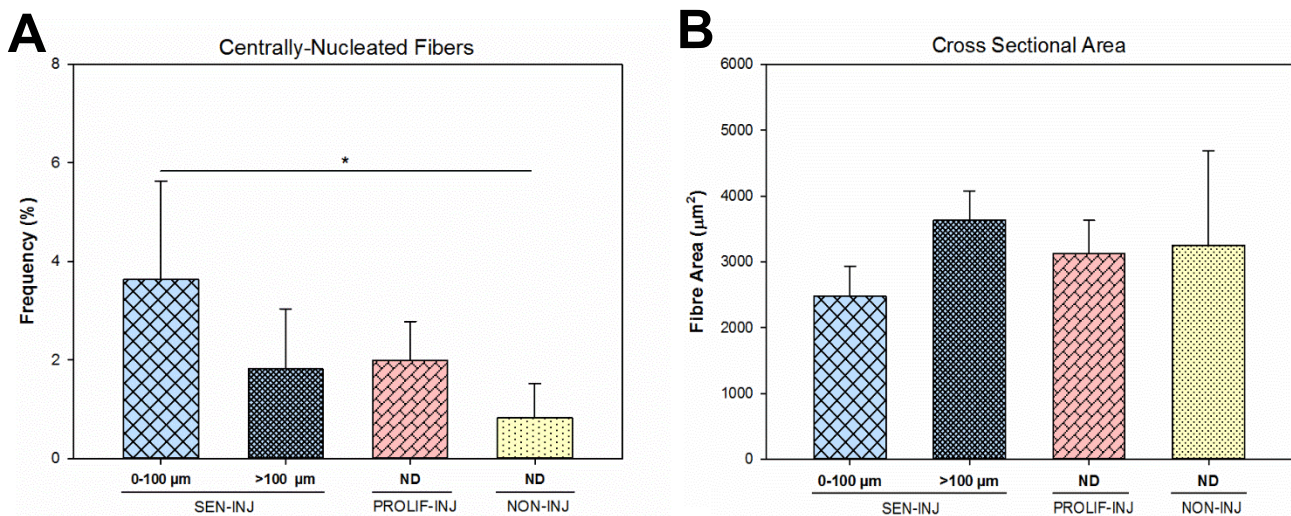
FIGURE 22. MUSCLE MORPHOLOGY ANALYSIS IN INJECTED AND NON-INJECTED TISSUES. A, Mean frequency of centrally-nucleated fibers within 100μm range of clusters of injected cells (0-100μm) and further distant from that same range (>100μm) from SEN-INJ tissues (n=6 for all groups) and from not defined, random regions (ND) from PROL-INJ (n=4) and NON-INJ (n=4) tissues. B, Cross-sectional area of fibers within 100μm range of clusters of injected cells (0-100μm) and further distant from that same range (>100μm) from SEN-INJ tissues and from not defined, random regions (ND) from PROL-INJ and NON-INJ tissues (n=3 for all groups). One-Way ANOVA followed by Holm-Sidak's multiple comparisons test were used to analyze the data. *, one-tailed p-value <0.05; n.s., not significant.

CHAPTER 4. DISCUSSION

Worldwide population ageing is currently increasing at rates never observed before. People are living longer and this increase in lifespan is shifting the distribution of countries' populations towards older ages. By 2050, the world's population over 60 years is expected to be more than the double of what it is today, reaching approximately 2 billion people, with 434 million of those being 80 years or older[169]. By itself, aging should not be considered a problem; there are, however, a number of pathological conditions associated with age-related loss of function. In fact, aging is the main risk factor for the development of cancer, cardiovascular diseases, sarcopenia, neurodegenerative diseases and many other pathological conditions[8,187]. Moreover, age also increases the chance of a person to develop several conditions at the same time (multimorbidity)[169]. For these reasons, improving our understanding of how and by what ageing is being driven and why there's an immense variability in what people experience with age is now more imperative than ever.

In 2013, Carlos López-Otín et al. attempted to identify the cellular and molecular hallmarks of ageing. The nine hallmarks proposed by the group included genomic instability, telomere attrition, altered intercellular communication, stem cell exhaustion, loss of proteostasis, epigenomic alterations, deregulated nutrient sensing, mitochondrial dysfunction and cellular senescence[160]. These are not isolated features; quite the contrary, all hallmarks are strongly interconnected. For instance, the onset of cellular senescence may be dependent on a myriad of factors including genomic instability, telomere erosion, mitochondrial dysfunction, loss of proteostasis and/or epigenomic alterations and, in turn, may be a driving agent mediating stem cell exhaustion, alterations in intercellular communication and deregulation of nutrient sensing mechanisms. Cellular senescence as also been linked to multiple age-related diseases, with both beneficial and detrimental effects (reviewed in[11]). For these reasons, the study of senescent cells, the mechanisms driving their accumulation within tissues with age and the processes contributing to alteration of tissue microenvironment are of extreme importance for a better understanding of the ageing process. The role of cell senescence as a causal factor in ageing is further exemplified by recent data showing that the rate of accumulation of senescent cells in diverse tissues predicts cohort lifespan in mice after genetic or dietary intervention[25] and that targeted ablation of senescent cells postponed age-related decline of function in multiple tissues including skeletal muscle and extended lifespan[162,188].

Cellular senescence is traditionally regarded as a state of irreversible cell cycle arrest elicited in response to diverse stressors[6,7]. Yet, some characteristics of senescent cells and emerging data regarding signaling pathways driving the establishment of senescence imply that senescence is much more complex than just proliferation arrest. As discussed earlier, mature postmitotic neurons were shown to develop a phenotype identical to the typical state of senescence, as a result of p21-mediated DDR signaling[40], which clearly suggest that the idea of growth arrest as the defining feature of senescent cells can no longer be sustained. Importantly, with this data, the hypothesis of other non-proliferative, postmitotic tissues possessing senescent cells *in vivo* cannot be discarded as it has mostly been before. This raises several questions regarding the effects of cellular senescence in postmitotic tissues and whether they can be comparable to the effects in tissues

constituted by proliferative cells. In addition, these new questions stress the need for further studies on cellular senescence using postmitotic tissue models in order to obtain an integrative understanding of the effects of senescent cells in organismal aging and their role in pathology and physiology. Considering this, mice skeletal muscle was chosen as the tissue model for this study.

In the first part of this work, we validated a panel of proposed senescence biomarkers in gastrocnemius skeletal muscle cryosections by comparing their expression in young versus old tissues. Classical markers of senescence, such as staining for SA-βGal have been used extensively, even though its use and specificity has its limitations, with analysis of human skin producing contradictory results[105,189]. Fortunately, the increasing availability of novel proposed biomarkers to detect cellular senescence *in vitro* and, importantly, *in vivo* allowed us to identify the most sensitive ones for the specific tissue model being evaluated in this study. We present here data for the expression of LB1, HMGB1 and p21 and the abundance of TAF and lipofuscin within muscle fibers, as well as a standard characterization of muscle morphology.

Our next objective was to assess whether senescent cells could induce a bystander effect in skeletal muscle *in vivo*, making use of the previously validated biomarkers. The bystander effect, previously reported in co-cultured fibroblasts *in vitro*[82], might be an important contributor to the age-dependent increase in senescent cell frequency observed in tissues and to the impact these cells have on their local microenvironment. However there is limited information regarding the relevance and roles of the bystander effect in non-pathological conditions *in vivo*. To shed some light over these questions, we set up to assess whether senescent cells in vivo can induce a bystander effect in skeletal muscle. For that, in the second part of this work, senescent and proliferative MRC5-GFP+Luc+ cells were injected into mice gastrocnemius skeletal muscle with the objective of comparing fibers adjacent and further away from sites of injection of senescent and proliferative cells with fibers from non-injected tissues. The original plan had to be adapted however, for it was not possible to identify proliferative cells within the injected tissues. Despite several slides emitting a positive chemoluminescence signal measured during the *in situ* luciferase assays, it was not possible to identify GFP-positive cells in PROL-INJ tissues during native GFP screens. This was probably due to the lower GFP fluorescence observed in proliferating MRC5-GFP+Luc+ fibroblasts in culture. Two factors, possibly combined, might explain these observations. First, senescent cells are larger and so contain about 5 to 10 times more protein than proliferating ones. In addition protein turnover is faster in young cells, and this together may be responsible for less accumulation of GFP and an overall weaker fluorescence signal. Secondly, proliferative cells are more capable to migrate in the tissue, causing the dispersion of injected cell aggregates, consequently dispersing the fluorescence signal throughout a bigger area, thus reducing signal intensity. For these reasons, it was not possible to identify sites of injection in PROL-INJ tissues; non-defined (ND) areas, which may or may not contain isolated injected proliferative MRC5-GFP+Luc+ cells were considered instead. This solution is not ideal though, as it excludes an important control for this study. By not analyzing fibers adjacent to sites of injection of proliferative cells we cannot surely claim the changes detected in fibers around sites with injected senescent cells are exclusively dependent on the bystander effect mediated by the aforementioned cells.

Without the analysis of fibers around injected proliferative cells, we will always have to consider the effect of the tissue disruption caused by the injection per se.

Nevertheless, in the last part of this project, we went on to confirm our hypothesis that senescent cells are capable of inducing persistent DNA damage and DDR in skeletal muscle bystander cells and *in vivo* contributing to skeletal muscle fiber ageing by inducing various senescence-like features. For that, we evaluated the same biomarkers validated during the first part of the project in fibers adjacent and further away from sites with injected senescent cells in SEN-INJ tissues and fibers from the ND regions selected for PROL-INJ and NON-INJ tissues. Next, a detailed discussion of the results obtained for each biomarker is presented.

Muscle Morphology:

In humans, body composition is widely altered during ageing, with skeletal muscle weakness and atrophy as major distinctive characteristics of older people. Here, we assessed gastrocnemius muscle fiber size by measuring fibers' cross-sectional area (CSA) and evaluated fiber regeneration through quantification of centrally-nucleated fibers (CNFs). Both are standard parameters, usually evaluated in studies assessing alterations in muscle morphology, sarcopenia and/or muscle dystrophy. There is general agreement that, in skeletal muscles from both old mice and humans, myofibre size is decreased (fibre atrophy)[170,179,190–193]. In turn, CNFs are recognized as newly regenerated myofibres, more resistant to mechanical stresses and believed to compensate the increase in fragility of skeletal muscle characteristic of several muscle dystrophies and ageing[194]. As such, in models of muscle dystrophy and ageing, increased CNFs, reflecting faster cycles of degeneration/regeneration, are usually reported. Our results, as expected, are in accordance with these observations. We report here a decrease in average fiber CSA of almost 50% between young (8 months) and old (32 months) mice, a clear increment of fibers with lower CSA but also a significant increase in CNFs in older mice. These results are a reflection of the accentuated phenotype of our old group of mice. At 32 months old, it is expected these mice display severe sarcopenia; nevertheless, their gastrocnemius muscles appear to still retain the ability to regenerate, in accordance to previous reports[195]. Coherently, fiber thinning and fiber regeneration take place in different fibers, and thus no differences were observed in CSA between CNFs and non-CNFs. Together, these results offer a valuable insight on the state of mice gastrocnemius skeletal muscle and give us reference values for comparison with injected muscles despite some limitations that should be considered. The CSA values we report are somewhat higher than what was observed in other studies[179] which can reflect the high heterogeneity between different models or difference dependent on the region of the muscle analyzed. Moreover, age-dependent shifts between type I and II fibers might contribute to our results. We did not assess fiber type. Nevertheless, the pattern of distribution of fibers according to CSA is very similar to what has been reported, for both age groups[179].

Both parameters, despite being related to tissue dysfunction and ageing do not appear to be extensively affected in regions adjacent to injected senescent cells. We observed an increment in frequency of CNFs around areas of injection; however that increment was only significant when

compared to NON-INJ tissues, with areas further away from sites of injected senescent cells and PROL-INJ tissues displaying somewhat intermediary frequencies between the other two. Overall though, the frequencies of CNFs within non-injected tissues are within the range observed for the young tissues analyzed for assessment of muscle morphology parameters. Regarding CSA measurements, no significant differences were observed between the groups, despite the 0-100μm, SEN-INJ group displaying a tendency to contain fibers with lower CSA than the remaining groups. The average value of CSA observed for that group was comparable to the value obtained for the fibers of older mice analyzed for assessment of muscle morphology parameters while the remaining groups displayed values between these two groups and the value obtained for fibers of young mice previously assessed. This apparent smaller size can be explained by the normal heterogeneity between individuals and models but also by the small age discrepancy between the mice in the two different studies. While young mice studied for the analysis of biomarkers were 8 months old, mice used for the assessment of the *in vivo* bystander effect were only 4-6 months old and could be expected to have somewhat smaller muscle fibers. In addition, reduction in fiber size reflects deep morphological alterations in skeletal muscle fibers, which probably develop long after the senescence state is elicited. This could explain why accentuated differences were not observed.

Lipofuscin-positive cells:

As discussed previously, the histochemical SBB staining can be a reliable approach to detect senescent cells[180]. SBB stains lipofuscin, an aggregate of oxidized proteins, lipids and metals known for a long time to accumulate with age, especially in post-mitotic cells[183,184]. This accumulation was proven to be not just a consequence of ageing, but also one of the many drivers of cellular senescence[183]. For these reasons, lipofuscin is considered a hallmark of aging[184,196]. As expected, we report an age-dependent increase in frequencies of SBB-stained/lipofuscin-positive fibers in mouse gastrocnemius muscle. Moreover, we report a significant decrease in the CSA of SBB-positive fibers when compared to SBB-negative fibers from older tissues. Even though the higher frequencies of SBB-positive fibers in older tissues can be responsible for lowering the average CSA of fibers in these tissues, the average value of CSA for only the SBB-negative fibers from older tissues is by itself lower than the average value reported for young tissues. These results suggest that, with age, the reduction in fiber size occur throughout the entire skeletal muscle; nonetheless, certain fibers display an accentuated phenotype, with lower CSA and accumulation of lipofuscin, which may be features of an aggravated condition. In accordance to this supposition, these two parameters – CSA and frequency of SBB-positive fibers – were also demonstrated to be negatively correlated by the Pearson's product moment correlation analysis. We also observed a higher cluster probability of SBB-positive cells in older tissues, with approximately 10% of SBB-positive cells being clustered, which might suggest some type of intercellular communication capable of propagating the senescent phenotype to adjacent fibers. This seems to be the case, as we also observe an increment of SBB-positive fibers in areas adjacent to sites with senescent injected cells. The frequency of SBB-positive fibers in this area was significantly higher than frequencies in the >100μm, SEN-INJ and NON-INJ groups and, even though it was not significantly higher when compared to the PROLIF-INJ group, the tendency remained. Together these results support our

hypothesis that senescent cells can induce a bystander effect in skeletal muscle *in vivo*, leading to the establishment of senescent-like phenotypes in adjacent cells.

p21-positive nuclei:

Despite being a key event in p53-mediated cell-cycle arrest, p21 did not appear to be a very sensitive biomarker to detect age-related changes in gastrocnemius muscle fibers. While accumulation of p21 in cytoplasm has been reported to prevent apoptosis and promote cell survival, with consequent oncogenic functions, its inhibitory effect on cell-cycle progression is correlated with its nuclear colocalization[197,198]. In concordance, we observed, in older tissues, a tendency for an increase in the nuclear colocalization of p21 and in the nucleus/cytoplasm ratio of p21 fluorescence signal intensity, even though no significant differences were detected. No apparent tendency was observed when comparing p21 cytoplasmic fluorescence intensity, though. In both young and old tissues, frequencies of p21-positive nuclei were high, with approximately 50% and 65% of the nuclei being considered positive, respectively. These values are not surprising though, as we are analyzing a non-proliferative tissue and p21 is involved in mediating cell-cycle arrest.

As previously discussed, p21 is involved in major signaling pathways that generate stable and self-sustainable feedback loops, possibly independent of proliferation arrest, necessary and sufficient for the establishment of senescence. p21 signaling also connects the DDR with downstream phenotypic alterations during the transition to senescence[40,76]. With this in consideration, p21 appears to have a prominent role in establishing the senescent phenotype it should be expected to also have an important role in mediating a senescent bystander effect. Our results strongly support this claim. Fibers adjacent to sites with aggregates of injected senescent cells contain significantly higher frequencies of p21-positive nuclei than fibers further away from the injected sites and fibers from PROL-INJ and NON-INJ tissues. No differences were detected between the remaining groups, restricting the effect to only the 100µm range established. Importantly, the average frequency of p21-positive nuclei reported in fibers within the 100µm range from the sites of injected cells is similar to the one reported for old gastrocnemius muscles in physiological conditions. Not surprisingly, the frequencies reported for the remaining groups are similar to the average frequency reported for young gastrocnemius muscle, suggesting fibers adjacent to aggregates of injected senescent cells are more akin to fibers from old muscles than to fibers from their own muscle, at least regarding p21 nuclear colocalization. This data represents strong evidence that senescent cells are able to modify their microenvironment and, through a bystander effect, induce senescent-like phenotypes in nearby fibers that resemble the phenotypes observed in much older muscles. To our knowledge this may constitute the first line of evidence of senescent cells generating a bystander effect inducing senescence-like features in postmitotic cells, *in vivo.* Moreover, we also report an effect of the abundance of injected senescent cells on the frequency of 21-positive nuclei in adjacent fibers. In fact, no increment was observed in fibers adjacent to two or less isolated, GFP-positive cells, with the average frequency of p21-positive nuclei in that group being comparable to the one reported for young muscles, meaning those

isolated senescent cells in their surroundings were not able to induce a bystander effect capable to alter, at least significantly, tissue microenvironment.

HMGB1-negative nuclei:

HMGB1 functions as a chromatin associated, high mobility group protein but also as a secreted cytokine, acting both as a regulator of transcription, replication and DNA repair, but also as an alerting danger signal[129,137]. In conditions of cellular stress, HMGB1 is released from the nuclei to promote cellular defense instead[139]. Accordingly, both loss and relocalization of HMGB1 into the cytoplasm were observed in senescent cells *in vitro* and *in vivo*, in both human and mouse models in a strain- and cell type-independent way. In pre-senescent cells HMGB1 can be abundant in the nuclei[186,199] whereas, in senescent cells, HMGB1 is barely detectable, with the exception of a faint cytoplasmic staining[186]. In mice given whole-body irradiation (9 Gy), approximately 80% of kidney cells presented faint nuclear and cytoplasmic HMGB1 staining, whereas it maintained mostly nuclear in cells from unirradiated mice[186]. The same group also demonstrated that the frequency of cells lacking nuclear HMGB1 increased with age in mice kidney[186], albeit no results were presented for HMGB1 localization in post-mitotic tissues. As expected, in older tissues we observed a significant increase in the frequency of HMGB1-negative nuclei and a tendency to decrease the mean nuclear HMGB1 fluorescence intensity. No apparent differences in HMGB1 fluorescence intensity in cytoplasm were detected between both types of tissue, indicating that, with age, HMGB1 was lost from muscle fibers instead of simply relocating from the nucleus to the cytoplasm. Surprisingly, the quantification of HMGB1-negative nuclei in SEN-INJ, PROLIF-INJ and NON-INJ tissues did not follow the pattern expected. No significant differences were detected between fibers within and further away from the established 100μm range from injected senescent cells, fibers from PROLIF-INJ tissues and fibers from NON-INJ tissues, with fibers from all these groups displaying mean frequencies very similar to the one reported for the young muscles in physiological conditions. The only significant difference detected was between GFP-positive cells, analyzed as controls, and the >100μm from SEN-INJ cells. Surprisingly, GFP-positive cells reported very low levels of HMGB1-negative nuclei. This, however, might reflect the fact that these cells are clustered together in a limited region of tissue. Because nuclei are in very close range of each other and cytoplasmic signal was very intense in these cells, measurements of mean nuclear intensity are not reliable because we are certainly quantifying signal from the cytoplasm of adjacent cells that is overlapping with nuclei being measured. Nonetheless, this is a problem only for injected GFP-positive cells and not for the nuclei of muscle fibers, thus the remaining results are still reliable. Finally, no significant differences were detected between fibers adjacent to clusters of injected senescent cells and fibers adjacent to isolated, two or less GFP-positive cells. These results strongly contrast with what was observed for p21. In this particular case, the presence of senescent cells did not alter HMGB1 nuclear content of nearby muscle fiber.

LB1 mean nuclear intensity and pixel-to-pixel variation:

LB1 loss, only recently validated as a biomarker of cellular senescence[116] is thought to be strongly associated with the morphological changes in the nuclei associated with cellular senescence[68,116,117] believed to be on the genesis of the alterations in gene expression characteristic

of these cells[185]. We observed a significant decrease of approximately 20% in LB1 mean intensity in older tissues, a value very similar to what was reported for livers of irradiated mice[116]. Consistently, we also observed an accumulation in older tissues of nuclei with lower mean LB1 fluorescence intensity signal. Contrary to expected though, no significant differences were detected for the standard deviation of the pixel-to-pixel variation of LB1 fluorescence intensity within a single nucleus. This parameter was measured as an indirect way to assess the presence of gaps in the nuclear lamina but the results obtained suggest that it is not a very sensitive parameter to detect differences between young an old gastrocnemius muscles. In the third part of the project, when assessing the effects of a possible bystander effect generated by the injected senescent cells, the results suggested the opposite. Neither differences nor tendencies were observed for the different groups considered in terms of LB1 mean nuclear fluorescence intensity; however, all groups from SEN-INJ tissues displayed higher values (significant for the >100μm group) of pixel-to-pixel variation when compared to fibers from PROLIF-INJ and NON-INJ tissues. All groups of SEN-INJ tissues displayed values of pixel-to-pixel variation similar to the mean value obtained for the old mice previously analyzed when validating biomarkers.

TAF-positive nuclei:

Telomeres are preferential sites for accumulation of DNA damage[38], being particularly susceptible to oxidative damage, which accelerates telomere shortening[17] and can elicit a DDR. In fact telomere shortening can contribute to the development of a permanent DNA damage response (DDR)[19], characterized by the formation of DNA-damage foci containing γH2A.X at telomeres. Importantly, telomere dysfunction/damage can induce a permanent DDR at telomeres (Telomere-associated Foci, TAF), and this occurs frequently during mouse ageing and has been validated as marker for senescent cells in ageing mouse tissues[25,38]. To measure cellular senescence in vivo, Immunofluorescence staining of γH2A.X alone is a less specific marker of senescence in aging mice because it can be indicative of many other processes than senescence, including DNA replication or repair. Here, we compared the frequencies of both γH2A.X- and TAF-positive cells by immunofluorescent *in situ* hybridization (Immuno-FISH) as previously reported by others[20,25,38]. Previous studies by Wang et al. 2009 and Jeyapalan et al. 2007 have reported very low frequencies of γH2A.X-positive nuclei in skeletal muscle fibers, with no age-dependent increment observed in both γH2A.X- and TAF-positive nuclei[39,157]. While we didn't observe any age-dependent increase in γH2A.X-positive nuclei, we did however observe higher frequencies than expected, with nuclei containing γH2A.X foci or bigger aggregates composing approximately 50% of total nuclei analyzed in muscles from old mice. In fact, we observed, what appeared as, different subpopulations of positive nuclei, with some nuclei displaying the expected dispersed foci, some nuclei displaying bigger aggregates at certain regions and nuclei completely stained for γH2A.X and extremely strong signal. These differences from what has been reported by other groups may be partially explained by differences in experimental conditions and models used and/or antibody limitations. In this study we opted for using gastrocnemius muscle cryosections from mice; in the study by Wang et al 2009, formalin-fixed, paraffin embedded quadriceps femoris sections were used while in the study by Jeyapalan et al 2007, cryosections of baboon vastus lateralis muscle were analyzed.

Quantification of TAF-positive nuclei proved to be a more sensitive way to assess frequencies of possible senescent cells in the tissue in agreement with earlier data[38]. Frequencies of TAF-positive nuclei were much lower and closer to what was expected and a significant increase in older tissues was observed, contrary to older publications[39,157] but in accordance with more recent data in livers and intestine of ageing mice[25,38]. To our knowledge, our data represents the first evaluation of the frequencies of γH2A.X- and TAF-positive nuclei in mice gastrocnemius muscle using tissue cryosections. Interestingly, we also report a positive correlation between TAF-positive nuclei and CNFs, detected by the Pearson's product moment correlation analysis, which might indicate a more specific role of TAFs in skeletal muscle aging and dysfunction than what is currently considered.

Due to time constraints, it was not possible to quantify TAF-positive nuclei in injected tissues, in order to assess a possible bystander effect affecting this parameter. However, it is definitely an important evaluation that should be done in the future in order to give a stronger confirmation of the effects of the injected senescent cells on the expression of the other biomarkers evaluated. Besides this, a stronger correlation analysis, with a higher n and more parameters evaluated should also be conducted to unveil other correlations that can easily appear as non-significant with this analysis but can hold physiological importance.

In conclusion, from four candidate markers for a senescent phenotype in muscle tested, we found that two of them were increased in muscle fibers in the vicinity of transplanted senescent cells, while the two others were essentially unchanged. This might suggest that senescent cells induce some features of senescence in adjacent muscle fibers *in vivo*, but not the full senescent phenotype as seen in muscles from old animals. It might be possible that the development of this 'deep senescence' might take longer than the time frame of the bystander experiment. However, the results might also indicate technical problems with some of the markers. In the cell transplantation experiments, the injected MRC5-GFP$^+$Luc$^+$ cells are expected to be the ideal internal control. Contrary to expectations, we saw high HMGB1 levels and no decrease in LB1 in the injected senescent fibroblasts (see Figs. 19 and 20). Therefore, results from these assays should be interpreted with extreme caution. Adding additional markers (especially TAF) will help to clarify the situation.

CHAPTER 5. CONCLUDING REMARKS

In this work, we first present a panel of candidate biomarkers to evaluate cellular senescence in skeletal muscle cryosections. We show here significant increases in frequencies of SBB-positive fibers, HMGB1-negative and TAF-positive nuclei, as well as decrease in mean LB1 fluorescence in tissues from old mice. While statistical significance was not detected, tissues from old mice displayed a tendency to increment frequencies of clustered SBB-positive cells and p21-positive nuclei and, congruently, to increase the p21 nucleus/cytoplasm ratio. Importantly, we also show significant correlations between some proposed biomarkers and evaluated parameters of muscle morphology. In particular, frequencies of SBB-positive cells and p21-positive nuclei both negatively correlate with fiber's CSA, while frequency of TAF-positive nuclei registers a positive correlation with CNFs. These results may prove useful in the future to generate robust tests for identification of senescent cells within postmitotic tissues.

Moreover, we show here that injection of senescent cells into skeletal muscle of young mice promotes accumulation of certain senescence biomarkers, specifically p21 and lipofuscin in adjacent, bystander muscle fibers. We report a significant increase in the frequency of nuclei positive for p21 and fibers positive for lipofuscin within a range of 100μm around injected senescent inducer cells. At least for p21, the accumulation appears to be dependent on the abundance of nearby senescent cells. No accumulation of HMGB1-negative cells, loss of LB1 and significant alteration of fibers' morphology parameters was observed, however. Our data suggest that senescent cells are capable of inducing persistent DNA damage and DDR in skeletal muscle bystander cells *in vivo* and engendering senescence-like features in those same cells. These results may be the first line of evidence of senescent cells generating a bystander effect inducing senescence-like features in postmitotic cells, *in vivo*. This not only adds a possible explanation on how senescent cells increase in several tissues with age but also might help explain how senescent cells may be driving ageing/age-related pathologies, possibly including sarcopenia.

CHAPTER 6. REFERENCES

1.   Martin, G. M. The biology of aging: 1985-2010 and beyond. *FASEB J.* **25,** 3756–3762 (2011).

2.   Ohtani, N. & Hara, E. Roles and mechanisms of cellular senescence in regulation of tissue homeostasis. *Cancer Sci.* **104,** 525–530 (2013).

3.   Burton, D. G. a & Krizhanovsky, V. Physiological and pathological consequences of cellular senescence. *Cell. Mol. Life Sci.* 4373–4386 (2014).

4.   Hayflick, L. The limited *in vitro* lifetime of human diploid cell strains. *Exp. Cell Res*. **37,** 614-636 (1965).

5.   Hayflick, L. & Moorhead, P. S. The serial cultivation of human diploid cell strains. *Exp. Cell Res.* **25,** 585–621 (1961).

6.   Campisi, J. & d'Adda di Fagagna, F. Cellular senescence: when bad things happen to good cells. *Nat. Rev. Mol. Cell Biol.* **8,** 729–740 (2007).

7.   Kuilman, T., Michaloglou, C., Mooi, W. J. & Peeper, D. S. The essence of senescence. *Genes Dev.* **24,** 2463–2479 (2010).

8.   Campisi, J. Aging, Cellular Senescence, and Cancer. *Annu. Rev. Physiol.* **75,** 685–705 (2013).

9.   Collado, M. & Serrano, M. Senescence in tumours: evidence from mice and humans. *Nat. Rev. Cancer* **10,** 51–57 (2010).

10.   Demaria, M., Desprez, P. Y., Campisi, J. & Velarde, M. C. Cell Autonomous and Non-Autonomous Effects of Senescent Cells in the Skin. *J. Invest. Dermatol.* **135,** 1722–1726 (2015).

11.   Muñoz-Espín, D. & Serrano, M. Cellular senescence: from physiology to pathology. *Nat. Rev. Mol. Cell Biol.* **15,** 482–96 (2014).

12.   Rodier, F. & Campisi, J. Four faces of cellular senescence. *J. Cell Biol.* **192,** 547–556 (2011).

13.   Campisi, J. Cellular senescence: Putting the paradoxes in perspective. *Curr. Opin. Genet. Dev.* **21,** 107–112 (2011).

14.   Salama, R., Sadaie, M., Hoare, M. & Narita, M. Cellular senescence and its effector programs Cellular senescence and its effector programs. 99–114 (2014).

15.   Young, A. R. J., Narita, M. & Narita, M. Cell senescence as both a dynamic and a static phenotype. *Methods Mol. Biol.* **965,** 1–13 (2013).

16.   Lu, T. & Finkel, T. Free radicals and senescence. *Exp. Cell Res.* **314,** 1918–1922 (2008).

17.   Von Zglinicki, T. Oxidative stress shortens telomeres. *Trends Biochem. Sci.* **27,** 339–344 (2002).

18.   Prieur, A. & Peeper, D. S. Cellular senescence in vivo: a barrier to tumorigenesis. *Curr. Opin. Cell Biol.* **20,** 150–5 (2008).

19.   d'Adda di Fagagna, F. *et al.* A DNA damage checkpoint response in telomere-initiated senescence. *Nature* **426,** 194–198 (2003).

20.   Nakamura, A. J. *et al.* Both telomeric and non-telomeric DNA damage are determinants of mammalian cellular senescence. *Epigenetics Chromatin* **1,** 6 (2008).

21.   Passos, J. F., Saretzki, G. & Von Zglinicki, T. DNA damage in telomeres and mitochondria during cellular senescence: Is there a connection? *Nucleic Acids Res.* **35,** 7505–7513 (2007).

22. Munro, J., Barr, N. I., Ireland, H., Morrison, V. & Parkinson, E. K. Histone deacetylase inhibitors induce a senescence-like state in human cells by a p16-dependent mechanism that is independent of a mitotic clock. *Exp. Cell Res.* **295,** 525–38 (2004).

23. Bhatia-Dey, N., Kanherkar, R. R., Stair, S. E., Makarev, E. O. & Csoka, A. B. Cellular Senescence as the Causal Nexus of Aging. *Front. Genet.* **7,** 13 (2016).

24. Moiseeva, O., Mallette, F. A., Mukhopadhyay, U. K., Moores, A. & Ferbeyre, G. DNA damage signaling and p53-dependent senescence after prolonged beta-interferon stimulation. *Mol. Biol. Cell* **17,** 1583–92 (2006).

25. Jurk, D. *et al.* Chronic inflammation induces telomere dysfunction and accelerates ageing in mice. *Nat. Commun.* **2,** 4172 (2014).

26. Quan, T. *et al.* Elevated matrix metalloproteinases and collagen fragmentation in photodamaged human skin: impact of altered extracellular matrix microenvironment on dermal fibroblast function. *J. Invest. Dermatol.* **133,** 1362–6 (2013).

27. Levy, M. Z., Allsopp, R. C., Futcher, A. B., Greider, C. W. & Harley, C. B. Telomere end-replication problem and cell aging. *J. Mol. Biol.* **225,** 951–960 (1992).

28. Allsopp, R. C. *et al.* Telomere shortening is associated with cell division in vitro and in vivo. *Exp. Cell Res.* **220,** 194–200 (1995).

29. de Lange, T. Shelterin: the protein complex that shapes and safeguards human telomeres. *Genes Dev.* **19,** 2100–10 (2005).

30. Carneiro, T. *et al.* Telomeres avoid end detection by severing the checkpoint signal transduction pathway. *Nature* **467,** 228–32 (2010).

31. Fumagalli, M. *et al.* Telomeric DNA damage is irreparable and causes persistent DNA-damage-response activation. *Nat. Cell Biol.* **14,** 355–65 (2012).

32. von Zglinicki, T., Saretzki, G., Ladhoff, J., d'Adda di Fagagna, F. & Jackson, S. P. Human cell senescence as a DNA damage response. *Mech. Ageing Dev.* **126,** 111–7 (2005).

33. Jiang, H., Ju, Z. & Rudolph, K. L. Telomere shortening and ageing. *Z. Gerontol. Geriatr.* **40,** 314–324 (2007).

34. Djojosubroto, M. W., Choi, Y. S., Lee, H.-W. & Rudolph, K. L. Telomeres and telomerase in aging, regeneration and cancer. *Mol. Cells* **15,** 164–175 (2003).

35. Harley, C. B., Futcher, a B. & Greider, C. W. Telomeres shorten during ageing of human fibroblasts. *Nature* **345,** 458–460 (1990).

36. Prowse, K. R. & Greider, C. W. Developmental and tissue-specific regulation of mouse telomerase and telomere length. *Proc. Natl. Acad. Sci. U. S. A.* **92,** 4818–4822 (1995).

37. Wright, W. E. & Shay, J. W. Telomere dynamics in cancer progression and prevention: fundamental differences in human and mouse telomere biology. *Nat. Med.* **6,** 849–51 (2000).

38. Hewitt, G. *et al.* Telomeres are favoured targets of a persistent DNA damage response in ageing and stress-induced senescence. *Nat. Commun.* **3,** 708 (2012).

39. Wang, C. *et al.* DNA damage response and cellular senescence in tissues of aging mice. *Aging Cell* **8,** 311–323 (2009).

40. Jurk, D. *et al.* Postmitotic neurons develop a p21-dependent senescence-like phenotype driven by a DNA damage response. *Aging Cell* **11,** 996–1004 (2012).

41. Toussaint, O., Medrano, E. E. & Von Zglinicki, T. Cellular and molecular mechanisms of stress-induced premature senescence (SIPS) of human diploid fibroblasts and melanocytes. *Exp. Gerontol.* **35,** 927–945 (2000).

42. Rodier, F. *et al.* DNA-SCARS: distinct nuclear structures that sustain damage-induced senescence growth arrest and inflammatory cytokine secretion. *J. Cell Sci.* **124,** 68–81 (2011).

43. Dierick, J. F. *et al.* Stress-induced premature senescence and replicative senescence are different phenotypes, proteomic evidence. *Biochem. Pharmacol.* **64,** 1011–1017 (2002).

44. Serra, V., von Zglinicki, T., Lorenz, M. & Saretzki, G. Extracellular superoxide dismutase is a major antioxidant in human fibroblasts and slows telomere shortening. *J. Biol. Chem.* **278,** 6824–30 (2003).

45. Van Remmen, H. *et al.* Life-long reduction in MnSOD activity results in increased DNA damage and higher incidence of cancer but does not accelerate aging. *Physiol. Genomics* **16,** 29–37 (2003).

46. Packer, L. & Fuehr, K. Low oxygen concentration extends the lifespan of cultured human diploid cells. *Nature* **267,** 423–425 (1977).

47. Serrano, M., Lin, A. W., McCurrach, M. E., Beach, D. & Lowe, S. W. Oncogenic ras provokes premature cell senescence associated with accumulation of p53 and p16(INK4a). *Cell* **88,** 593–602 (1997).

48. Gorgoulis, V. G. & Halazonetis, T. D. Oncogene-induced senescence: The bright and dark side of the response. *Curr. Opin. Cell Biol.* **22,** 816–827 (2010).

49. Nelson, D. M., McBryan, T., Jeyapalan, J. C., Sedivy, J. M. & Adams, P. D. A comparison of oncogene-induced senescence and replicative senescence: implications for tumor suppression and aging. *Age (Dordr).* **36,** 9637 (2014).

50. Wei, S., Wei, W. & Sedivy, J. M. Expression of Catalytically Active Telomerase Does Not Prevent Premature Senescence Caused by Overexpression of Oncogenic Ha-Ras in Normal Human Fibroblasts. *Cancer Res.* **59,** 1539–1543 (1999).

51. Di Micco, R. *et al.* Oncogene-induced senescence is a DNA damage response triggered by DNA hyper-replication. *Nature* **444,** 638–42 (2006).

52. Bartkova, J. *et al.* Oncogene-induced senescence is part of the tumorigenesis barrier imposed by DNA damage checkpoints. *Nature* **444,** 633–7 (2006).

53. d'Adda di Fagagna, F. Living on a break: cellular senescence as a DNA-damage response. *Nat. Rev. Cancer* **8,** 512–522 (2008).

54. Chen, Z. *et al.* Crucial role of p53-dependent cellular senescence in suppression of Pten-deficient tumorigenesis. *Nature* **436,** 725–30 (2005).

55. Shiloh, Y. The ATM-mediated DNA-damage response: taking shape. *Trends Biochem. Sci.* **31,** 402–410 (2006).

56. D'Amours, D. & Jackson, S. P. The Mre11 complex: at the crossroads of dna repair and checkpoint signalling. *Nat. Rev. Mol. Cell Biol.* **3,** 317–27 (2002).

57. Zou, L. Single- and double-stranded DNA: building a trigger of ATR-mediated DNA damage response. *Genes Dev.* **21,** 879–85 (2007).

58. Downey, M. & Durocher, D. gammaH2AX as a checkpoint maintenance signal. *Cell Cycle* **5,** 1376–81 (2006).

59. Buscemi, G. *et al.* Activation of ATM and Chk2 kinases in relation to the amount of DNA strand breaks. *Oncogene* **23,** 7691–700 (2004).

60. Toledo, L. I., Murga, M., Gutierrez-Martinez, P., Soria, R. & Fernandez-Capetillo, O. ATR signaling can drive cells into senescence in the absence of DNA breaks. *Genes Dev.* **22,** 297–302 (2008).

61. Freund, A., Patil, C. K. & Campisi, J. p38MAPK is a novel DNA damage response-independent regulator of the senescence-associated secretory phenotype. *EMBO J.* **30,** 1536–48 (2011).

62. Muñoz-Espín, D. *et al.* Programmed cell senescence during mammalian embryonic development. *Cell* **155,** 1104–18 (2013).

63. Storer, M. *et al.* Senescence is a developmental mechanism that contributes to embryonic growth and patterning. *Cell* **155,** 1119–30 (2013).

64. Olsen, C. L., Gardie, B., Yaswen, P. & Stampfer, M. R. Raf-1-induced growth arrest in human mammary epithelial cells is p16-independent and is overcome in immortal cells during conversion. *Oncogene* **21,** 6328–39 (2002).

65. Bartkova, J. *et al.* DNA damage response as a candidate anti-cancer barrier in early human tumorigenesis. *Nature* **434,** 864–70 (2005).

66. Sherr, C. J. & McCormick, F. The RB and p53 pathways in cancer. *Cancer Cell* **2,** 103–12 (2002).

67. Zhang, J., Pickering, C. R., Holst, C. R., Gauthier, M. L. & Tlsty, T. D. p16INK4a modulates p53 in primary human mammary epithelial cells. *Cancer Res.* **66,** 10325–31 (2006).

68. Narita, M. *et al.* Rb-Mediated Heterochromatin Formation and Silencing of E2F Target Genes during Cellular Senescence. *Cell* **113,** 703–716 (2003).

69. Beauséjour, C. M. *et al.* Reversal of human cellular senescence: roles of the p53 and p16 pathways. *EMBO J.* **22,** 4212–22 (2003).

70. Takahashi, A. *et al.* Mitogenic signalling and the p16INK4a-Rb pathway cooperate to enforce irreversible cellular senescence. *Nat. Cell Biol.* **8,** 1291–1297 (2006).

71. Harman, D. Aging: a theory based on free radical and radiation chemistry. *J. Gerontol.* **11,** 298–300 (1956).

72. Harman, D. Free radical theory of aging: dietary implications. *Am. J. Clin. Nutr.* **25,** 839–43 (1972).

73. Quinlan, C. L., Perevoshchikova, I. V, Hey-Mogensen, M., Orr, A. L. & Brand, M. D. Sites of reactive oxygen species generation by mitochondria oxidizing different substrates. *Redox Biol.* **1,** 304–312 (2013).

74. Murphy, M. P. *et al.* How mitochondria produce reactive oxygen species. *Biochem. J.* **417,** 1–13 (2009).

75. Cadet, J. & Wagner, J. R. Oxidatively generated base damage to cellular DNA by hydroxyl radical and one-electron oxidants: Similarities and differences. *Arch. Biochem. Biophys.* **557,** 47–54 (2014).

76. Passos, J. F. *et al.* Feedback between p21 and reactive oxygen production is necessary for cell senescence. *Mol. Syst. Biol.* **6,** 347 (2010).

77. Passos, J. F., von Zglinicki, T. & Kirkwood, T. B. L. Mitochondria and ageing: winning and losing in the numbers game. *Bioessays* **29,** 908–17 (2007).

78. Passos, J. F. *et al.* Mitochondrial dysfunction accounts for the stochastic heterogeneity in telomere-dependent senescence. *PLoS Biol.* **5,** e110 (2007).

79. Saretzki, G., Murphy, M. P. & von Zglinicki, T. MitoQ counteracts telomere shortening and elongates lifespan of fibroblasts under mild oxidative stress. *Aging Cell* **2,** 141–3 (2003).

80. von Zglinicki, T., Pilger, R. & Sitte, N. Accumulation of single-strand breaks is the major cause of telomere shortening in human fibroblasts. *Free Radic. Biol. Med.* **28,** 64–74 (2000).

81. Torres, M. & Forman, H. J. Redox signaling and the MAP kinase pathways. *BioFactors* **17,** 287–296 (2003).

82. Nelson, G. *et al.* A senescent cell bystander effect: Senescence-induced senescence. *Aging Cell* **11,** 345–349 (2012).

83. Van Raamsdonk, J. M. & Hekimi, S. Superoxide dismutase is dispensable for normal animal lifespan. *Proc. Natl. Acad. Sci. U. S. A.* **109,** 5785–90 (2012).

84. Lawless, C. *et al.* A stochastic step model of replicative senescence explains ROS production rate in ageing cell populations. *PLoS One* **7,** e32117 (2012).

85. Correia-Melo, C. *et al.* Mitochondria are required for pro-ageing features of the senescent phenotype. *EMBO J.* **35,** 724–42 (2016).

86. Correia-Melo, C. & Passos, J. F. Mitochondria: Are they causal players in cellular senescence? *Biochim. Biophys. Acta - Bioenerg.* **1847,** 1373–1379 (2015).

87. Ziegler, D. V, Wiley, C. D. & Velarde, M. C. Mitochondrial effectors of cellular senescence: beyond the free radical theory of aging. *Aging Cell* **14,** 1–7 (2015).

88. Yoon, Y.-S., Byun, H.-O., Cho, H., Kim, B.-K. & Yoon, G. Complex II defect via down-regulation of iron-sulfur subunit induces mitochondrial dysfunction and cell cycle delay in iron chelation-induced senescence-associated growth arrest. *J. Biol. Chem.* **278,** 51577–86 (2003).

89. Moiseeva, O., Bourdeau, V., Roux, A., Deschênes-Simard, X. & Ferbeyre, G. Mitochondrial dysfunction contributes to oncogene-induced senescence. *Mol. Cell. Biol.* **29,** 4495–507 (2009).

90. Miwa, S. *et al.* Low abundance of the matrix arm of complex I in mitochondria predicts longevity in mice. *Nat. Commun.* **5,** 3837 (2014).

91. Kayo, T., Allison, D. B., Weindruch, R. & Prolla, T. A. Influences of aging and caloric restriction on the transcriptional profile of skeletal muscle from rhesus monkeys. *Proc. Natl. Acad. Sci. U. S. A.* **98,** 5093–8 (2001).

92. Balaban, R. S., Nemoto, S. & Finkel, T. Mitochondria, Oxidants, and Aging. *Cell* **120,** 483–495 (2005).

93. Wang, W., Yang, X., López de Silanes, I., Carling, D. & Gorospe, M. Increased AMP:ATP ratio and AMP-activated protein kinase activity during cellular senescence linked to reduced HuR function. *J. Biol. Chem.* **278,** 27016–23 (2003).

94. Mihaylova, M. M. & Shaw, R. J. The AMPK signalling pathway coordinates cell growth, autophagy and metabolism. *Nat. Cell Biol.* **13,** 1016–1023 (2011).

95. Jones, R. G. *et al.* AMP-Activated Protein Kinase Induces a p53-Dependent Metabolic Checkpoint. *Mol. Cell* **18,** 283–293 (2005).

96. Haigis, M. C. & Sinclair, D. A. Mammalian sirtuins: biological insights and disease relevance. *Annu. Rev. Pathol.* **5,** 253–95 (2010).

97. Lee, S. *et al.* Mitochondrial Fission and Fusion Mediators, hFis1 and OPA1, Modulate Cellular Senescence. *J. Biol. Chem.* **282,** 22977–22983 (2007).

98. Park, Y.-Y. *et al.* Loss of MARCH5 mitochondrial E3 ubiquitin ligase induces cellular senescence through dynamin-related protein 1 and mitofusin 1. *J. Cell Sci.* **123,** 619–26 (2010).

99. Mai, S. *et al.* Decreased expression of Drp1 and Fis1 mediates mitochondrial elongation in senescent cells and enhances resistance to oxidative stress through PINK1. *J. Cell Sci.* **123,** 917–26 (2010).

100. Frank, S. *et al.* The Role of Dynamin-Related Protein 1, a Mediator of Mitochondrial Fission, in Apoptosis. *Dev. Cell* **1,** 515–525 (2001).

101. Trougakos, I. P., Saridaki, A., Panayotou, G. & Gonos, E. S. Identification of differentially expressed proteins in senescent human embryonic fibroblasts. *Mech. Ageing Dev.* **127,** 88–92 (2006).

102. Shelton, D. N., Chang, E., Whittier, P. S., Choi, D. & Funk, W. D. Microarray analysis of replicative senescence. *Curr. Biol.* **9,** 939–945 (1999).

103. Seluanov, A. *et al.* Change of the death pathway in senescent human fibroblasts in response to DNA damage is caused by an inability to stabilize p53. *Mol. Cell. Biol.* **21,** 1552–64 (2001).

104. Hampel, B., Malisan, F., Niederegger, H., Testi, R. & Jansen-Dürr, P. Differential regulation of apoptotic cell death in senescent human cells. *Exp. Gerontol.* **39,** 1713–21 (2004)

105. Dimri, G. P. *et al.* A biomarker that identifies senescent human cells in culture and in aging skin in vivo. *Proc. Natl. Acad. Sci. U. S. A.* **92,** 9363–9367 (1995).

106. Choudhury, A. R. *et al.* Cdkn1a deletion improves stem cell function and lifespan of mice with dysfunctional telomeres without accelerating cancer formation. *Nat. Genet.* **39,** 99–105 (2007).

107. Romanov, V. S., Pospelov, V. A. & Pospelova, T. V. Cyclin-dependent kinase inhibitor p21(Waf1): contemporary view on its role in senescence and oncogenesis. *Biochem. Biokhimii͡a* **77,** 575–84 (2012).

108. Ohtani, N., Yamakoshi, K., Takahashi, A. & Hara, E. The p16INK4a-RB pathway: molecular link between cellular senescence and tumor suppression. *J. Med. Invest.* **51,** 146–53 (2004).

109. Waaijer, M. E. C. *et al.* The number of p16INK4a positive cells in human skin reflects biological age. *Aging Cell* **11,** 722–5 (2012).

110. Bernardi, R. & Pandolfi, P. P. Structure, dynamics and functions of promyelocytic leukaemia nuclear bodies. *Nat. Rev. Mol. Cell Biol.* **8,** 1006–16 (2007).

111. Pearson, M. *et al.* PML regulates p53 acetylation and premature senescence induced by oncogenic Ras. *Nature* **406,** 207–10 (2000).

112. Herbig, U., Ferreira, M., Condel, L., Carey, D. & Sedivy, J. M. Cellular senescence in aging primates. *Science* **311,** 1257 (2006).

113. Rodier, F. *et al.* Persistent DNA damage signalling triggers senescence-associated inflammatory

cytokine secretion. *Nat. Cell Biol.* **11,** 973–979 (2009).

114. Weilner, S., Schraml, E., Redl, H., Grillari-Voglauer, R. & Grillari, J. Secretion of microvesicular miRNAs in cellular and organismal aging. *Exp. Gerontol.* **48,** 626–33 (2013).

115. Coppé Jean-Philippe , Pierre-Yves Desprez, Ana Krtolica, and J. C. The Senescence-Associated Secretory Phenotype: The Dark Side of Tumor Suppression. *Annu Rev Pathol.* 99–118 (2010).

116. Freund, A., Laberge, R.-M., Demaria, M. & Campisi, J. Lamin B1 loss is a senescence-associated biomarker. *Mol. Biol. Cell* **23,** 2066–75 (2012).

117. Reddy, K. L., Zullo, J. M., Bertolino, E. & Singh, H. Transcriptional repression mediated by repositioning of genes to the nuclear lamina. *Nature* **452,** 243–7 (2008).

118. Shimi, T. *et al.* The role of nuclear lamin B1 in cell proliferation and senescence. *Genes Dev.* **25,** 2579–93 (2011).

119. Lee, B. Y. *et al.* Senescence-associated beta-galactosidase is lysosomal beta-galactosidase. *Aging Cell* **5,** 187–95 (2006).

120. Coppé, J.-P. *et al.* Senescence-associated secretory phenotypes reveal cell-nonautonomous functions of oncogenic RAS and the p53 tumor suppressor. *PLoS Biol.* **6,** 2853–2868 (2008).

121. Kuilman, T. & Peeper, D. S. Senescence-messaging secretome: SMS-ing cellular stress. *Nat. Rev. Cancer* **9,** 81–94 (2009).

122. Coppé, J.-P., Kauser, K., Campisi, J. & Beauséjour, C. M. Secretion of vascular endothelial growth factor by primary human fibroblasts at senescence. *J. Biol. Chem.* **281,** 29568–74 (2006).

123. Xue, W. *et al.* Senescence and tumour clearance is triggered by p53 restoration in murine liver carcinomas. *Nature* **445,** 656–60 (2007).

124. Tchkonia, T. *et al.* Fat tissue, aging, and cellular senescence. *Aging Cell* **9,** 667–684 (2010).

125. Freund, A., Orjalo, A. V, Desprez, P.-Y. & Campisi, J. Inflammatory networks during cellular senescence: causes and consequences. *Trends Mol. Med.* **16,** 238–46 (2010).

126. Acosta, J. C. *et al.* Chemokine signaling via the CXCR2 receptor reinforces senescence. *Cell* **133,** 1006–18 (2008).

127. Hoenicke, L. & Zender, L. Immune surveillance of senescent cells--biological significance in cancer- and non-cancer pathologies. *Carcinogenesis* **33,** 1123–6 (2012).

128. Kuilman, T. *et al.* Oncogene-Induced Senescence Relayed by an Interleukin-Dependent Inflammatory Network. *Cell* **133,** 1019–1031 (2008).

129. Salminen, A., Kauppinen, A. & Kaarniranta, K. Emerging role of NF-κB signaling in the induction of senescence-associated secretory phenotype (SASP). *Cell. Signal.* **24,** 835–845 (2012).

130. Coppé, J.-P. *et al.* Tumor suppressor and aging biomarker p16(INK4a) induces cellular senescence without the associated inflammatory secretory phenotype. *J. Biol. Chem.* **286,** 36396–403 (2011).

131. Orjalo, A. V, Bhaumik, D., Gengler, B. K., Scott, G. K. & Campisi, J. Cell surface-bound IL-1alpha is an upstream regulator of the senescence-associated IL-6/IL-8 cytokine network. *Proc. Natl. Acad. Sci. U. S. A.* **106,** 17031–6 (2009).

132. Chien, Y. *et al.* Control of the senescence-associated secretory phenotype by NF-κB promotes senescence and enhances chemosensitivity. *Genes Dev.* **25,** 2125–2136 (2011).

133. Chien, Y. *et al.* Control of the senescence-associated secretory phenotype by NF-κB promotes senescence and enhances chemosensitivity. *Genes Dev.* **25,** 2125–36 (2011).

134. Rovillain, E. *et al.* Activation of nuclear factor-kappa B signalling promotes cellular senescence. *Oncogene* **30,** 2356–2366 (2011).

135. Maruyama, J., Naguro, I., Takeda, K. & Ichijo, H. Stress-activated MAP kinase cascades in cellular senescence. *Curr. Med. Chem.* **16,** 1229–35 (2009).

136. Debacq-Chainiaux, F., Boilan, E., Dedessus Le Moutier, J., Weemaels, G. & Toussaint, O. p38(MAPK) in the senescence of human and murine fibroblasts. *Adv. Exp. Med. Biol.* **694,** 126–37 (2010).

137. Castiglioni, A., Canti, V., Rovere-Querini, P. & Manfredi, A. A. High-mobility group box 1 (HMGB1) as a master regulator of innate immunity. *Cell Tissue Res.* **343,** 189–99 (2011).

138. Tang, D., Kang, R., Zeh, H. J. & Lotze, M. T. High-mobility group box 1, oxidative stress, and disease. *Antioxid. Redox Signal.* **14,** 1315–35 (2011).

139. Tang, D. *et al.* Endogenous HMGB1 regulates autophagy. *J. Cell Biol.* **190,** 881–892 (2010).

140. Acosta, J. C. *et al.* A complex secretory program orchestrated by the inflammasome controls paracrine senescence. *Nat. Cell Biol.* **15,** 978–90 (2013).

141. Hubackova, S., Krejcikova, K., Bartek, J. & Hodny, Z. IL1- and TGFβ-Nox4 signaling, oxidative stress and DNA damage response are shared features of replicative, oncogene-induced, and drug-induced paracrine 'bystander senescence'. *Aging (Albany. NY).* **4,** 932–51 (2012).

142. Krtolica, a, Parrinello, S., Lockett, S., Desprez, P. Y. & Campisi, J. Senescent fibroblasts promote epithelial cell growth and tumorigenesis: a link between cancer and aging. *Proc. Natl. Acad. Sci. U. S. A.* **98,** 12072–12077 (2001).

143. Liu, D. & Hornsby, P. J. Senescent human fibroblasts increase the early growth of xenograft tumors via matrix metalloproteinase secretion. *Cancer Res.* **67,** 3117–26 (2007).

144. Kodama, R. *et al.* ROS-generating oxidases Nox1 and Nox4 contribute to oncogenic Ras-induced premature senescence. *Genes to Cells* **18,** 32–41 (2013).

145. Hodny, Z., Hubackova, S. & Bartek, J. Cytokine-induced 'bystander' senescence in DDR and immuno-surveillance. *Oncotarget* **4,** 1552–3 (2013).

146. Mikuła-Pietrasik, J. *et al.* Bystander senescence in human peritoneal mesothelium and fibroblasts is related to thrombospondin-1-dependent activation of transforming growth factor-β1. *Int. J. Biochem. Cell Biol.* **45,** 2087–2096 (2013).

147. Widel, M., Krzywon, A., Gajda, K., Skonieczna, M. & Rzeszowska-Wolny, J. Induction of bystander effects by UVA, UVB, and UVC radiation in human fibroblasts and the implication of reactive oxygen species. *Free Radic. Biol. Med.* **68,** 278–287 (2014).

148. Jaiswal, H. & Lindqvist, A. Bystander communication and cell cycle decisions after DNA damage. *Front. Genet.* **6,** 1–6 (2015).

149. Hanahan, D. & Weinberg, R. A. Hallmarks of cancer: the next generation. *Cell* **144,** 646–74 (2011).

150. Morales, C. P. *et al.* Absence of cancer-associated changes in human fibroblasts immortalized with telomerase. *Nat. Genet.* **21,** 115–8 (1999).

151. Suram, A. *et al.* Oncogene-induced telomere dysfunction enforces cellular senescence in human cancer precursor lesions. *EMBO J.* **31,** 2839–51 (2012).

152. Laberge, R.-M., Awad, P., Campisi, J. & Desprez, P.-Y. Epithelial-mesenchymal transition induced by senescent fibroblasts. *Cancer Microenviron.* **5,** 39–44 (2012).

153. Sun, Y. *et al.* Treatment-induced damage to the tumor microenvironment promotes prostate cancer therapy resistance through WNT16B. *Nat. Med.* **18,** 1359–68 (2012).

154. Demaria, M. *et al.* An Essential Role for Senescent Cells in Optimal Wound Healing through Secretion of PDGF-AA. *Dev. Cell* **31,** 722–733 (2014).

155. Jun, J.-I. & Lau, L. F. The matricellular protein CCN1 induces fibroblast senescence and restricts fibrosis in cutaneous wound healing. *Nat. Cell Biol.* **12,** 676–85 (2010).

156. Telgenhoff, D. & Shroot, B. Cellular senescence mechanisms in chronic wound healing. *Cell Death Differ.* **12,** 695–8 (2005).

157. Jeyapalan, J. C., Ferreira, M., Sedivy, J. M. & Herbig, U. Accumulation of senescent cells in mitotic tissue of aging primates. *Mech. Ageing Dev.* **128,** 36–44 (2007).

158. Campisi, J. Senescent Cells, Tumor Suppression, and Organismal Aging: Good Citizens, Bad Neighbors. *Cell* **120,** 513–522 (2005).

159. Janzen, V. *et al.* Stem-cell ageing modified by the cyclin-dependent kinase inhibitor p16INK4a. *Nature* **443,** 421–6 (2006).

160. López-Otín, C., Blasco, M. A., Partridge, L., Serrano, M. & Kroemer, G. The Hallmarks of Aging. *Cell* **153,** 1194–1217 (2013).

161. Blagosklonny, M. V. Geroconversion: irreversible step to cellular senescence. *Cell Cycle* **13,** 3628–35 (2014).

162. Baker, D. J. *et al.* Clearance of p16Ink4a-positive senescent cells delays ageing-associated disorders. *Nature* **479,** 232–6 (2011).

163. Maier, B. *et al.* Modulation of mammalian life span by the short isoform of p53. *Genes Dev.* **18,** 306–319 (2004).

164. Bowen, J. M., Chamley, L., Keelan, J. A. & Mitchell, M. D. Cytokines of the placenta and extra-placental membranes: roles and regulation during human pregnancy and parturition. *Placenta* **23,** 257–73 (2002).

165. Huang, T. & Rivera-Pérez, J. A. Senescence-associated β-galactosidase activity marks the visceral endoderm of mouse embryos but is not indicative of senescence. *Genesis* **52,** 300–8 (2014).

166. Ullah, Z., Lee, C. Y., Lilly, M. A. & DePamphilis, M. L. Developmentally programmed endoreduplication in animals. *Cell Cycle* **8,** 1501–9 (2009).

167. Chuprin, A. *et al.* Cell fusion induced by ERVWE1 or measles virus causes cellular senescence. *Genes Dev.* **27,** 2356–66 (2013).

168. Rauser, C. L., Mueller, L. D. & Rose, M. R. The evolution of late life. *Ageing Res. Rev.* **5,** 14–32 (2006).

169. World Health Organization (WHO) [Internet]. Ageing and health fs404 [cited 2016 Jul 25]. Available from: http://www.who.int/. *WHO* (2016).

170. Miljkovic, N., Lim, J.-Y., Miljkovic, I. & Frontera, W. R. Aging of skeletal muscle fibers. *Ann. Rehabil. Med.* **39,** 155–62 (2015).

171. Brady, A. O., Straight, C. R. & Evans, E. M. Body composition, muscle capacity, and physical function in older adults: an integrated conceptual model. *J. Aging Phys. Act.* **22,** 441–52 (2014).

172. Cruz-Jentoft, A. J. *et al.* Sarcopenia: European consensus on definition and diagnosis: Report of the European Working Group on Sarcopenia in Older People. *Age Ageing* **39,** 412–23 (2010).

173. Goodpaster, B. H., Kelley, D. E., Thaete, F. L., He, J. & Ross, R. Skeletal muscle attenuation determined by computed tomography is associated with skeletal muscle lipid content. *J. Appl. Physiol.* **89,** 104–10 (2000).

174. Broskey, N. T. *et al.* Skeletal muscle mitochondria in the elderly: effects of physical fitness and exercise training. *J. Clin. Endocrinol. Metab.* **99,** 1852–61 (2014).

175. Renault, V. *et al.* Regenerative potential of human skeletal muscle during aging. *Aging Cell* **1,** 132–9 (2002).

176. Arthur, S. T. & Cooley, I. D. The effect of physiological stimuli on sarcopenia; impact of Notch and Wnt signaling on impaired aged skeletal muscle repair. *Int. J. Biol. Sci.* **8,** 731–60 (2012).

177. Cheung, T. H. & Rando, T. A. Molecular regulation of stem cell quiescence. *Nat. Rev. Mol. Cell Biol.* **14,** 329–40 (2013).

178. Yin, H., Price, F. & Rudnicki, M. A. Satellite cells and the muscle stem cell niche. *Physiol. Rev.* **93,** 23–67 (2013).

179. Sousa-Victor, P. *et al.* Geriatric muscle stem cells switch reversible quiescence into senescence. *Nature* **506,** 316–21 (2014).

180. Georgakopoulou, E. A. *et al.* Specific lipofuscin staining as a novel biomarker to detect replicative and stress-induced senescence. A method applicable in cryo-preserved and archival tissues. *Aging (Albany. NY).* **5,** 37–50 (2013).

181. Feeney, E. J. *et al.* The value of muscle biopsies in Pompe disease: identifying lipofuscin inclusions in juvenile- and adult-onset patients. *Acta Neuropathol. Commun.* **2,** 2 (2014).

182. García-Prat, L. *et al.* Autophagy maintains stemness by preventing senescence. *Nature* **529,** 37–42 (2016).

183. von Zglinicki, T., Nilsson, E., Döcke, W. D. & Brunk, U. T. Lipofuscin accumulation and ageing of fibroblasts. *Gerontology* **41 Suppl 2,** 95–108 (1995).

184. Jung, T., Bader, N. & Grune, T. Lipofuscin: formation, distribution, and metabolic consequences. *Ann. N. Y. Acad. Sci.* **1119,** 97–111 (2007).

185. Shah, P. P. *et al.* Lamin B1 depletion in senescent cells triggers large-scale changes in gene expression and the chromatin landscape. *Genes Dev.* **27,** 1787–99 (2013).

186. Davalos, A. R. *et al.* p53-dependent release of Alarmin HMGB1 is a central mediator of senescent phenotypes. *J. Cell Biol.* **201,** 613–29 (2013).

187. Niccoli, T. & Partridge, L. Ageing as a Risk Factor for Disease. *Curr. Biol.* **22,** R741–R752 (2012).

188. Baker, D. J. *et al.* Naturally occurring p16(Ink4a)-positive cells shorten healthy lifespan. *Nature* **530,** 184–9 (2016).

189. Cristofalo, V. J. SA β Gal staining: Biomarker or delusion. *Experimental Gerontology* **40,** 836–838 (2005).

190. Lexell, J. Human aging, muscle mass, and fiber type composition. *J. Gerontol. A. Biol. Sci. Med. Sci.* **50 Spec No,** 11–6 (1995).

191. Demontis, F., Piccirillo, R., Goldberg, A. L. & Perrimon, N. Mechanisms of skeletal muscle aging: insights from Drosophila and mammalian models. *Dis. Model. Mech.* **6,** 1339–52 (2013).

192. Fujisawa, K. Some observations on the skeletal musculature of aged rats: Part 1. Histological aspects. *J. Neurol. Sci.* **22,** 353–366 (1974).

193. Fujisawa, K. Some observations on the skeletal musculature of aged rats. Part 2. Fine morphology of diseased muscle fibres. *J. Neurol. Sci.* **24,** 447–69 (1975).

194. Narita, S. & Yorifuji, H. Centrally nucleated fibers (CNFs) compensate the fragility of myofibers in mdx mouse. *Neuroreport* **10,** 3233–5 (1999).

195. Lee, A. S. J. *et al.* Aged skeletal muscle retains the ability to fully regenerate functional architecture. *Bioarchitecture* **3,** 25–37

196. Terman, A. & Brunk, U. T. Lipofuscin. *Int. J. Biochem. Cell Biol.* **36,** 1400–1404 (2004).

197. Ćmielová, J. & Řezáčová, M. Protein and its function based on a subcellular localization. *J. Cell. Biochem.* **112,** 3502–3506 (2011).

198. Karimian, A., Ahmadi, Y. & Yousefi, B. Multiple functions of p21 in cell cycle, apoptosis and transcriptional regulation after DNA damage. *DNA Repair (Amst).* **42,** 63–71 (2016).

199. Falciola, L. *et al.* High mobility group 1 protein is not stably associated with the chromosomes of somatic cells. *J. Cell Biol.* **137,** 19–26 (1997).